

Analysis and Synthesis of Eutrophication-Related Conditions in Narragansett Bay (RI/MA USA): Updated Through 2019

Daniel L. Codiga, Sole Proprietor

Academic Affiliation: University of Rhode Island,
Graduate School of Oceanography

**NARRAGANSETT BAY
ESTUARY PROGRAM**



FINAL REPORT

September 10, 2021

Narragansett Bay Estuary Program

Funded by the Environmental Protection Administration
through
New England Interstate Water Pollution Control Commission

NEI Job Code: 0349-001

Project Code: 2020-031

NBEP Contribution Number: NBEP-21-243

EPA Grant Number: USEPA CE00A00407

Full citation:

Codiga, D.L. 2021. Analysis and Synthesis of Eutrophication-Related Conditions in Narragansett Bay (RI/MA USA): Updated Through 2019. NBEP Technical Report. NBEP-21-243. URL: <https://figshare.com/s/a421d07c711a212ca7b2> DOI: 10.6084/m9.figshare.14830890

Abstract

The response of eutrophication-related conditions in Narragansett Bay to managed long-term declines in nitrogen load is investigated, with emphasis on the whole-estuary perspective, using multiple independent monitoring datasets through 2019. Since 2013 when bay-wide load declines were substantially complete, there has been a notable decline, over at least several years, in excess chlorophyll and a decline in hypoxia at least as substantial. Although an upcoming year with summer river flow comparable to the wettest earlier years will be necessary for a more complete assessment, the bay appears to have reached a new state characterized by reduced chlorophyll levels and effectively free from all but mild hypoxia.

There are clear relationships among nitrogen load, chlorophyll, and hypoxia for both inter-annual variability and long-term declines. Variability of both nitrogen load and stratification closely follows that of river flow, the most important driver of inter-annual changes. Stratification is more tightly correlated to river flow than nitrogen load, due to the long-term decline in the latter, which best explains the long-term chlorophyll and oxygen trends. Investigations of the potential importance of other physical influences (salinity, winds, tidal range, non-tidal sea level gradients) demonstrate that they play minor roles. In this sense, changes in the bay have followed expectations from conventional understanding of eutrophication: long-term load reductions have led to declines in chlorophyll and hypoxia. Until now this has been somewhat obscured by both the large range of inter-annual variability relative to the long-term changes and the difficulties in defining bay-wide indicators given the complex system geometry, numerous river flow and nitrogen load sources, and differing characteristics of available datasets. Similarity of results from two key complementary datasets for chlorophyll and oxygen supports confidence in the findings. To the extent climate-driven long-term warming (see next paragraph) is causing long-term increases in oxygen consumption through metabolic rates, and reducing the oxygen saturation concentration, the observed declines in hypoxia are slower than they otherwise would be.

Long-term trends in temperature, salinity, and density stratification are evaluated for 2006-2019 using multiple independent monitoring datasets. Statistical strength of results is marginal but key results are consistent across datasets. For the summer-centered May to October period surface waters are warming at rates consistent with prior published results throughout the region, and near-seafloor temperatures are warming about 80% faster than at the surface, likely in association with offshore waters entering the bay as the deep inward limb of estuarine exchange flow. Annual-mean temperatures are warming but more weakly, due to long-term cooling of the winter-centered November to April period. Salinities are increasing, more strongly at the surface, consistent with the influence of relatively low river flow since 2013. Stratification is decreasing, at a rate that is weak in the sense that it would require at least a few decades to cause a substantial reduction to typical stratification strength; the decrease is predominantly due to salinity, which is increasing faster near the surface, but also due to the faster temperature increases at depth.

Executive Summary

The response of eutrophication-related conditions in Narragansett Bay to managed long-term declines in nitrogen load is investigated, with emphasis on the whole-estuary perspective, using multiple independent monitoring datasets through 2019. Baseline hypotheses center on the expectation that reduced nitrogen load will cause declines in overabundant phytoplankton, thus less oxygen will be consumed during its bacterial decomposition, and hypoxia severity will be reduced, particularly in deep waters isolated by density stratification from reaeration through the air-sea interface.

May to October is the main focus because it is when treatment plants implement upgraded nitrogen removal, it brackets development and breakdown of seasonal stratification, and it includes late summer when hypoxia occurs. Bay-wide measures of river flow and load of total nitrogen are defined and tabulated at daily resolution. River flow is from 11 sources and uses United States Geological Service gauge measurements. Nitrogen load is from 18 sources including 11 treatment plants discharging directly the bay, 6 rivers with load including inputs from plants upstream, and runoff from ungauged bay-adjacent areas; data are provided by the Rhode Island Department of Environmental Management (RIDEM), Narragansett Bay Commission (NBC), and Fall River Treatment Plant. Two independent monitoring datasets for in situ chlorophyll and oxygen are analyzed, each spanning the water column and with spatial coverage extending beyond the most eutrophication-prone northern and western parts of the bay. Time series of the Narragansett Bay Fixed Site Monitoring Network are from an array of 11 sites, mostly in deeper areas on or near channels, and have strong temporal sampling (15-minute resolution); stratification is computed from their temperature and salinity measurements. They result from efforts of University of Rhode Island, NBC, and the Narragansett Bay National Estuarine Research Reserve. Complementary vessel-based surveys on typically 5-7 late spring to early fall dates have strong spatial sampling (60-70 stations) and cover both shallower and deeper areas. They result from efforts of several institutions led by Brown University.

The time series are characterized by a sequence of high-chlorophyll events, each lasting from about a day to a week, and a distinct asynchronous sequence of fewer low-oxygen events of similar durations during late summer. The metric used to quantify each surface chlorophyll event is the area swept out by the concentration vs time curve above a fixed threshold. The sum of such areas for all May-Oct events is denoted the Chlorophyll Index, a single summary indicator reflecting variations in the number, durations, and severity of events; its average across multiple stations, excluding a few in far-inshore markedly shallower embayments, is used to identify year to year changes in bay-wide conditions. Three thresholds are used, denoted mild, moderate, and severe: 4.9, 9.4, and 17.6 mg/L , the 20th, 50th, and 80th percentiles, respectively, of time series from all stations and years. The Hypoxia Index is defined similarly (the sum, over all May-Oct events, of the area below a fixed threshold swept out by near-seafloor oxygen concentration vs time) and averaged over the same stations. Mild, moderate, and severe hypoxia thresholds (4.8, 2.9, and 1.4 mg/L , respectively) are regulatory and based on harm to organisms.

Each vessel-based survey yields the percent of sampled geographic area of the bay with surface chlorophyll above a threshold, and the percent area with near-bottom oxygen below a threshold. Averages of results from all surveys in a year are used to identify year to year changes. Chlorophyll thresholds (8.0, 14.0, and 27.4 mg/L) are the 20th, 50th, and 80th percentiles, respectively, of surveys from all stations and years; these are higher than the time series thresholds due to the surveys sampling more of shallow areas where chlorophyll is highest. Oxygen thresholds are the same as for the time series.

For many parameters system-wide the most important control of year to year changes in May-Oct averages is the pronounced inter-annual variability of river flow, which is a dominant driver of nitrogen loads and the primary influence on stratification. Inter-annual variations in nitrogen load closely follow those of river flow, but with a long-term decline superposed, due to treatment plant upgrades. Stratification also parallels river flow, more closely than does nitrogen load as it has no long-term decline, indicating that load is more important to the long-term changes in chlorophyll and oxygen. The long-term decline in load occurred over a period of at least 8 years, with contributions from individual treatment plant upgrades during different time periods. The decline has magnitude comparable to or less than inter-annual load variations and was effectively complete bay-wide during 2013.

Chlorophyll metrics from both datasets and three thresholds show inter-annual variability generally parallel to that of load, as expected. During a several year period after 2013 there is a slow decline in chlorophyll metrics superposed on the inter-annual variations, with the most recent few years among the lowest to date. Similarly, for hypoxia metrics from both datasets and three thresholds the inter-annual variability generally follows that of load and chlorophyll; the relationship is less tight than between chlorophyll and load, consistent with the expectation that oxygen is influenced by load through chlorophyll as intermediary. Since 2013 there has been a decline in hypoxia metrics, and during the most recent few years hypoxia has been essentially absent for the moderate and severe thresholds.

It is important to note that no year since 2013 had May-Oct river flow comparable to the several wettest years of the prior decade, which include 2013. Under this extended period of relatively dry summers it could be expected that load, chlorophyll, and hypoxia would be reduced even without treatment plant upgrades—especially with the magnitude of load reductions by plant upgrades comparable to or smaller than inter-annual load variations due to river flow. However, comparisons of chlorophyll and hypoxia metrics during years before and after 2013 having similar river flow, which includes dry to moderately wet years with 2018 and 2019 being in the latter group, indicates they are lower after 2013. It follows that the nitrogen load declines are more responsible than the recent period of relatively low river flow.

In summary, in response to nitrogen load reductions there has been a notable decline, over at least several years, in excess chlorophyll and a decline in hypoxia at least as substantial. Although an upcoming year with river flow comparable to the wettest earlier years will be necessary for a more complete assessment, the bay appears to have reached a new state characterized by reduced chlorophyll levels and effectively free from all but mild hypoxia. There are clear relationships of both inter-annual variability and long-term declines among nitrogen load, chlorophyll, and hypoxia. Investigations of the potential importance of other physical influences (salinity, winds, tidal range, non-tidal sea level gradients) demonstrate that they play minor roles. In this sense, changes in the bay have followed expectations from conventional understanding of eutrophication: long-term load reductions have caused long-term declines in chlorophyll and hypoxia. Until now this has been somewhat obscured by both the large range of inter-annual variability relative to the declines and difficulties in defining bay-wide indicators given the complex system geometry, numerous river flow and nitrogen load sources, and differing characteristics of available datasets. Similarity of results from the two key datasets supports confidence in the findings. To the extent climate-driven long-term warming (see below) is causing long-term increases in oxygen consumption through metabolic rates, and reducing the oxygen saturation concentration, the observed declines in hypoxia are slower than they otherwise would be.

While those conclusions hold overall, there remain aspects less well understood. Although flushing and residence time estimates are no longer than a month or two, the response to reduced load occurred over multiple years, with a lag of at least a year. Load reductions were first substantially complete bay-wide in 2013, but due to high river flow, hypoxia that year was comparable to the most severe prior years; in addition, 2018 and 2019 river flow and nitrogen load were higher than the immediately preceding few years but chlorophyll and hypoxia metrics did not increase as much as expected. The influence of sediment fluxes is among the possible explanations for these lags.

Long-term trends in temperature, salinity, and density stratification. Data from multiple independent monitoring programs are treated including primarily the time series described above and also the Graduate School of Oceanography (GSO) Fish Trawl, GSO Long-term Plankton, RIDEM Coastal Fish Trawl, and National Oceanic and Atmospheric Administration Newport datasets. The most suitable common period is treated, 2006-2019. To investigate trends during different parts of the year, summer-centered (May-Oct) and winter-centered (Nov-Apr) six-month periods, as well as the 12-month Nov-Oct period, are treated. Overall statistical confidence suggests the datasets are at best marginally suitable for the analyses applied. However, surface temperature trends are consistent with those reported elsewhere, and there are clear patterns in differences from season to season and between near-surface and near-seafloor depths that occur across multiple datasets and multiple sites, lending the results credence.

Trends identified, that are applicable at the bay-wide scale and mainly for portions of the bay with bathymetric depths deeper than the typical mixed layer depth of 4m, include the following:

- Warming of near-surface summer temperatures at about 0.4-0.5 deg C per decade.
- Stronger warming of near-seafloor summer temperatures, about 80% faster than near-surface.
- Trends of whole-year warming but at rates slower than summer by up to about 50%, and with a smaller difference between near-surface and near-seafloor rates than in summer, as a result of winter temperatures that are cooling at similar near-surface and near-seafloor rates.
- Salinity increasing during summer at average rates of about 0.8 and 0.3 PSU per decade near the surface and near the seafloor, respectively, and at similar rates in winter.
- Density stratification decreasing at about 0.4 kg m⁻³ per decade in summer, mainly due to the salinity trends (slower increases at depth), but also due to the temperature trends (faster warming at depth).

With respect to processes causing the identified trends, many aspects are understood reasonably well. Increasing temperatures are due to global climate warming, which has a strong regional signature. Faster warming at depth is most likely associated with the influence of offshore conditions through the deep inward limb of estuarine exchange flow. Increasing salinities are linked to relatively low river inputs in years since 2013, roughly the second half of the analyzed period, particularly during summer; increases are faster near the surface because less-dense river flow influences the upper portion of the water column more strongly. Due to the seawater equation of state the dominant cause of declining stratification is the different near-surface and near-seafloor salinity trends, rather than temperature. The rate of stratification decline is weak, in the sense that at least a few decades would be required to substantially reduce the typical stratification; as noted, to the extent that warming is increasing oxygen consumption rates and lowered the oxygen saturation concentration, it likely has more influence on eutrophication processes than the long-term trend in stratification.

Products. Data files and documentation, for all datasets and analysis code developed, are provided online at <https://figshare.com/s/a421d07c711a212ca7b2>.

Contents

Abstract.....	1
Executive Summary.....	2
List of Figures	7
List of Tables	10
Acronyms	11
Task 1 River Flow, Wind, Tidal Range, and Sea Level.....	12
1.1 Scope.....	12
1.2 Methods.....	12
1.3 Results.....	14
Task 2 Nitrogen Loads.....	19
2.1 Scope.....	19
2.2 Methods.....	19
2.3 Results.....	19
Task 3 Fixed-Site Monitoring Network: Data Reduction.....	44
3.1 Scope.....	44
3.2 Methods.....	44
3.3 Results.....	44
Task 4 Fixed-Site Monitoring Network: Hypoxia Index.....	48
4.1 Scope.....	48
4.2 Methods.....	48
4.3 Results.....	48
Task 5 Fixed-Site Monitoring Network: Chlorophyll Index	55
5.1 Scope.....	55
5.2 Methods.....	55
5.3 Results.....	58
Task 6 Synthesis of Hypoxia, Chlorophyll, Nitrogen Load, Physical Drivers.....	64
6.1 Scope.....	64
6.2 Methods.....	64
6.3 Results.....	64
6.3.1 Nitrogen load by source.....	65
6.3.2 Nitrogen load and river flow: long-term changes, seasonality.....	66
6.3.3 Role of stratification.....	67
6.3.4 Changes in chlorophyll and hypoxia due to nitrogen load reductions	68
6.3.5 Physical drivers: temperature, wind, tidal range, sea level differences.....	70
6.3.6 Additional discussion	71
Task 7 Long-Term Trends in Temperature, Salinity, and Stratification	89
7.1 Scope.....	89
7.2 Methods.....	89
7.2.1 Data reduction	90

7.2.2	Trend analysis	91
7.2.3	Bootstrap: weekly/monthly vs 15-minute sampling.....	93
7.3	Results	93
7.3.1	Fixed site monitoring network.....	93
7.3.2	Bootstrap quantification of weaker statistics for weekly/monthly sampling.....	96
7.3.3	GSO Fish Trawl	96
7.3.4	GSO Long-term Plankton.....	97
7.3.5	RIDEM Coastal Fish Trawl.....	98
7.3.6	NOAA Newport station	98
7.3.7	Conclusions	99
	Some Recommended Future Research Needs	116
	All Tasks: Data and Code Files Documentation.....	118
1.	River Flow, Wind, Tidal Range, and Sea Level.....	118
2.	Nitrogen Load.....	119
3.	Fixed-Site Monitoring Network: Data Reduction.....	121
4.	Fixed-Site Monitoring Network: Hypoxia Index.....	121
5.	Fixed-Site Monitoring Network: Chlorophyll Index	122
6.	Synthesis of Hypoxia, Chlorophyll, Nitrogen Load, Physical Drivers.....	122
7.	Long-Term Trends in Temperature, Salinity, and Stratification.....	122
	References Cited	124
	Acknowledgements.....	127

List of Figures

Figure 1-1. Daily river flows 2001-2019, 10 rivers and ungauged area: basin-wide flow. Inset shows 2016 only, as example of a single year.	17
Figure 1-2. Median daily basin-wide flow, June to September (black line), 2001-2019.....	18
Figure 2-1. Nitrogen load sources, on background of Figure A-2 from Appendix of NBEP (2017).....	22
Figure 2-2. Taunton River and upstream WWTFs.....	23
Figure 2-3. Blackstone River and upstream WWTFs.....	24
Figure 2-4. Fields Point WWTF.....	25
Figure 2-5. Pawtuxet River and upstream WWTFs.....	26
Figure 2-6. Fall River WWTF.....	27
Figure 2-7. Ungauged runoff from riparian areas.....	28
Figure 2-8. Bucklin Point WWTF.....	29
Figure 2-9. Ten Mile River and upstream WWTFs.....	30
Figure 2-10. Newport WWTF.....	31
Figure 2-11. Bristol WWTF.....	32
Figure 2-12. East Providence WWTF.....	33
Figure 2-13. Woonasquatucket River and upstream WWTF.....	34
Figure 2-14. Somerset WWTF.....	35
Figure 2-15. Moshassuck River.....	36
Figure 2-16. Warren WWTF.....	37
Figure 2-17. Quonset WWTF.....	38
Figure 2-18. East Greenwich WWTF.....	39
Figure 2-19. Jamestown WWTF.....	40
Figure 2-20. TN load time series, 18 sources superposed on same figure. Linear y-axis scale.....	41
Figure 2-21. TN load time series, 18 sources superposed on same figure. Logarithmic y-axis scale (otherwise same as Figure 2-20).....	42
Figure 2-22. Total TN load (summed loads from 18 sources) to Narragansett Bay.....	43
Figure 3-1. Near-bottom dissolved oxygen measurements (units mg L^{-1}) from 2018 and 2019 at the 11 NBFSMN sites. The percent time with valid measurements is shown at upper right in each frame (and in Table 3-1).	46
Figure 3-2. Near-surface chlorophyll measurements (mg L^{-1}) from 2018 and 2019 at the 11 NBFSMN sites. The percent time with valid measurements is shown at upper right in each frame (and in Table 3-2). Values higher than the vertical axis maximum, 250 mg L^{-1} , are green.	47

Figure 4-1. Hypoxia Index relative to 4.8 mg L ⁻¹ (highest of the three thresholds; a measure of all relatively low oxygen conditions including the most mild hypoxia) for individual sites (each frame showing a station group).....	51
Figure 4-2. Hypoxia Index relative to 2.9 mg L ⁻¹ (intermediate of the three thresholds; used by regulators to designate impaired areas), shown as in Figure 4-1.....	52
Figure 4-3. Hypoxia Index relative to 1.4 mg L ⁻¹ (lowest of the three thresholds; a measure of the most severe hypoxic conditions), shown as in Figure 4-1.	53
Figure 4-4. Hypoxia Index results, station-group averages. Threshold 4.8 mg L ⁻¹ , 2.9 mg L ⁻¹ , and 1.4 mg L ⁻¹ are shown in the top, middle, and bottom panels respectively.....	54
Figure 5-1. Chlorophyll Index relative to 4.9 µg L ⁻¹ (lowest of the three thresholds; a measure of all high-chlorophyll events including the most mild) for individual sites (each frame showing a station group). Shown as in Figure 4-1 for the Hypoxia Index.....	60
Figure 5-2. Chlorophyll Index relative to 9.4 µg L ⁻¹ (intermediate of the three thresholds), shown as in Figure 5-1.....	61
Figure 5-3. Chlorophyll Index relative to 17.6 µg L ⁻¹ (highest of the three thresholds; a measure of the most severe high-chlorophyll events), shown as in Figure 5-1.	62
Figure 5-4. Chlorophyll Index results, station-group averages. Threshold 4.9 µg L ⁻¹ , 9.4 µg L ⁻¹ , and 17.6 µg L ⁻¹ are shown in the top, middle, and bottom panels respectively.	63
Figure 6-1. TN load timeseries for 18 individual sources to the bay (left axis), with bay-wide river flow superposed as thick black line (right axis); both are the mean over the May-Oct period.	74
Figure 6-2. TN load from sources to the east and west of the Mt Hope bridge, May-Oct, with river flow superposed.	75
Figure 6-3. Scatter plot of bay-wide TN load vs bay-wide river flow, means over the June-September period. Years prior to 2013 are circles and years from 2013 onward are triangles. The latter are all notably lower, for each range of river flow, which quantifies the extent to which treatment plant upgrades have reduced loads. Linear regressions to the two year ranges have r ² values 0.94 and 0.98, respectively (both p < 0.05).	75
Figure 6-4. Bay-wide TN load (left axis, solid curves) and river flow (right axis, dashed curves) sums (TN load in lb; river flow in m ³) broken out by time of year: all 12 months (red); Nov-Apr, the 6 months centered on winter (blue), and May-Oct, the 6 months centered on summer (black). Note scale factor at top of each y-axis.....	76
Figure 6-5. Bay-wide stratification vs bay-wide river flow, June to September mean. Linear regression in scatterplot is based on all years and has r ² value 0.94 with p < 0.05.	77
Figure 6-6. Time series 2005-2019 of bay-wide eutrophication-related summer conditions in relation to river flow and TN load.....	78
Figure 6-7. Bay-wide chlorophyll metrics vs June to September mean bay-wide TN load. Upper frame: severe thresholds. The r ² values for Chlorophyll Index and percent high-chlorophyll area are 0.73 and 0.66 respectively (both p < 0.05). Lower frame: moderate thresholds. The r ² values for Chlorophyll Index and percent high-chlorophyll area are 0.71 and 0.64 respectively (both p < 0.05).	79

Figure 6-8. Bay-wide hypoxia metrics vs June to September mean bay-wide TN load. Upper frame: severe threshold. (No regression lines because of the high fractions of zero values.) Lower frame: moderate threshold. Regression lines for Hypoxia Index and percent hypoxic area have r^2 values 0.68 and 0.67 respectively (both $p < 0.05$).	80
Figure 6-9. Physical drivers, mean June to September: temperature (frame 3), wind speed and direction (frame 4), tidal range (frame 5 left), and Providence less Newport non-tidal sea level (frame 5 right). To provide context, in frames 1 and 2 the river flow, TN load, Chlorophyll Index, and Hypoxia Index results from Figure 6-6 are shown.	81
Figure 7-1. Station location map of datasets used in trend analysis. See Table 7-1 for variables sampled, and characteristics of temporal sampling, for each dataset.	104
Figure 7-2. Post data-reduction GSO Fish Trawl measurements, Fox Island station.....	105
Figure 7-3. Post data-reduction GSO Fish Trawl measurements, Whale Rock station.....	106
Figure 7-4. Post data-reduction GSO Long-term Plankton Time Series measurements.....	107
Figure 7-5. Post data-reduction RIDEM Coastal Trawl Survey measurements.....	108
Figure 7-6. Post data-reduction NOAA Newport tidal station measurements.....	109
Figure 7-7. Example time series treatment and trend calculation results.	110
Figure 7-8. Trend results for all fixed site (NBFSMN) stations, year range 2006-2019, 5-month mid-May to mid-Oct date range.....	111
Figure 7-9. Trend results for the four fixed site stations where year-round sampling occurs, presented similarly to Figure 7-8 (same ranges on vertical axes, and colors, for the four variables).	112
Figure 7-10. Bootstrap results. From monthly means from raw 15-min data, denoted “q” for quarter-hour, are same as in Figure 7-8. Weekly “w” and monthly “m” results are from bootstrap.	113
Figure 7-11. Trend results for GSO Long-term Plankton (station S2), GSO Fish Trawl (stations FI and WR), and Newport. Shown as in Figure 7-9 (same ranges on vertical axes, and colors, for the four variables), with S, A, and W indicating summer, annual, and winter periods.....	114
Figure 7-12. Trend results for DEM Coastal Trawl dataset. Presented as in prior two figures except that the range for the vertical axis is two times as large.	115

List of Tables

Table 1-1. Gauges used for river flow observations. Same as in Codiga (2020a).....	16
Table 1-2. Scale-up factors based on Table 7 of Ries (1990). The first 8 rows are the scale-up factors from the gauge (see left column of Table 1 above) to the mouth of each river. The last row is the scale-up factor from the sum of the 8 river mouth flows to the basin-wide flow. Same as in Codiga (2020a).....	16
Table 1-3. Threshold values, for median daily basin-wide flow between June and September based on 1990 to 2017 (not 2019; see text) conditions, to designate individual years as wet, dry, or intermediate. Same as in Codiga (2020a).....	16
Table 1-4. Designation of bay-wide Jun-Sep river flow conditions each year from 2001 to 2019 as “wet”, “intermediate”, or “dry”, using the criterion in Table 1-3.....	16
Table 2-1. The eighteen sources treated in this analysis, listed in descending order based on their mean TN load from the estimated 2001-2019 timeseries.....	21
Table 3-1. Percent of time during mid-May to mid-October analysis period with valid near-bottom dissolved oxygen values, at each of the eleven sites during 2018 and 2019.	45
Table 3-2. Percent of time during mid-May to mid-October analysis period with valid surface chlorophyll values, at each of the eleven sites during 2018 and 2019.....	45
Table 7-1. Summary of sampled variables (T = temperature, S = salinity), and spatial locations and temporal characteristics of the sampling, for each of the different datasets treated by the long-term trend analysis. Station locations are shown in Figure 7-1. The most recent year included in the analysis is 2019.....	101
Table 7-2. Years duration statistic, NBFMSMN sites with 12-month sampling.	102
Table 7-3. Same as Table 7-2 but showing bootstrap results for weekly (“w”) and monthly (“m”) sub-sampling of the 15-minute resolution measurements (“q” for quarter-hourly; values repeated from Table 7-2). Asterisks indicate the results were not finite.	102
Table 7-4. Years duration statistic, for datasets other than NBFMSMN. Based on the bootstrap results, results for these weekly- and monthly-sampled datasets are underestimates.	103

Acronyms

BR	Bullock Reach site of NBFSMN
CP	Conimicut Point site of NBFSMN
DO	Dissolved Oxygen
GB	Greenwich Bay site of NBFSMN
GRBY	Greenwich Bay group of NBFSMN stations
GSO	Graduate School of Oceanography
MH	Mount Hope Bay site of NBFSMN
MV	Mount View site of NBFSMN
NARR	North American Regional Reanalysis
NBFSMN	Narragansett Bay Fixed Site Monitoring Network
NBEP	Narragansett Bay Estuary Program
NBNERR	Narragansett Bay National Estuarine Research Reserve
NEIWPC	New England Interstate Pollution Control Commission
NOAA	National Oceanic and Atmospheric Administration
NP	North Prudence Island site of NBFSMN
PD	Phillipsdale Landing site of NBFSMN
PP	Poppasquash Point site of NBFSMN
PRUB	Providence River and Upper Bay group of NBFSMN stations
QP	Quonset Point site of NBFSMN
RIDEM	Rhode Island Department of Environmental Management
SNBIW	State of Narragansett Bay and Its Watershed, published 2017 by NBEP
SR	Sally Rock site of NBFSMN
TW	Prudence Island T-Wharf site of NBFSMN
URI	University of Rhode Island
UEP	Upper East Passage group of NBFSMN stations
UWP	Upper West Passage group of NBFSMN stations

Task 1 River Flow, Wind, Tidal Range, and Sea Level

1.1 Scope

Time series for river flow, wind, tidal range, and sea level parameters were generated previously (Codiga 2020a) for years up to 2017; here the years 2018-2019 are produced and appended.

1.2 Methods

River flow. Available daily flow observations were obtained from the USGS website for all gauges in Table 1-1 from 1990 to the end of 2019. Gaps less than 3 days long were filled by linear interpolation. Three rivers had gaps longer than 3 days, which were filled by regression against a nearby river (right column of Table 1-1 shows the correlation coefficients). Gap-filled records from the 8 gauges in the left column are used in the remainder of the analysis.

Freshwater runoff to the Narragansett Bay basin is taken to consist of 11 sources: 8 gauged rivers, 2 ungauged rivers both estimated by correlation to a gauged river, and ungauged flow from outside those riversheds. The ungauged Hardig Brook and Maskerchugg River are included as sources, in addition to the 8 gauged rivers. They are included in order to capture flow entering Greenwich Bay, and because of their proximity to sites of long term time series observations to be analyzed; their flows are estimated from regressions against the Hunt River flow, to which they are highly correlated, using coefficients from Ullman et al (2019) where the method is explained.

The aggregate basin-wide runoff, including all ungauged areas, is computed from the 8 gauge observation records by a two-stage scale-up process using scale factors (Ries, 1990) based on drainage areas and historical records. The first stage is to scale up each of the 8 gauged flows to the flow at the mouth of the river each gauge is on, to account for ungauged flow within its rivershed. A monthly-varying unitless scale-up factor equal to or greater than 1.0 is applied to flow of each gauge, to account for flow entering the river from drainage areas downstream of the gauge, between the gauge and the river mouth. If the gauge was located at the mouth, the factor would be 1.0. For rivers that have the gauge located near the mouth, or that have little flow entering the river from the drainage area between the gauge and the mouth, the factor will exceed 1.0 by a small amount. The highest scale-up factor is for the Taunton River, because the gauge used is far upstream from the mouth. For the gauged rivers except the Hunt, the 12 long-term mean monthly river mouth scale-up factors (Table 1-2) are from Table 7 in Ries (1990), computed as the ratio of the long-term mean monthly river mouth flow and the corresponding gauge flow. For the Hunt, Ries did not consider mouth flow separately, so the value of one is used for the river mouth scale-up factor. The monthly scale-up factors are assigned to the 15th of every month and interpolated to daily resolution in order to avoid unrealistic step functions from month to month. These daily values are then multiplied by the daily gauge observations to yield the end product of stage one: daily records for the 8 mouths that include ungauged flow within their riversheds.

The second stage is to determine basin-wide flow including ungauged areas both inside and outside the riversheds of the 8 gauged rivers, by scaling up the sum of the records for the 8 mouth flows from the first stage so that flow from ungauged areas outside the riversheds is also included. Twelve monthly values of the basin-wide scale-up factor (last row of Table 1-2) are from Table 7 in Ries (1990), computed as the ratio between the long-term mean monthly basin-wide flow which includes all ungauged areas and the long-term mean sum of the 8 mouth flows. The monthly basin-wide scale-up factors are

assigned to the 15th of every month and interpolated to daily resolution in order to avoid unrealistic step functions from month to month. These daily values are then multiplied by the sum of the mouth flows, to yield the daily basin-wide flow including all ungauged areas.

Finally, the ungauged flow from areas outside the 10 riversheds is computed as the difference of the basin-wide flow result from stage two, and the sum of mouth flows from stage one plus the Hardig and the Maskerchugg. Figure 1-1 shows the results, for the period from 2001-2019.

The median daily flow during June through September each year from 1990 to 2017 (not through 2019, as explained below) was computed and used to determine its 66.7th and 33.3rd percentiles; these are the thresholds (Table 1-3) applied to designate years as wet, intermediate, or dry.

The years 2001-2019, corresponding to when records are available from the Narragansett Bay Fixed-Site Monitoring Network, are the primary focus of the analysis in this report. For each individual year 2001-2019, if the median June to September daily flow is higher than $52.43 \text{ m}^3 \text{ s}^{-1}$ it is designated “wet”, if it is lower than $34.53 \text{ m}^3 \text{ s}^{-1}$ it is designated “dry”, and if it is between the two thresholds it is designated “intermediate” (Table 1-3; same as in Codiga 2020a). Results are shown in Figure 1-2 and Table 1-4.

The threshold values ($52.43 \text{ m}^3 \text{ s}^{-1}$ and $34.53 \text{ m}^3 \text{ s}^{-1}$) were computed using the year range from 1990 through 2017 (Codiga 2020a). The start of the range, 1990, was chosen so the range spans at least a few cycles of multiyear variability, while also not being influenced by conditions prior to 1990, which are less representative of the period since 2001 due to decadal variability (Kellogg, 2018). Years earlier than 1990 were also not included because their records are not available for all of the 8 gauges used (Table 1-1), and the records that are available include more substantial gaps. For the end of the range, 2017 was used rather than 2019, for two reasons. The first reason is that wet/intermediate/dry designations were previously assigned to 2001-2017 (Codiga, 2020a) based on these thresholds ($52.43 \text{ m}^3 \text{ s}^{-1}$ and $34.53 \text{ m}^3 \text{ s}^{-1}$) as computed using 1990-2017. Computing new thresholds using 2001-2019 could lead to confusion due to some individual years having different designations in this report than in the earlier report. The second reason is that the range 1990-2019 only includes 2 additional years compared to the 28-year period 1990-2017, so the thresholds based on using 1990-2019 are only different by small amounts ($53.07 \text{ m}^3 \text{ s}^{-1}$ and $35.56 \text{ m}^3 \text{ s}^{-1}$). An appropriate time to compute and use new thresholds could be after there are perhaps 5 or more additional years available more recent than 2017, to make up a more substantial fraction by which the 28 year period currently being used is extended.

It is important to note that for an individual year, the designation of wet, intermediate or dry will be assigned even though the flow conditions may be very near the boundary between two of these classifications. A prominent example is 2017, which is at the very high end of the intermediate range, with median of daily June to September flow just lower than the $52.43 \text{ m}^3 \text{ s}^{-1}$ threshold defining a wet year. In fact, exploration of sensitivity to use of the May to September period (instead of the June to September period), with all other aspects of the method unchanged, indicated that 2017 would be designated wet in that case (not shown). In this context, while the ability to classify years as wet, intermediate, or dry is useful and the method presented here is defined in a clear and justifiable way, it should nonetheless be borne in mind that distinctions between wet and intermediate, or intermediate and dry, can be minor so use of the numerical values (Figure 1-2) is more informative.

In plots for Tasks 4 and 5 below, the wet/intermediate/dry years are denoted as light, medium, and dark gray bars in the backgrounds of figures. Versions of the figures using white, light gray, and dark gray were made (not shown) but it was decided they were not as clear.

Winds. The 10-m elevation wind from the North American Regional Reanalysis (“NARR”; Mesinger et al., 2006), a meteorological model product based on assimilation of observed atmospheric conditions, is used because it has no missing-data gaps, in contrast to local wind gauges. Its grid over Rhode Island has ~32 km resolution, which is coarse relative to the bay, so it does not capture details of small-scale local wind patterns. This trade-off is considered acceptable to gain the benefits of gap-free records for the entire period. The years 1999 through 2019 from the over-land NARR gridpoint nearest to Narragansett Bay, just north of Greenwich Bay but representative of the region, are used. They were retrieved remotely from the NOAA server where large files containing data from all gridpoints are provided; the small desired subset (from one grid point) of these files was extracted using built-in Matlab functionality for data access protocols. They are instantaneous winds, with a value each 3 hours. The wind speed and wind components toward a range of cardinal directions were computed. All quantities were low-pass filtered (25-hr halfwidth, triangle-weight) and the 12-hour subsampled low-passed results computed.

Tidal range. Tidal ranges are computed from NOAA CO-OPS (Center for Operational Oceanographic Products and Services) tidal predictions, available via web services. Hourly predictions for the Newport station (<https://tidesandcurrents.noaa.gov/noaatidepredictions.html?id=8452660>), which is representative of bay-wide tidal conditions, are obtained and used to compute the difference between successive high and low tides. The daily tidal range is computed as the mean of all such differences during each day, typically two or one. The tidal range cubed, a measure of mixing energy, is also computed. Values are interpolated to a 12 hour grid, to match the low-passed sub-sampled winds.

Sea Level. Non-tidal sea level observations from Providence and Newport, and their difference, are computed to enable inclusion of weather-band variability in the analyses. Raw hourly sea level observations (including both tidal and non-tidal components) were obtained, along with atmospheric pressure data in order to do the inverse barometer correction, from NOAA servers for Providence (<https://tidesandcurrents.noaa.gov/stationhome.html?id=8454000>) and Newport (<https://tidesandcurrents.noaa.gov/stationhome.html?id=8452660>). Atmospheric pressure is used to correct sea level for the inverse barometer effect. The hourly water level and inverse-barometer adjusted hourly water level at each station, and their differences between Providence and Newport, are computed. Where data gaps precluded the inverse barometer correction unadjusted values were used. All quantities are low-pass filtered (25-hr halfwidth triangle-weight) to isolate the non-tidal component, and subsampled to 12-hour resolution to match winds and tidal range. Substantial gaps were present in the dataset during 2018 and 2019.

See page 118 for information about supporting code and data files, and how to use them.

1.3 Results

Products developed here are useful as indicators of physical processes active in the bay. They are available for use in support of analyses in later sections of this report and by other researchers.

A summary of results for daily river flow 2001-2019 is shown in Figure 1-1. The purpose of this figure is not to enable identification of specific features of individual curves from each other, which is recognized to be difficult due to the large number of sources and years included, but rather to provide a general sense of the relative magnitudes of the sources and how they vary through the 19-year period.

The median bay-wide daily flow during the June to September period of each year is shown in Figure 1-2, annotated by corresponding designations (also in Table 1-4) as wet, intermediate, or dry. The year

2018 was intermediate and 2019 was wet. Among the 6 years that are designated wet, 2019 had the least runoff, a substantial amount less than the next-higher other wet year (2013).

Further analysis of these products is included in Task 6 below.

Table 1-1. Gauges used for river flow observations. Same as in Codiga (2020a).

River used in analysis	River used for regression and gap-filling
Taunton (Bridgewater 01108000)	Threemile (North Dighton 01109060) $r^2 = 0.940$
Blackstone (Pawtucket 01113895)	Blackstone (Woonsocket 01112500) $r^2 = 0.993$
Pawtuxet (Cranston 01116500)	
Ten Mile (East Providence 01109403)	
Woonasquatucket (Centerdale 01114500)	
Moshassuck (Providence 01114000)	
Palmer (Reed St, South Rehoboth 01109220)	Ten Mile (East Providence 01109403) $r^2 = 0.968$
Hunt (East Greenwich 01117000)	

Table 1-2. Scale-up factors based on Table 7 of Ries (1990). The first 8 rows are the scale-up factors from the gauge (see left column of Table 1 above) to the mouth of each river. The last row is the scale-up factor from the sum of the 8 river mouth flows to the basin-wide flow. Same as in Codiga (2020a).

	Jan	Feb	Mar	Apr	May	Jun	Jul	Aug	Sep	Oct	Nov	Dec
Taunton	2.29	2.20	2.20	2.23	2.23	2.49	2.03	2.17	1.91	2.27	2.13	2.29
Blackstone	1.07	1.07	1.07	1.07	1.07	1.07	1.07	1.07	1.07	1.07	1.07	1.07
Pawtuxet	1.21	1.21	1.19	1.19	1.20	1.20	1.20	1.21	1.20	1.21	1.17	1.20
Ten Mile	1.02	1.02	1.02	1.03	1.03	1.03	1.03	1.03	1.03	1.03	1.02	1.02
Woonasquatucket	1.37	1.36	1.36	1.36	1.36	1.36	1.36	1.36	1.36	1.36	1.37	1.36
Moshassuck	1.47	1.45	1.48	1.50	1.49	1.53	1.59	1.56	1.57	1.53	1.46	1.44
Palmer	1.02	1.02	1.02	1.02	1.02	1.02	1.02	1.02	1.02	1.02	1.02	1.02
Hunt	1.00	1.00	1.00	1.00	1.00	1.00	1.00	1.00	1.00	1.00	1.00	1.00
Basin-wide	1.30	1.29	1.25	1.27	1.33	1.37	1.64	1.79	1.72	1.59	1.45	1.35

Table 1-3. Threshold values, for median daily basin-wide flow between June and September based on 1990 to 2017 (not 2019; see text) conditions, to designate individual years as wet, dry, or intermediate. Same as in Codiga (2020a).

Period of year	"Wet" above (66.7 th percentile):	"Dry" below (33.3 rd percentile):
June to September	52.43 m ³ s ⁻¹	34.53 m ³ s ⁻¹

Table 1-4. Designation of bay-wide Jun-Sep river flow conditions each year from 2001 to 2019 as "wet", "intermediate", or "dry", using the criterion in Table 1-3.

Wet	2003, 2006, 2009, 2011, 2013, 2019
Intermediate	2001, 2004, 2005, 2007, 2008, 2012, 2017, 2018
Dry	2002, 2010, 2014, 2015, 2016

Figure 1-1. Daily river flows 2001-2019, 10 rivers and ungauged area: basin-wide flow. Inset shows 2016 only, as example of a single

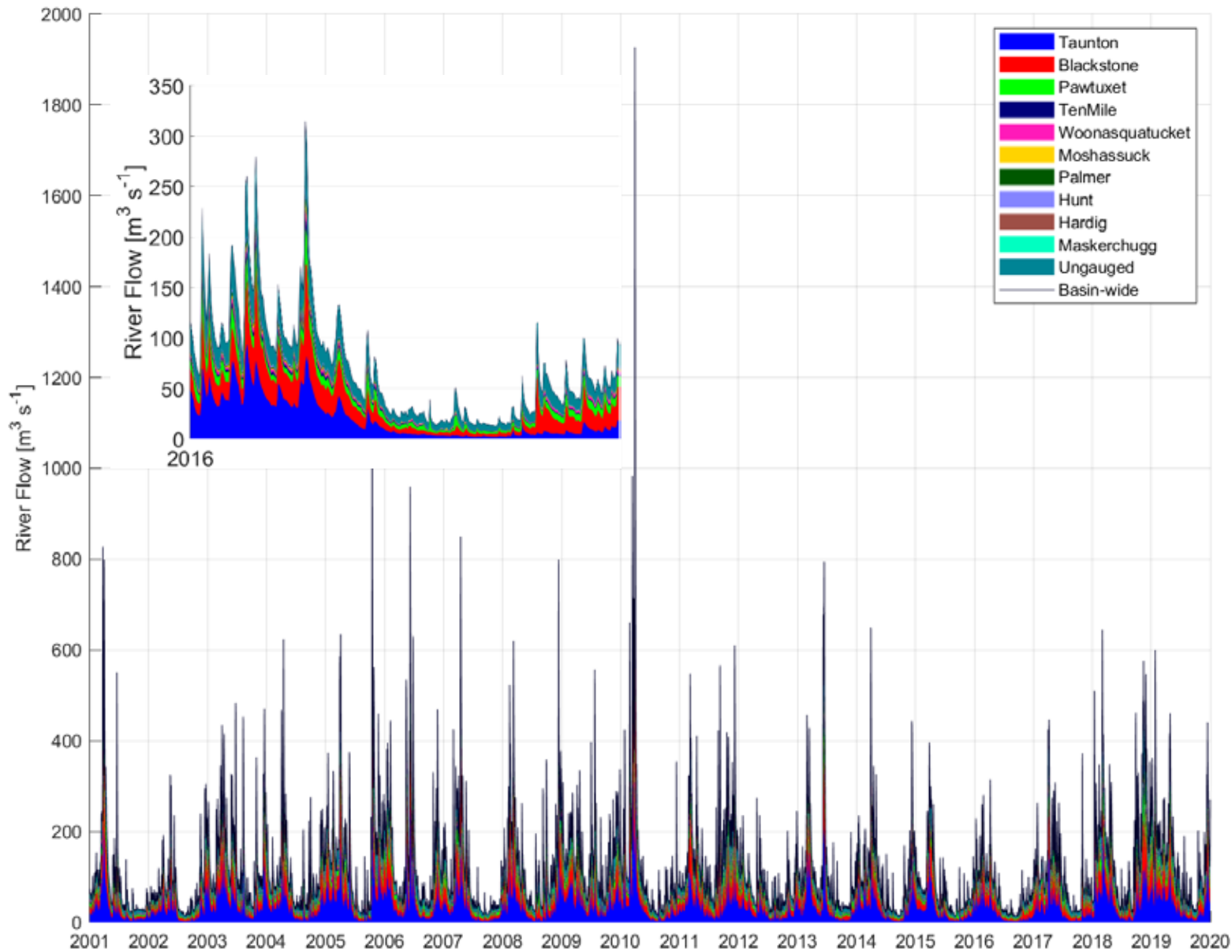
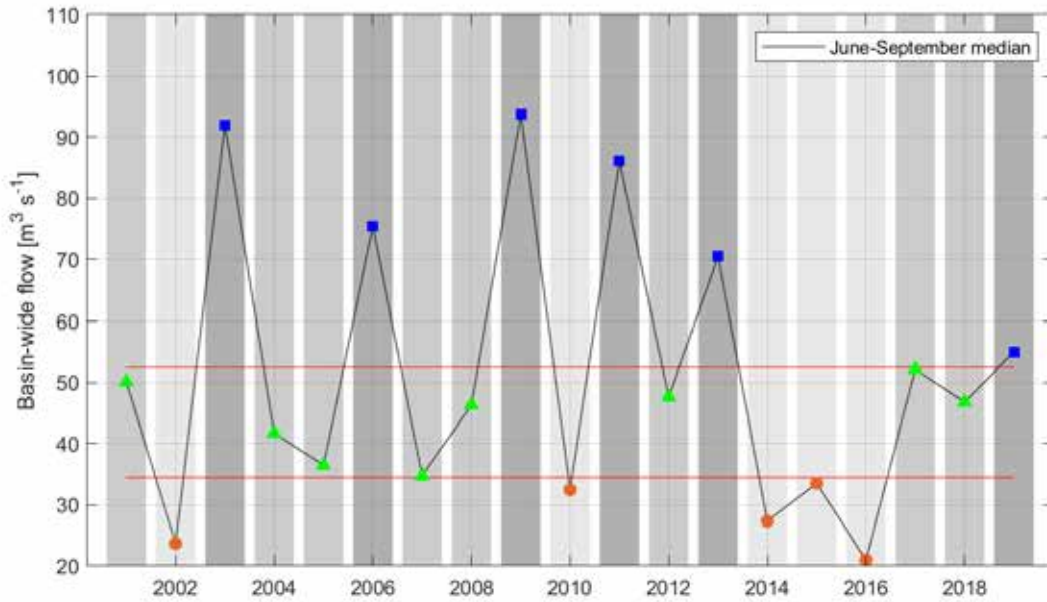


Figure 1-2. Median daily basin-wide flow, June to September (black line), 2001-2019.

Thresholds (red lines) and resulting designations of wet (blue squares), intermediate (green triangles) and dry (orange circles) years as in Table 1-4. The gray background bars (darkest wet, medium intermediate, lightest dry) demonstrate how wet, intermediate, and dry flow conditions are indicated on plots of other quantities in other sections of this report.



Task 2 Nitrogen Loads

2.1 Scope

The time series of daily bay-wide total nitrogen (TN) load, partitioned across 18 wastewater treatment facility (WWTF) and watershed sources, were generated previously (Codiga 2020b) for years 2001-2017; here the years 2018-2019 are produced and appended.

2.2 Methods

Measurements of nutrient concentration and flow rates were obtained from the Rhode Island Department of Environmental Management (RIDEM), the Narragansett Bay Commission (NBC), and the Fall River treatment facility.

The total load to the bay is taken to consist of loads from 18 sources (Table 2-1): eleven WWTFs with direct discharge to the bay, six rivers (which include the load of any WWTFs that discharge to them upstream from the site; sites are generally near where each river enters the bay), and runoff from ungauged riparian area direct to the bay (Figure 2-1). This approach follows NBEP (2017), except for two differences: the South Kingstown and Scarborough treatment facility loads are not included here, as they discharge at locations outside the bay to the south of the Lower East Passage; and the Somerset WWTF, though not considered by the SNBIW analysis to be a plant that discharges directly to NB, is treated as one here because it discharges to the Taunton River downstream from the site where its riverine input is estimated.

The methods are as detailed in Codiga (2020b). For each source, the method used for the years leading up to and including 2017 was applied to 2018 and 2019.

For the Ten Mile river, the concentration measurements in 2018 and 2019 were from the Roger Williams Ave site whereas in earlier years they were from the Omega Pond site; the analysis used values available from either site, as the two sites are near each other and both are near the mouth of the river. In addition, for the Ten Mile river, no concentration measurements were available from Nov 2017 through Jul 2018, so this period was filled using the mean seasonal cycle based on 2013-2016.

See page 118 for information about supporting code and data files, and page 119 for how to use them.

2.3 Results

Results for the 18 sources are shown in Figure 2-2 to 2-19, in order of decreasing long-term mean load (same order as they appear in Table 2-1). Each figure has three frames: the TN load, the TN concentration, and the flow.

Plots of the 18 load timeseries all superposed (Figure 2-20 and Figure 2-21; these show the same results, but with linear and logarithmic y-axes, respectively), and of the total summed TN load of all 18 sources with the contributions of each source annotated by color (Figure 2-22), give useful summary information. The purpose of these figures is not to enable identification of specific features of individual curves from each other, which is recognized to be difficult due to the large number of sources and years

included, but rather to provide a general sense of the relative magnitudes of the sources and how they vary through the 19-year period.

Codiga (2020b) presents comparisons of these loads to prior independent estimates of annual-mean loads for selected earlier years, with a discussion of the applicability and limitations of these results.

The 2018-2019 the loads are generally similar to the prior few years leading up to and including 2017, continuing the overall patterns for seasonality and long-term trends during 2001-2017 described by Codiga (2020b). The seasonality is characterized by a sharp decrease starting in May and a sharp increase starting in November, reflecting the beginning and end of the period when regulatory compliance is required, respectively. The long-term trends include secular decreases from roughly 2008 through 2014, due to upgraded nitrogen removal at treatment facilities, primarily during the summer compliance months.

During the last few months of 2018 and the first few months of 2019 the flows, and therefore the loads, were relatively high for many of the sources compared to that time of year during the prior few years.

Further analysis is presented in Task 6 below.

Table 2-1. The eighteen sources treated in this analysis, listed in descending order based on their mean TN load from the estimated 2001-2019 timeseries.

WWTF sources (11) blue, riverine sources (6) green, ungauged runoff purple.

Source	Figure below
Taunton River and upstream WWTFs	2
Blackstone River and upstream WWTFs	3
Fields Point WWTF	4
Pawtuxet River and upstream WWTFs	5
Fall River WWTF	6
Ungauged direct runoff to bay	7
Bucklin Point WWTF	8
Ten Mile River and upstream WWTFs	9
Newport WWTF	10
Bristol WWTF	11
East Providence WWTF	12
Woonasquatucket River and upstream WWTF	13
Somerset WWTF	14
Moshassuck River	15
Warren WWTF	16
Quonset WWTF	17
East Greenwich WWTF	18
Jamestown WWTF	19

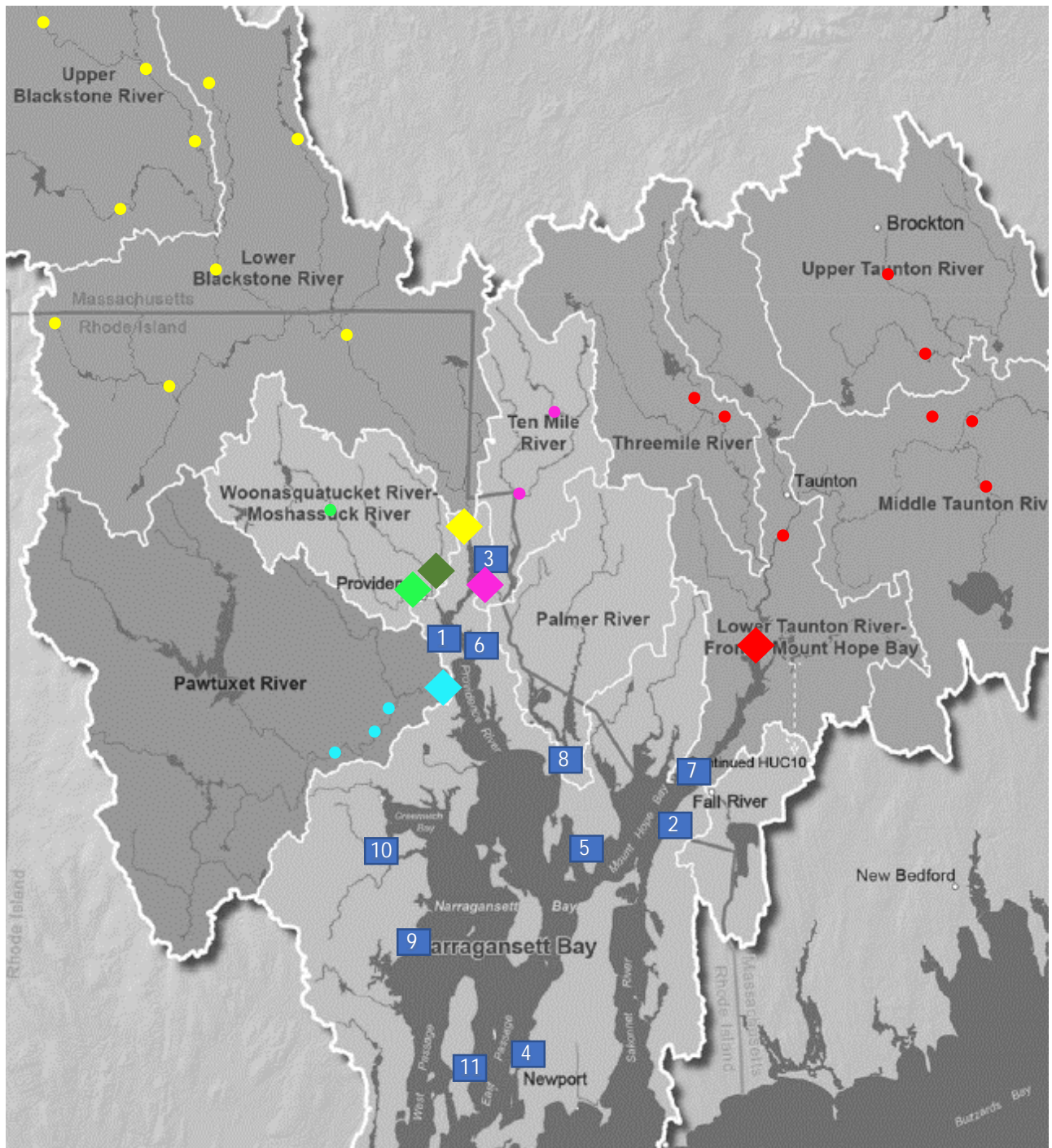


Figure 2-1. Nitrogen load sources, on background of Figure A-2 from Appendix of NBEP (2017).

Blue rectangles are treatment facilities discharging direct to bay: Fields Point (1), Fall River (2), Bucklin Point (3), Newport (4), Bristol (5), East Providence (6), Somerset (7), Warren (8), Quonset (9), East Greenwich (10), and Jamestown (11). Diamonds are river mouth sampling sites: Taunton (red), Blackstone (yellow), Pawtuxet (cyan), Ten Mile (magenta), Woonasquatucket (light green), and Moshassuck (dark green) Rivers. Colored circles are treatment facilities upstream on rivers (color-coded to diamonds). Ungauged runoff direct to the bay from riparian areas is gray land adjacent the bay (excluding riversheds of the Ten Mile, Woonasquatucket, and Moshassuck Rivers).

Figure 2-2. Taunton River and upstream WWTFs.

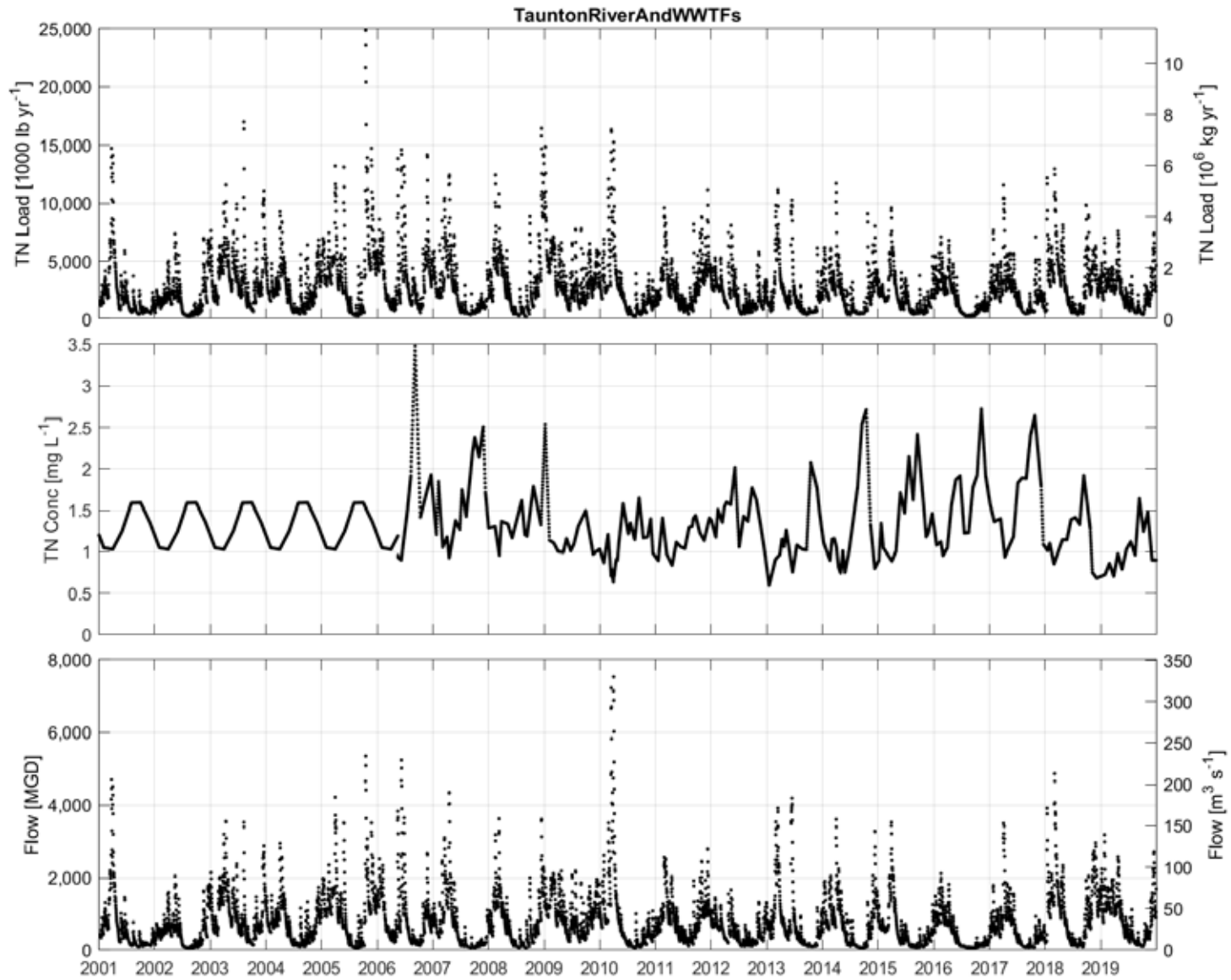


Figure 2-3. Blackstone River and upstream WWTFs.

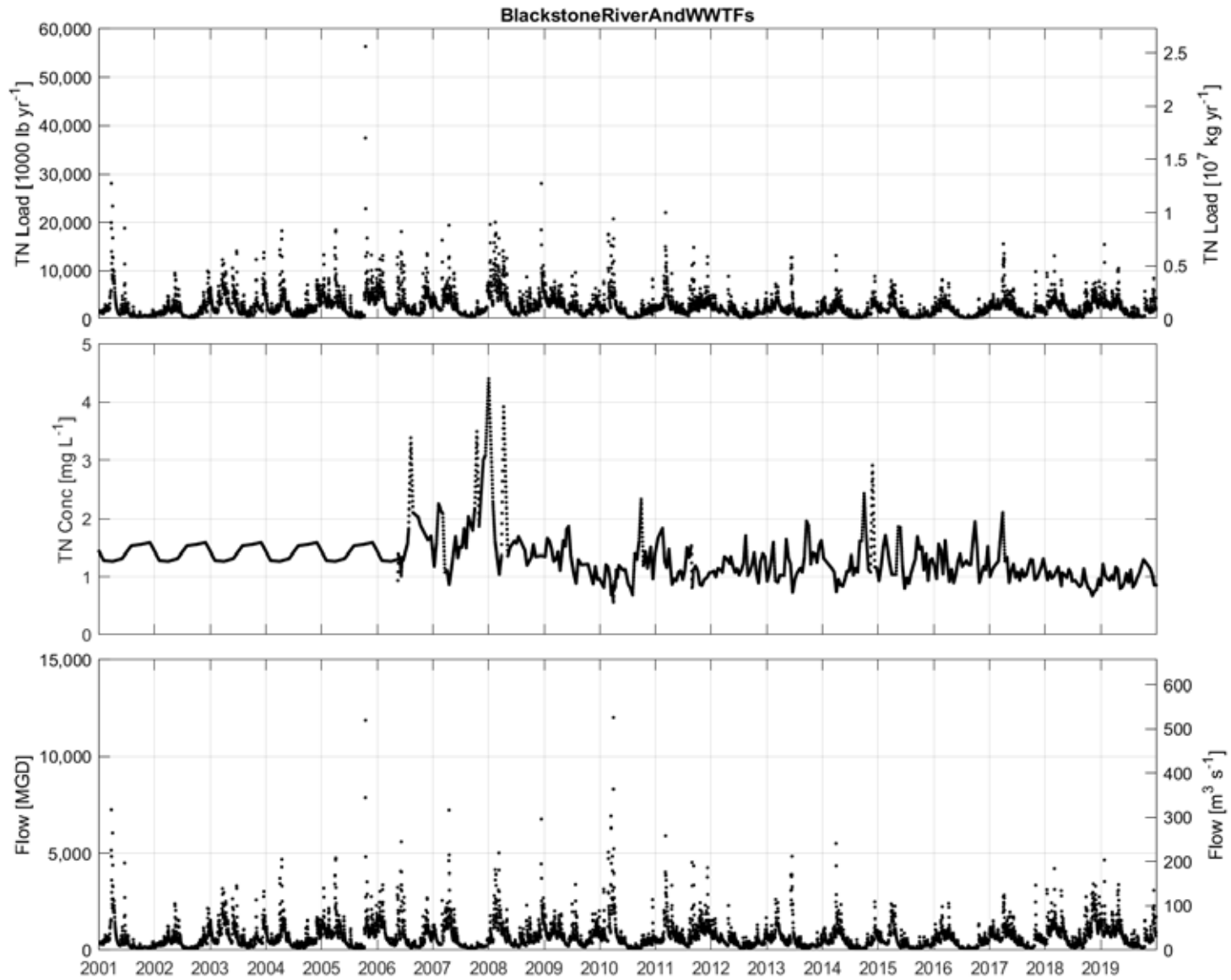


Figure 2-4. Fields Point WWTF.

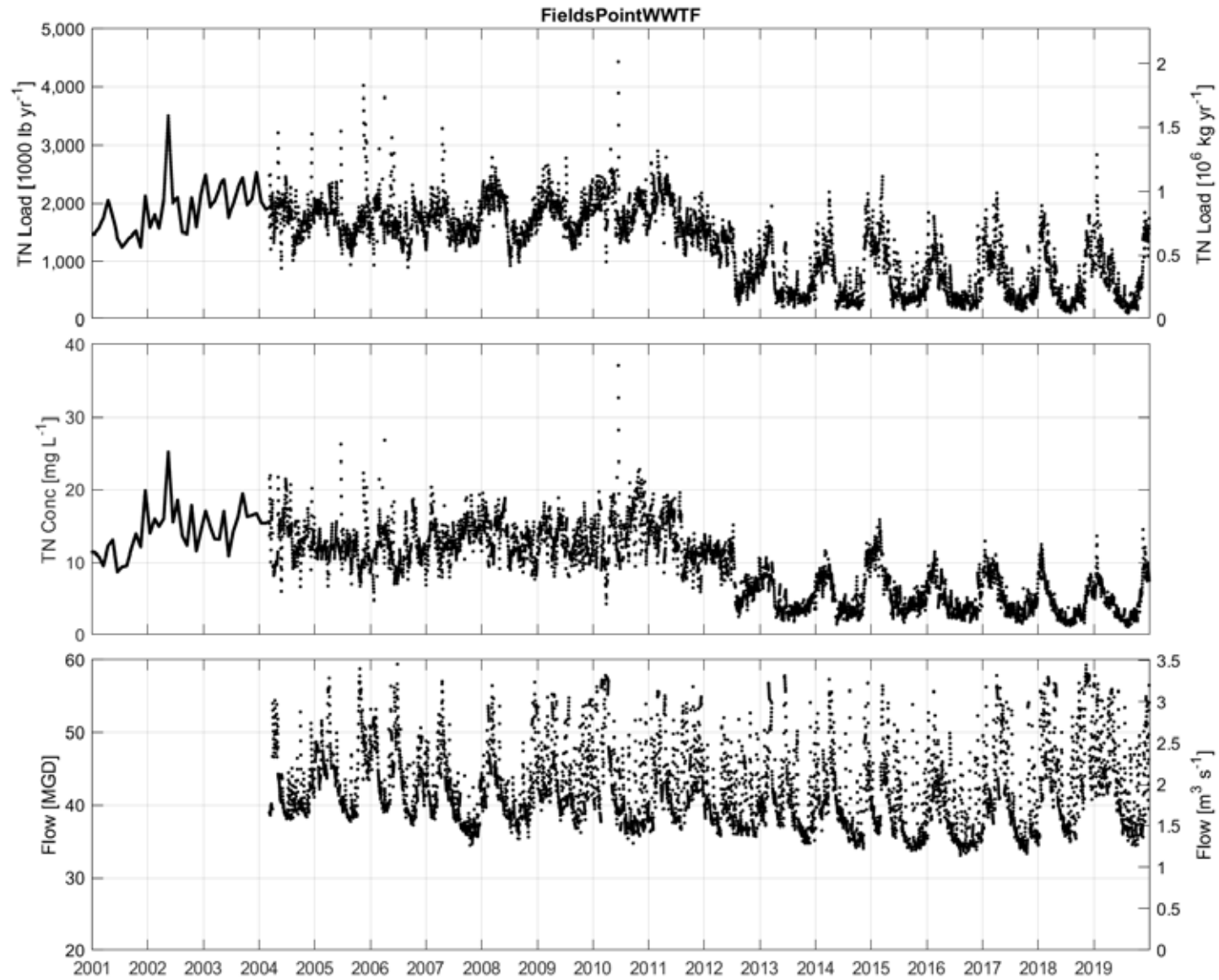


Figure 2-5. Pawtuxet River and upstream WWTFs.

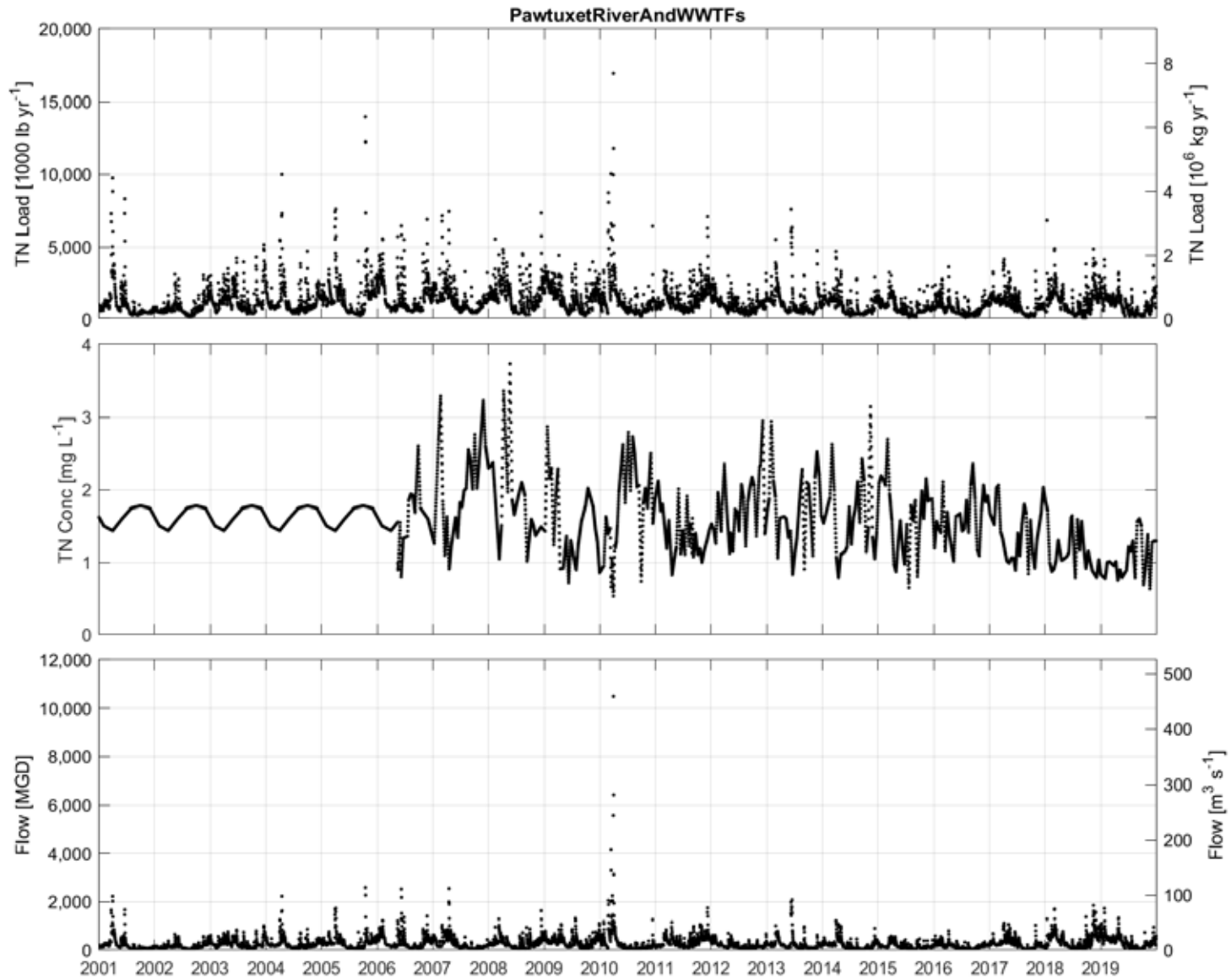


Figure 2-6. Fall River WWTF.

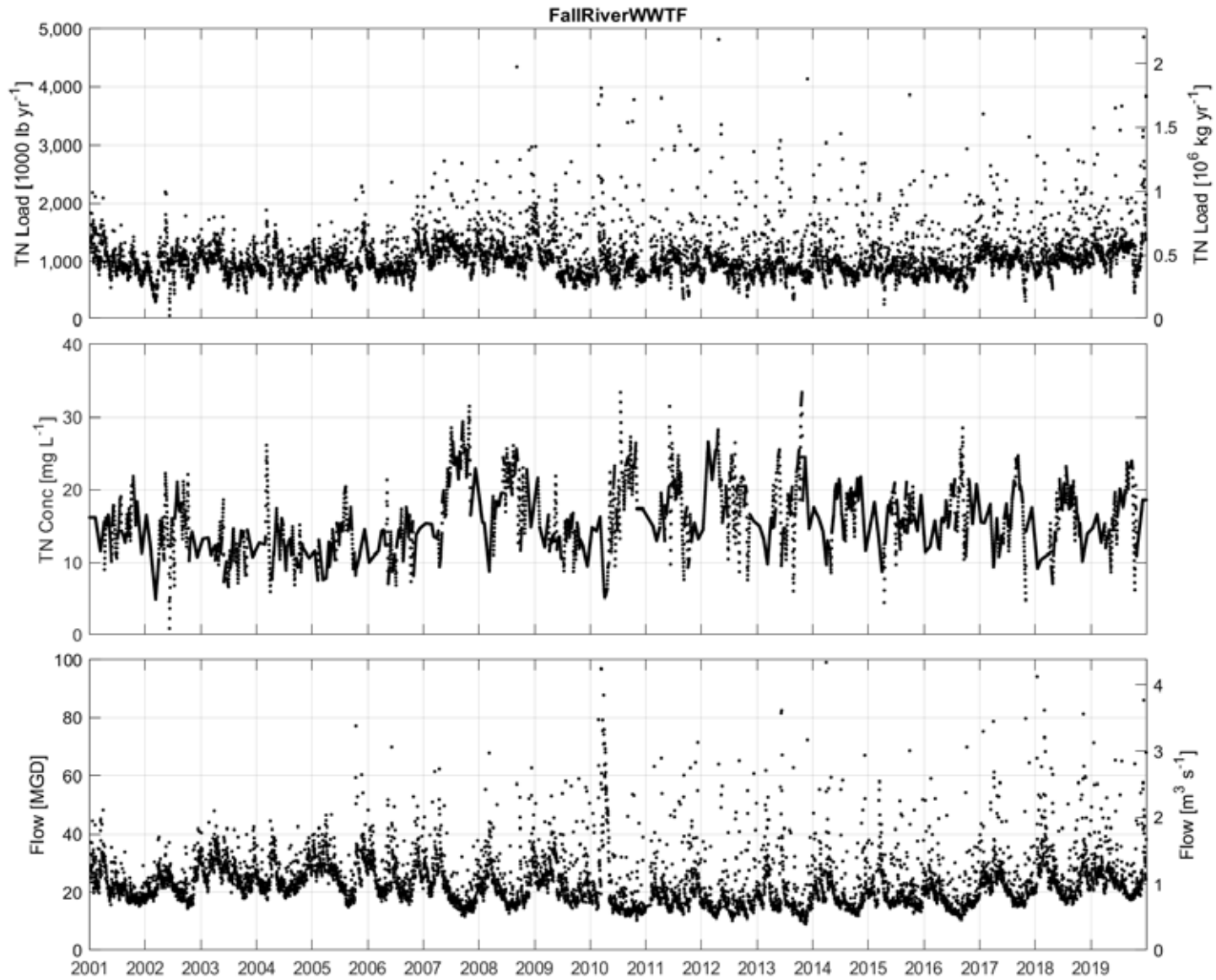


Figure 2-7. Ungauged runoff from riparian areas.

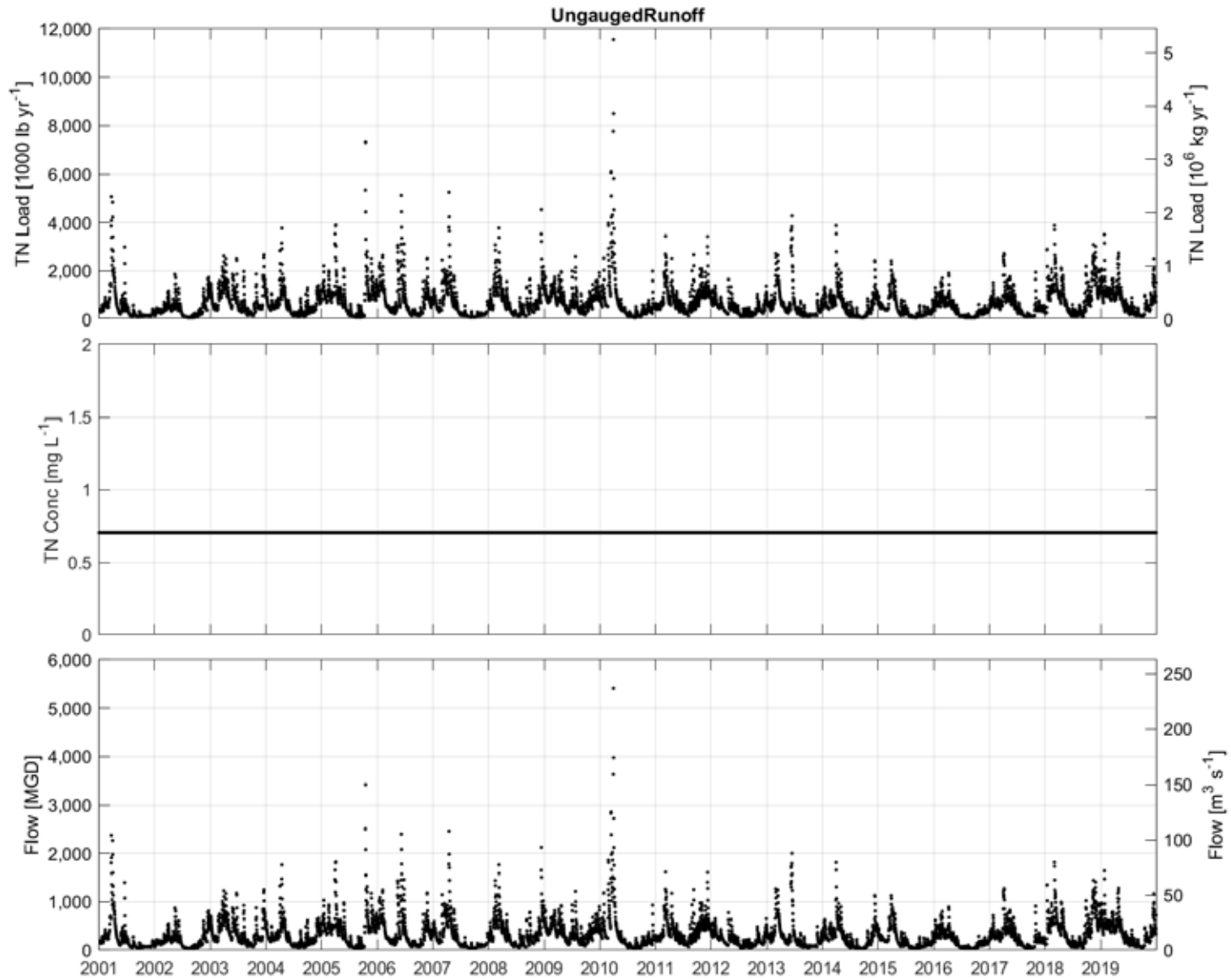


Figure 2-8. Bucklin Point WWTF.

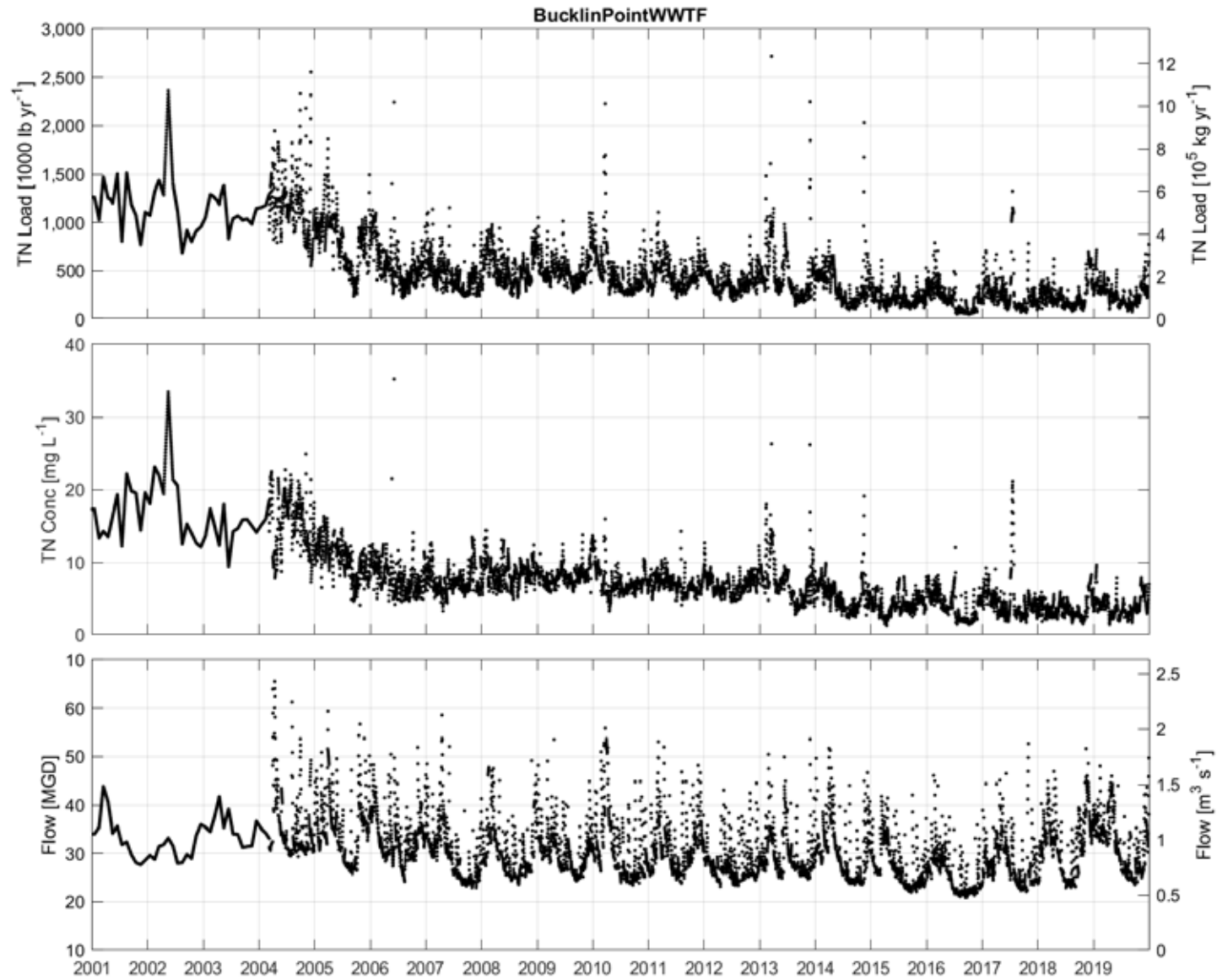


Figure 2-9. Ten Mile River and upstream WWTFs.

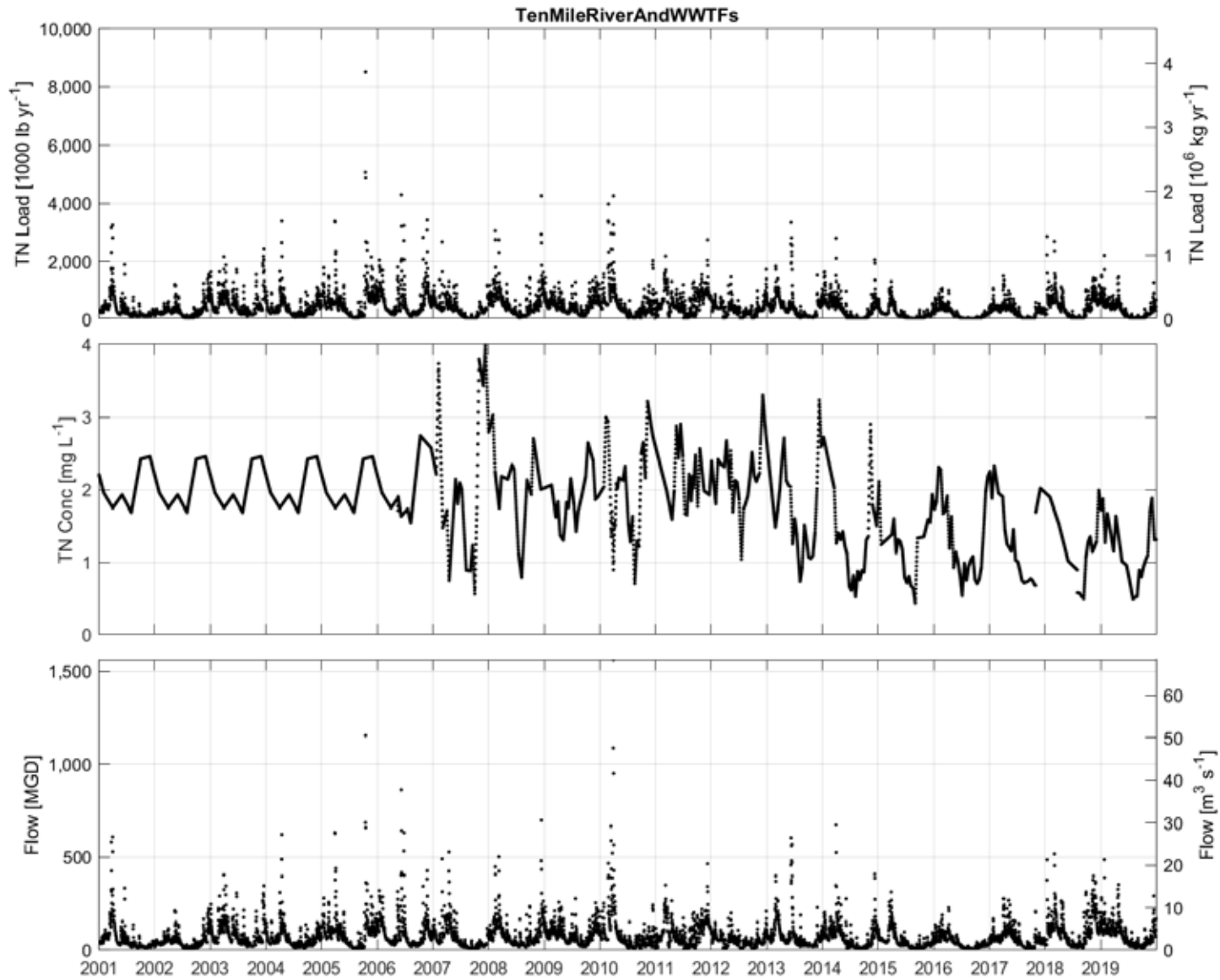


Figure 2-10. Newport WWTF.

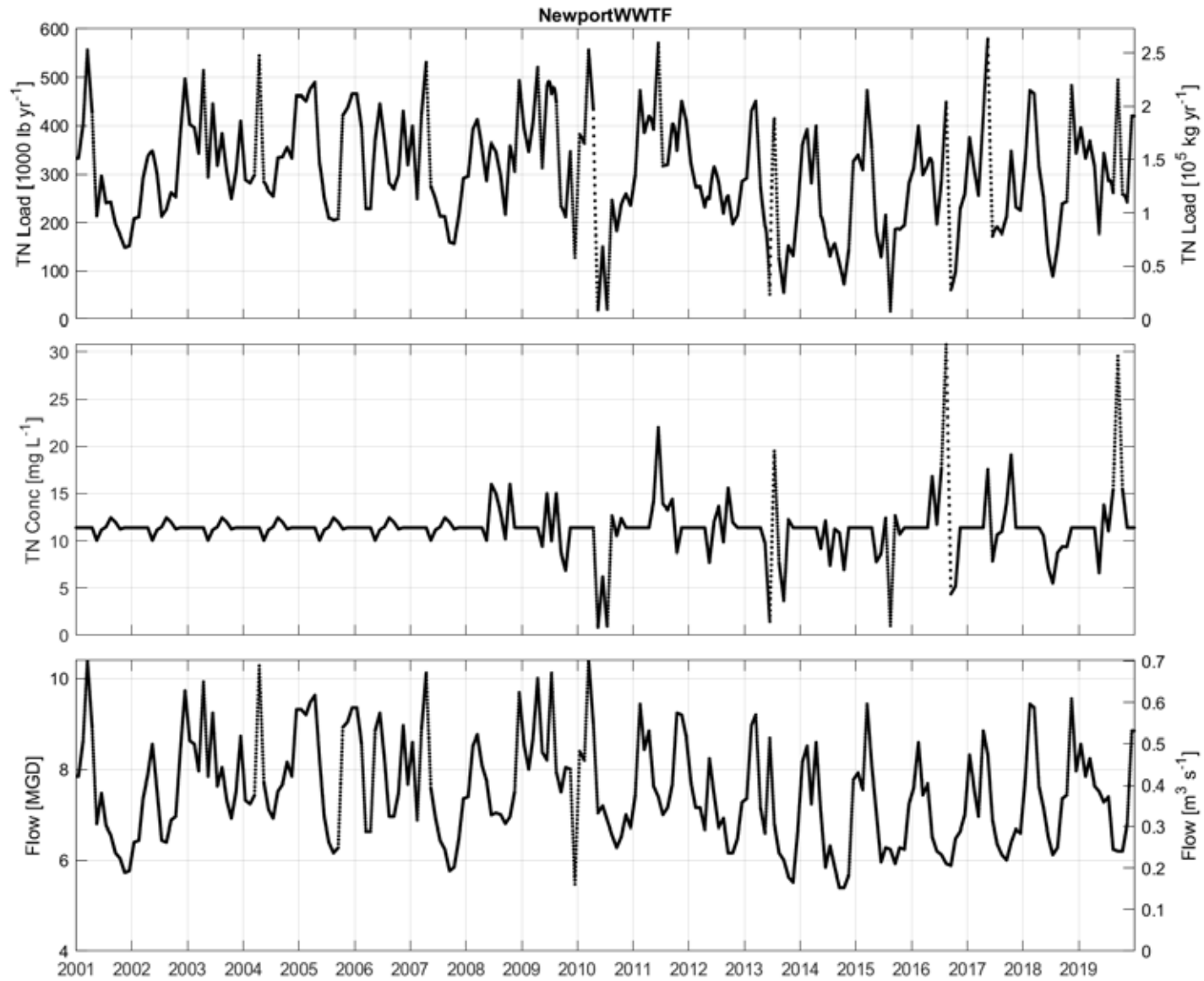


Figure 2-11. Bristol WWTF.

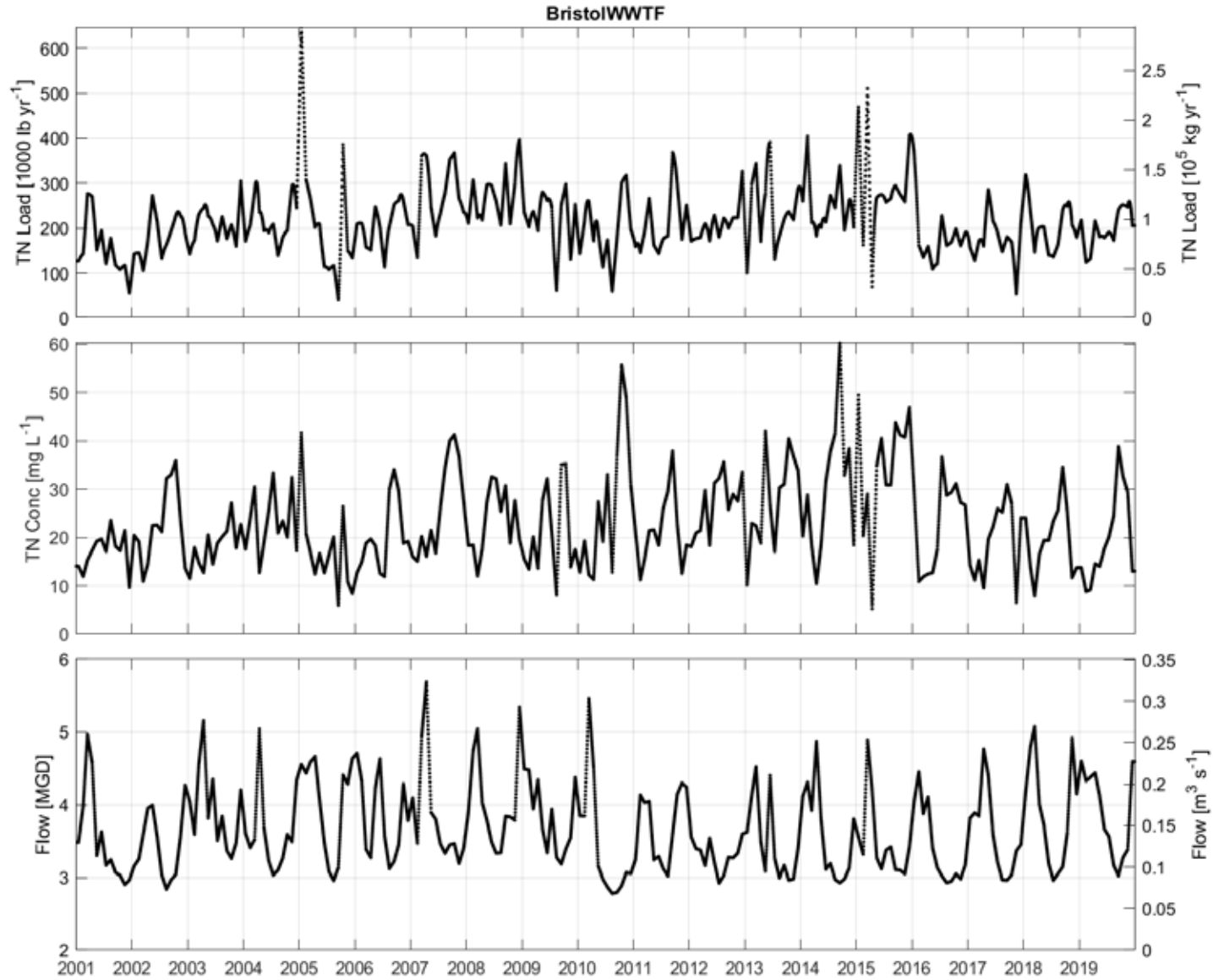


Figure 2-12. East Providence WWTF.

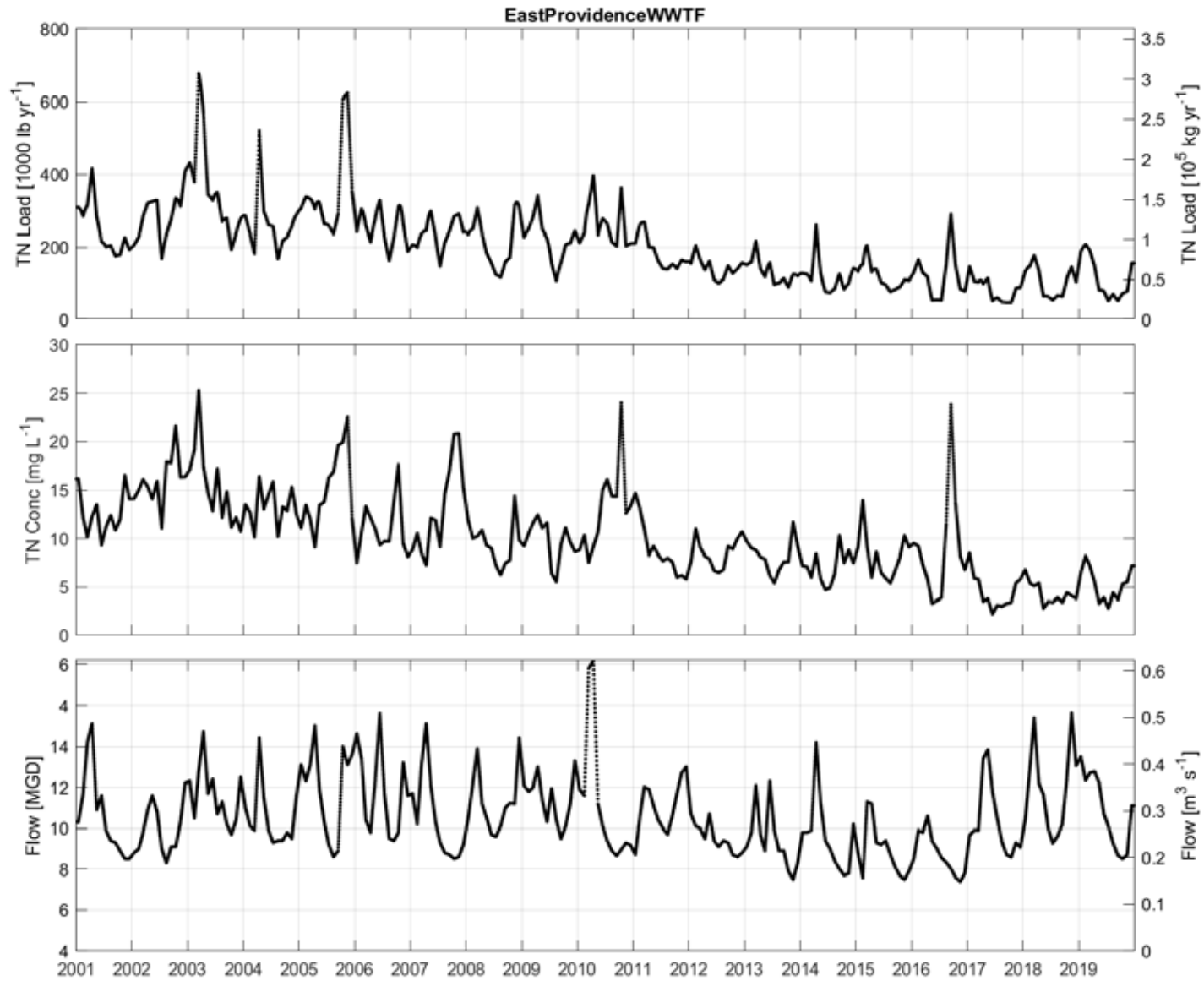


Figure 2-13. Woonasquatucket River and upstream WWTF.

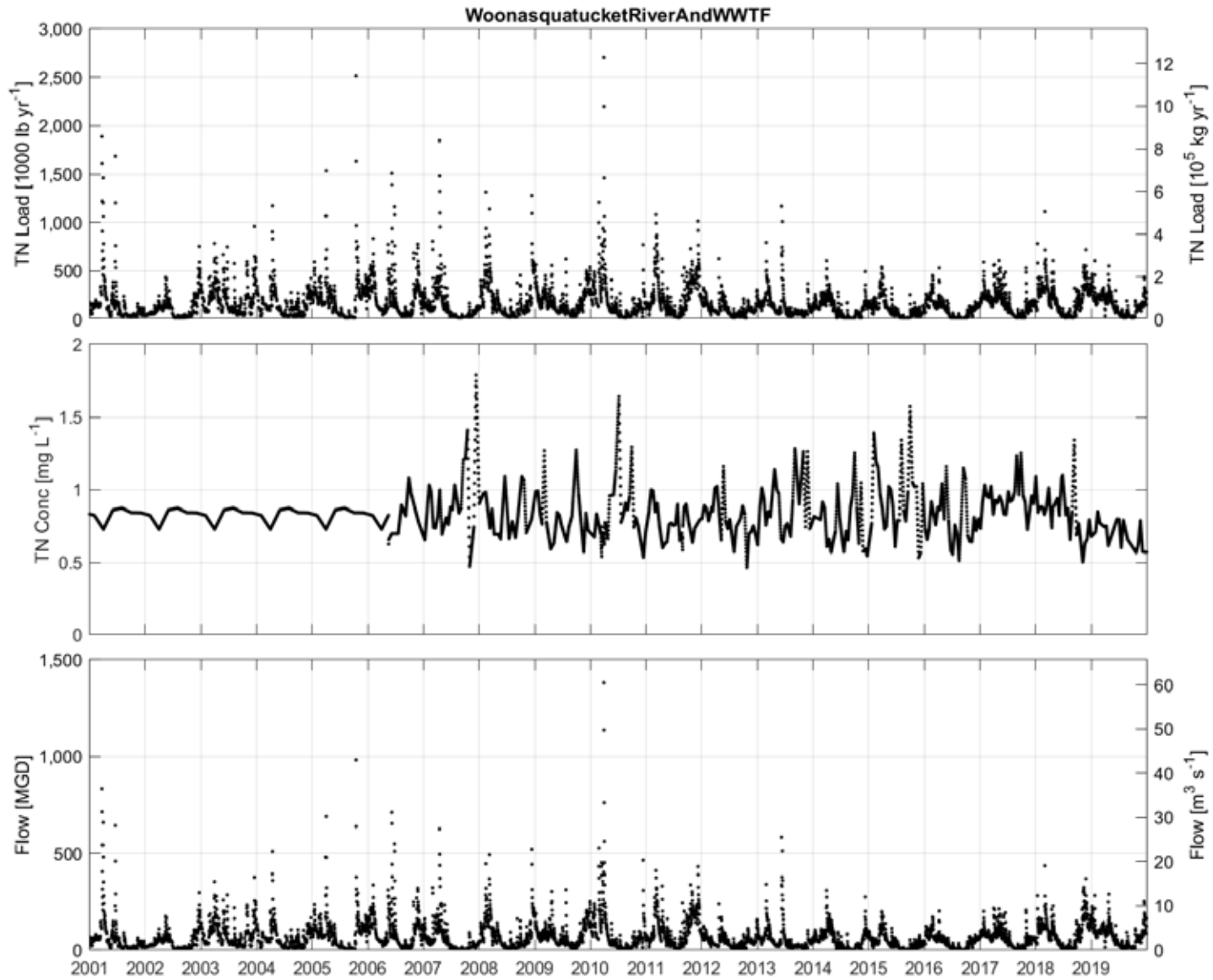


Figure 2-14. Somerset WWTF.

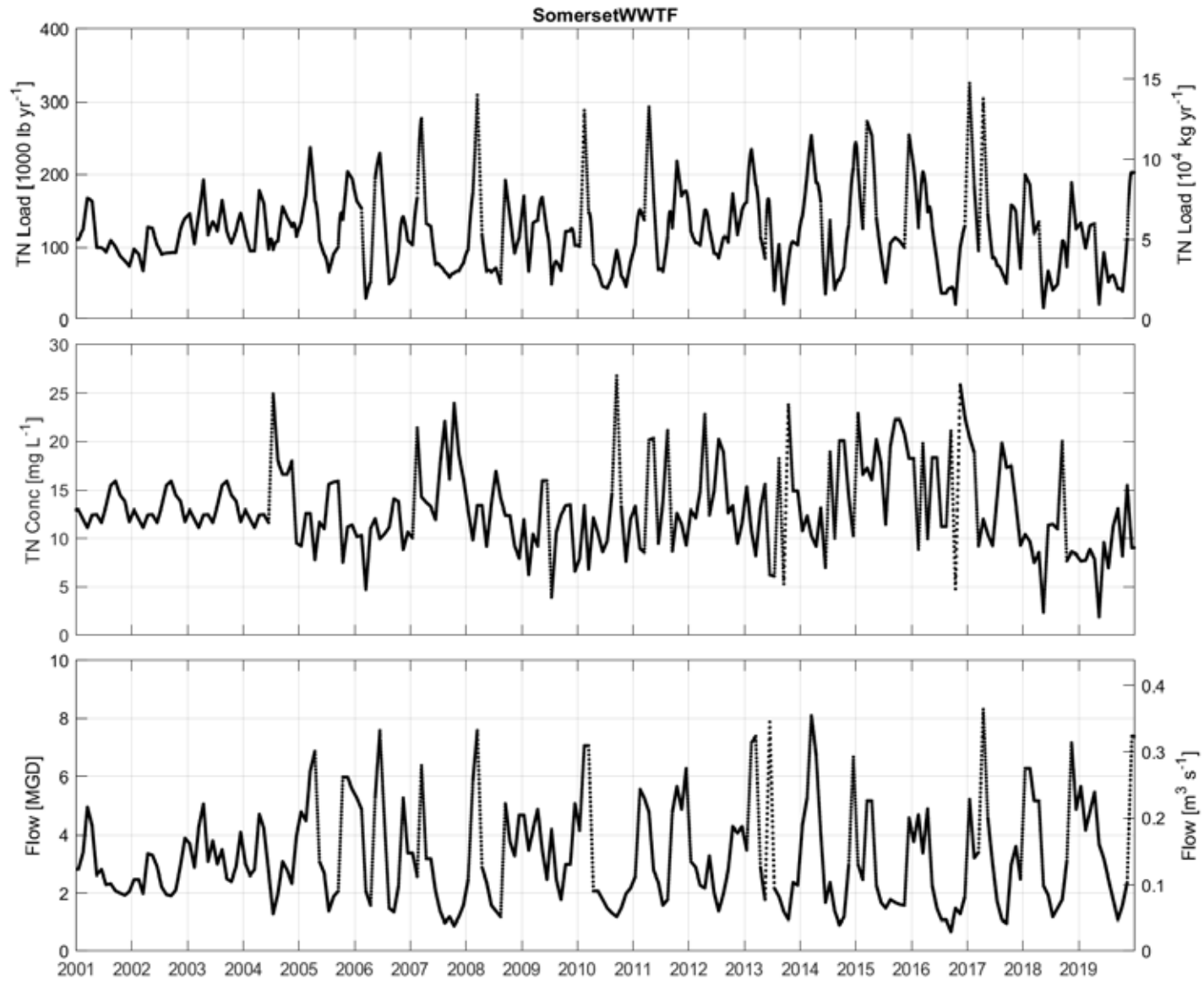


Figure 2-15. Moshassuck River.

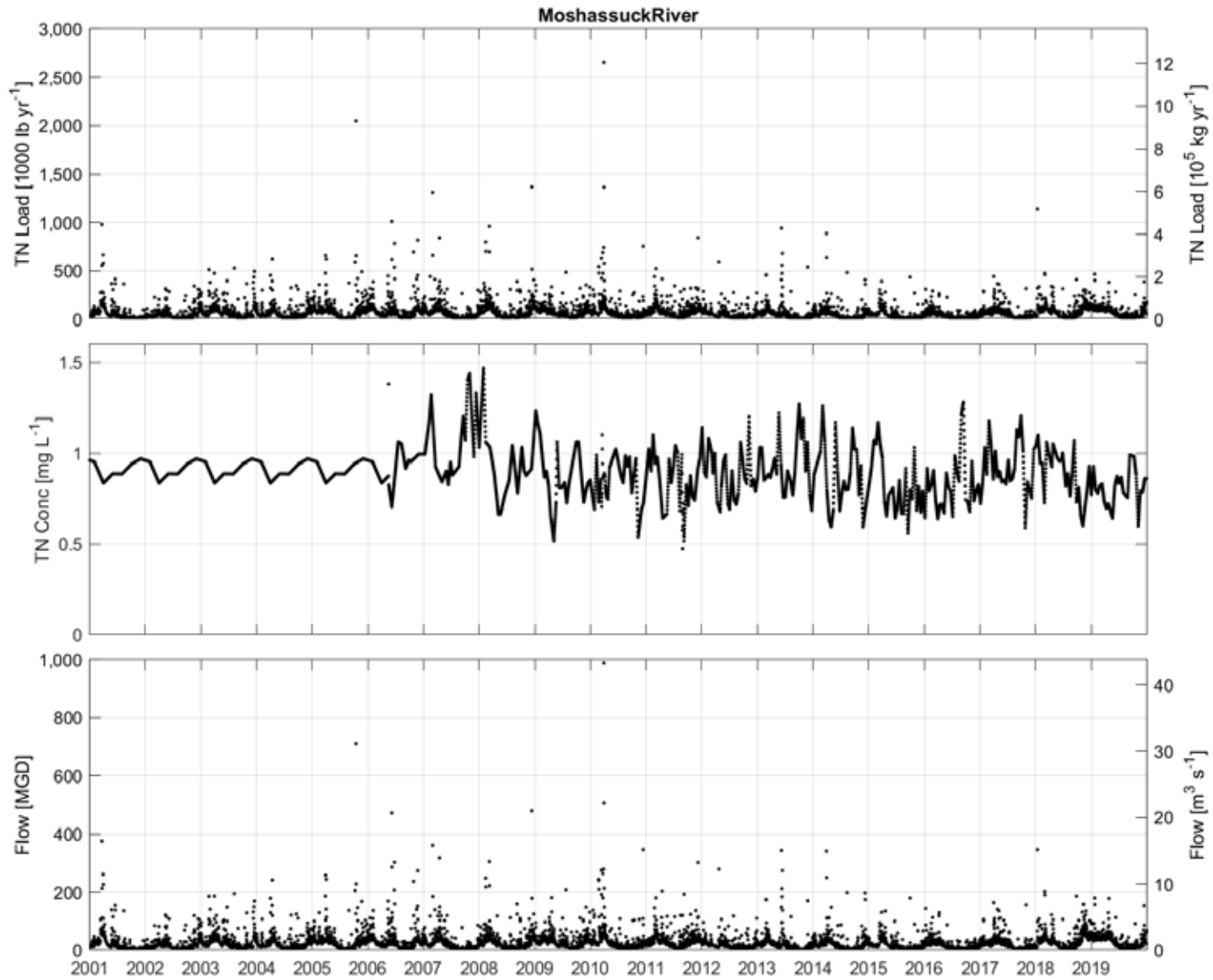


Figure 2-16. Warren WWTF.

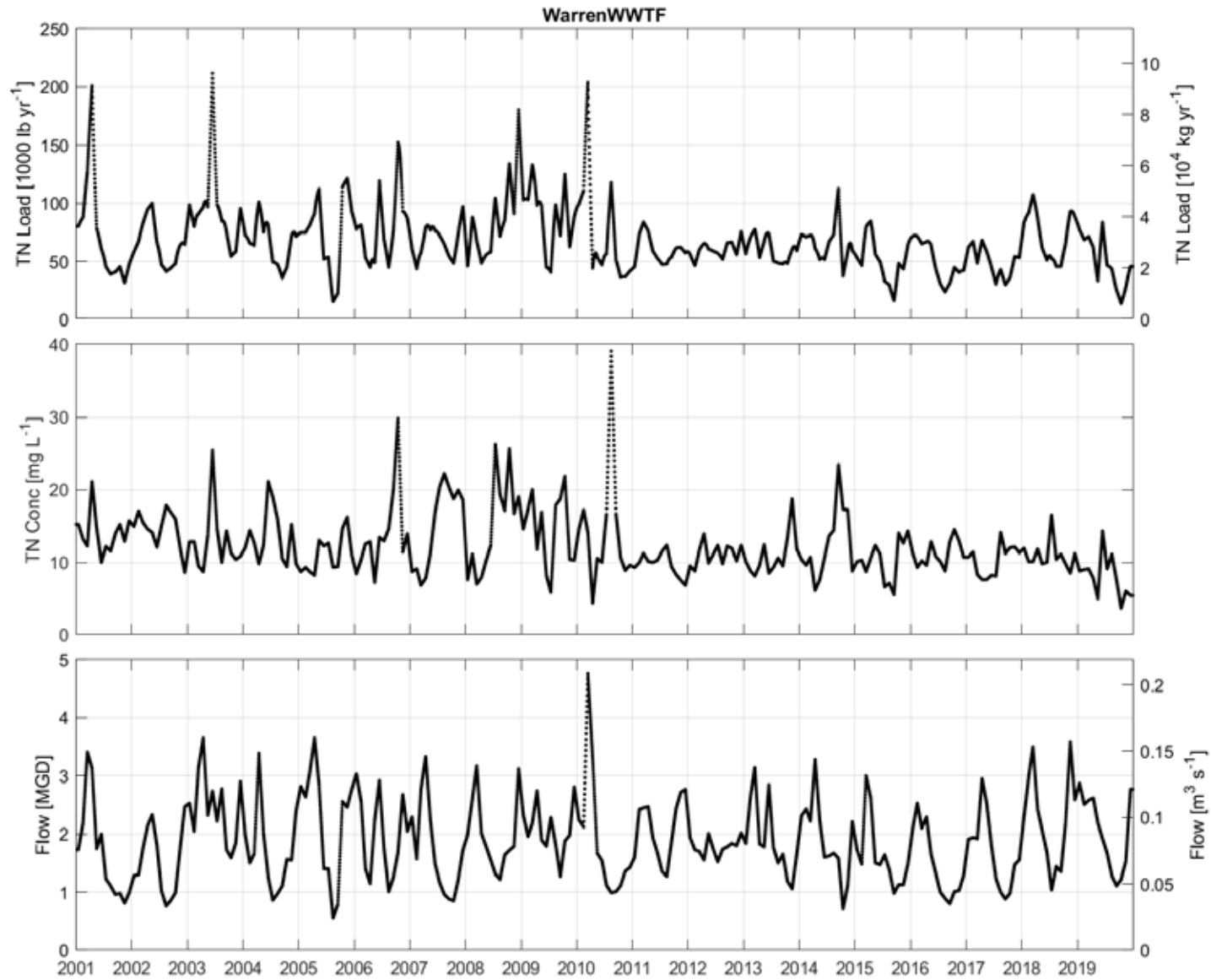


Figure 2-17. Quonset WWTF.

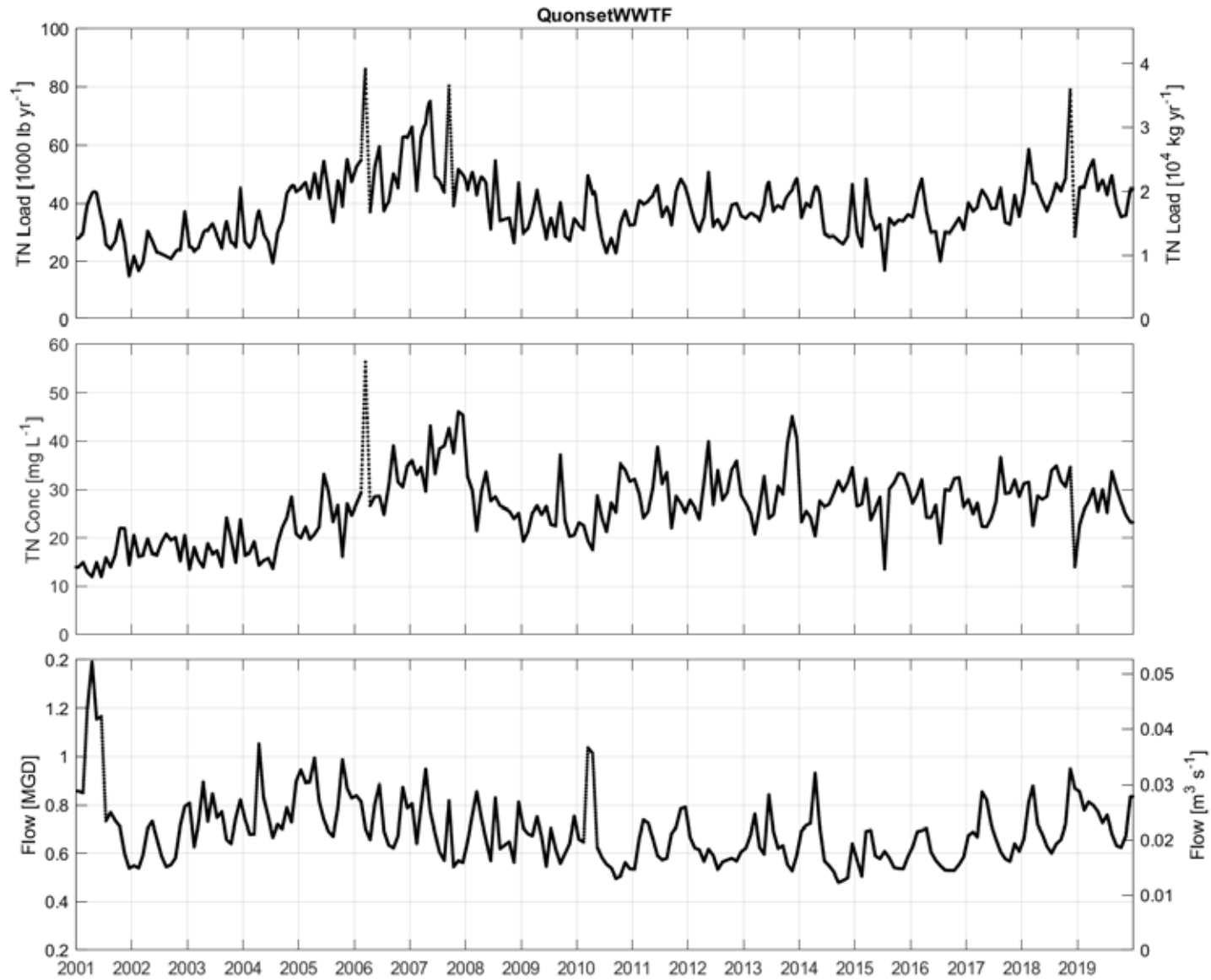


Figure 2-18. East Greenwich WWTF.

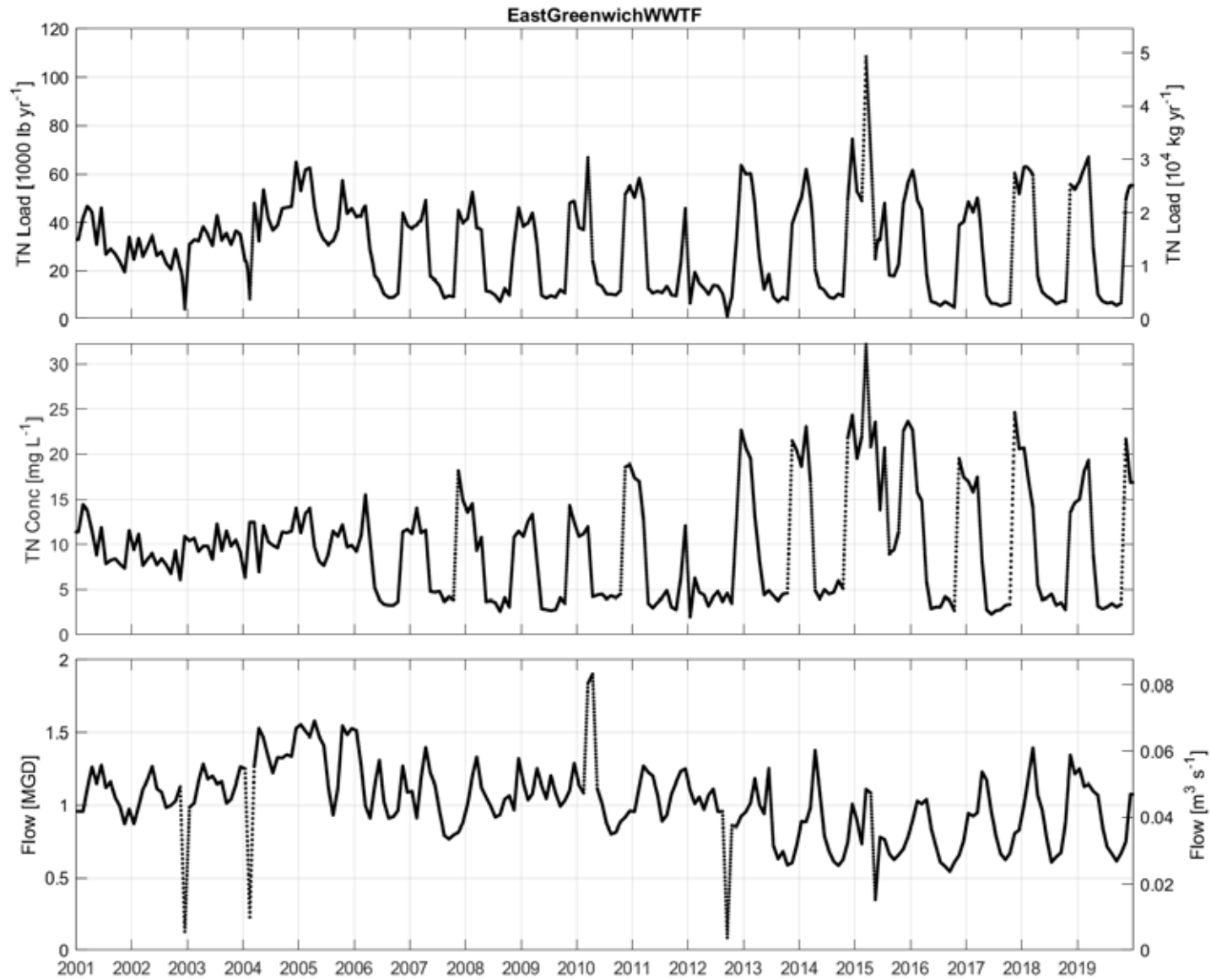


Figure 2-19. Jamestown WWTF.

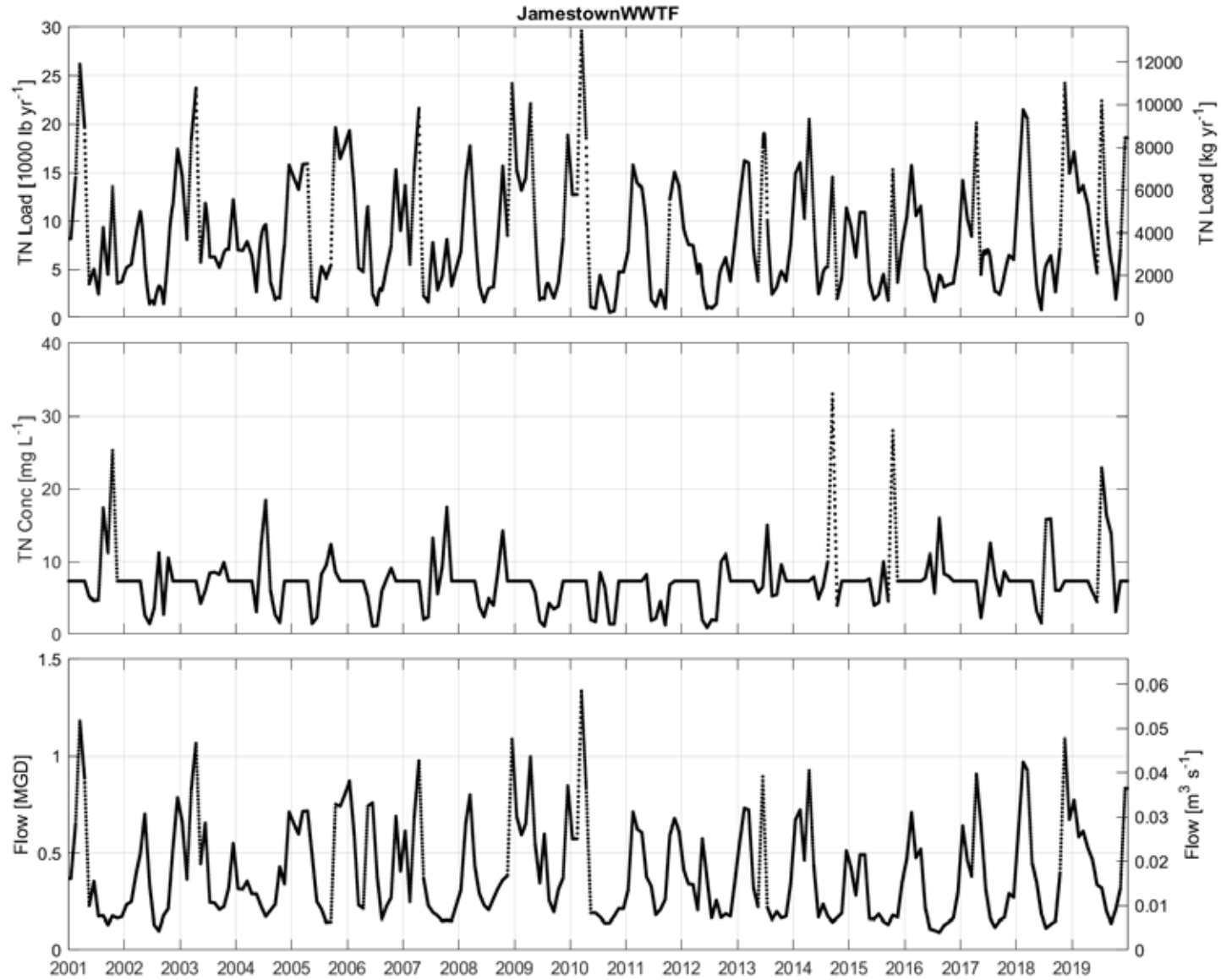


Figure 2-20. TN load time series, 18 sources superposed on same figure. Linear y-axis scale.

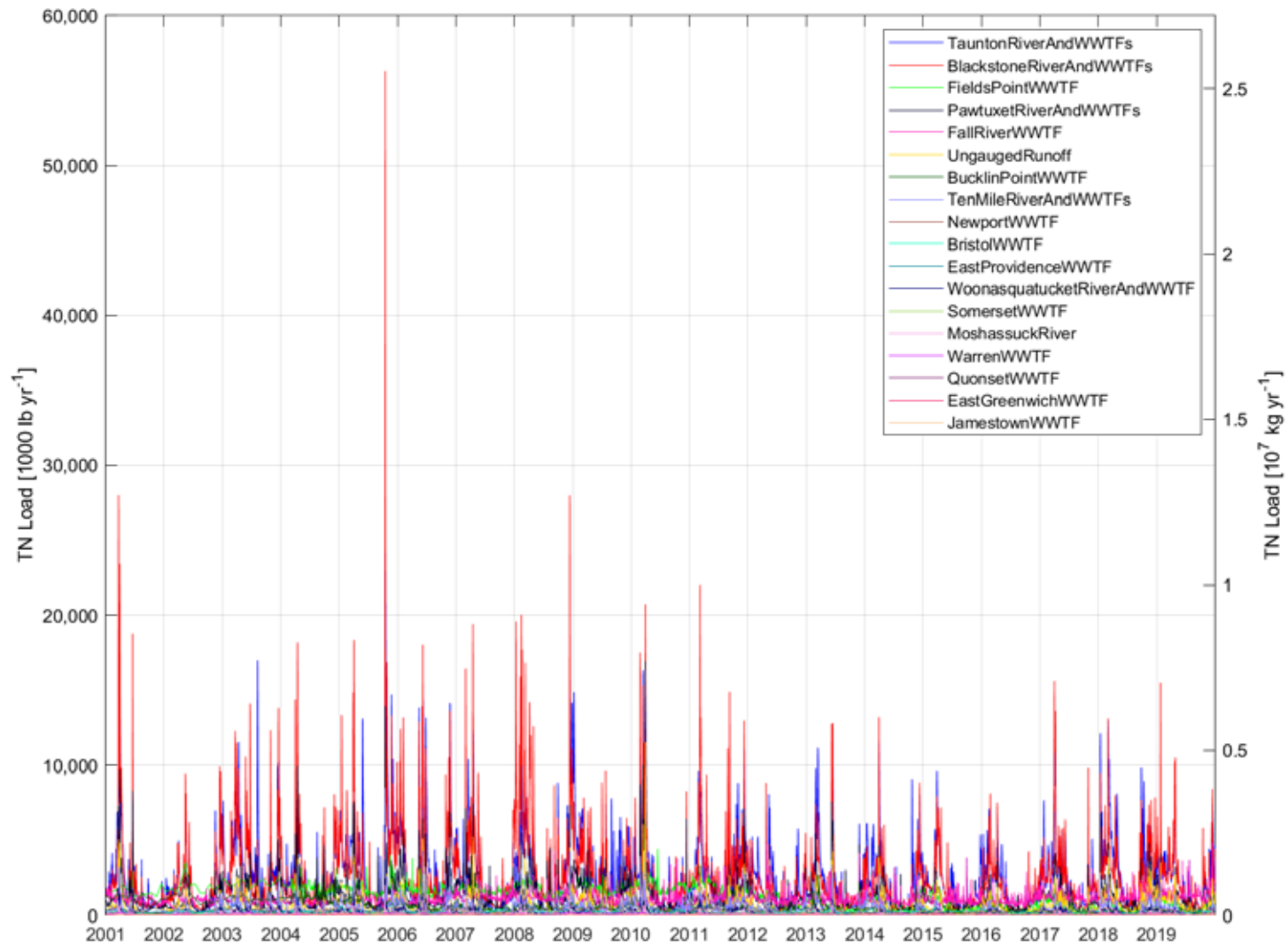


Figure 2-21. TN load time series, 18 sources superposed on same figure. Logarithmic y-axis scale (otherwise same as Figure 2-20).

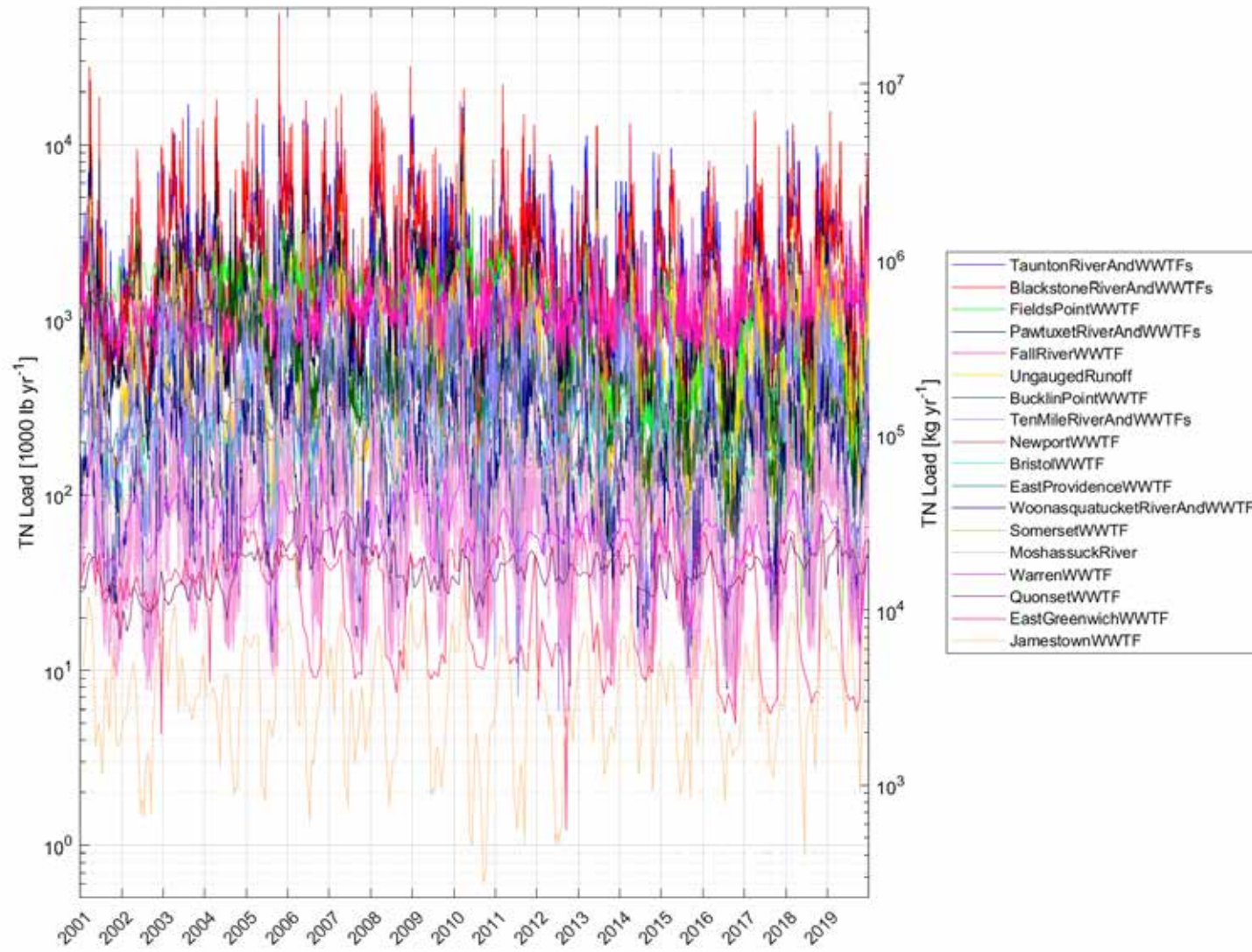
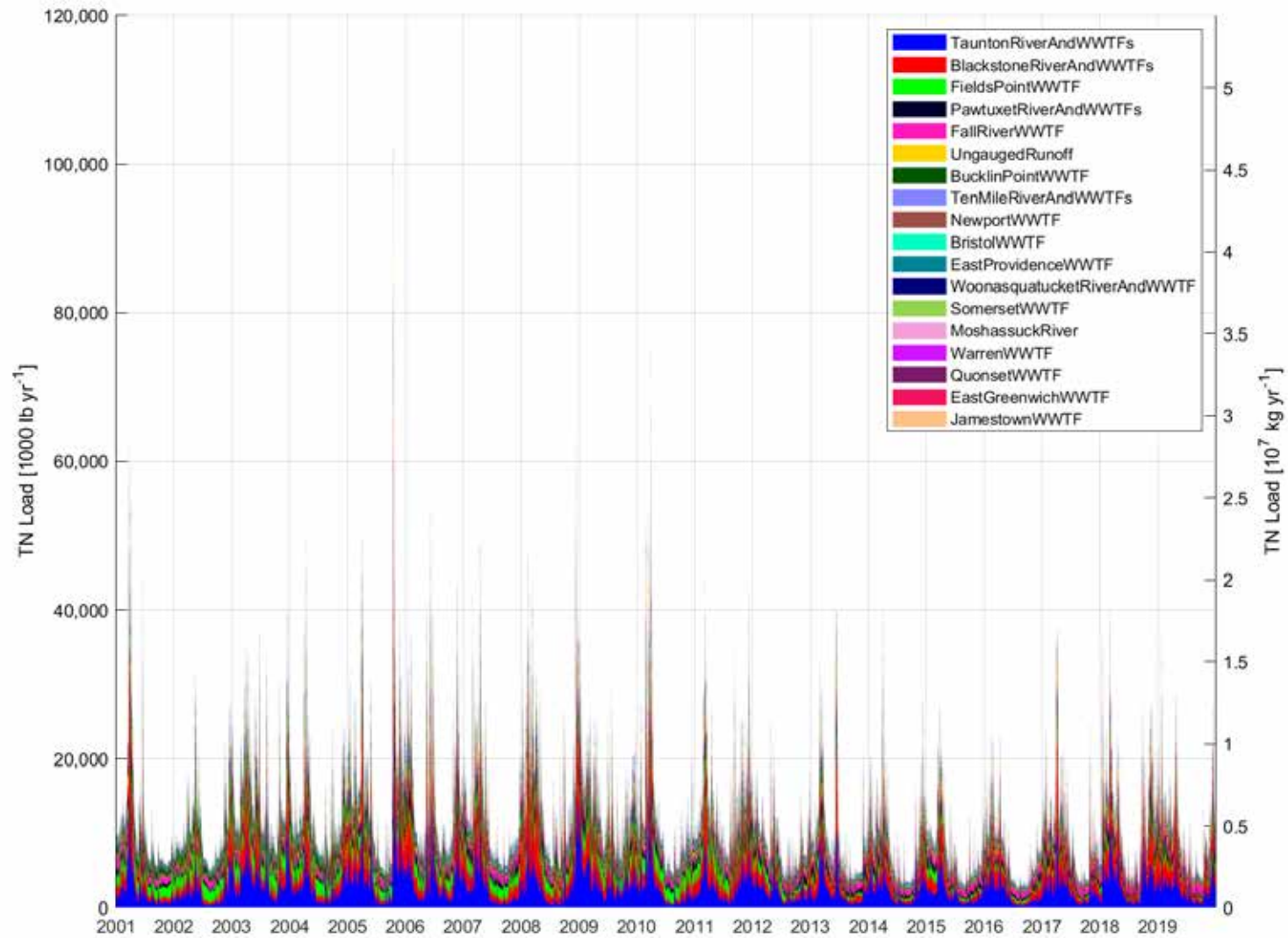


Figure 2-22. Total TN load (summed loads from 18 sources) to Narragansett Bay.



Task 3 Fixed-Site Monitoring Network: Data Reduction

3.1 Scope

Obtain the 2018 and 2019 measurements (for near-bottom oxygen, near-surface chlorophyll, and near-surface and near-bottom temperature and salinity) for the Narragansett Bay Fixed-Site Monitoring Network (NBFSMN) from Heather Stoffel (URI-GSO/RIDEM). Apply the data reduction methods from earlier analyses (NBEP, 2017; Codiga 2020a) and append the results to the products (including oxygen, chlorophyll, and density stratification) of Codiga (2020a) for prior years up through 2017.

3.2 Methods

Methods for oxygen are as explained in NBEP (2017; Chapter 15) and Codiga (2020a). Methods for chlorophyll are the bay-wide thresholds approach explained in Codiga (2020a; Task 10). Methods for density stratification are as explained in Codiga (2020a; Task 5).

See page 118 for information about supporting code and data files, and page 121 for how to use them.

3.3 Results

The “corrected” spreadsheet files for the 11 NBFSMN sites were obtained from Heather Stoffel (URI). The sites are Phillipsdale Landing (PD) in the Seekonk River, Bullocks Reach (BR), Conimicut Point (CP), and North Prudence Island (NP) in the Providence River and Upper Bay (PRUB), Mount View (MV) and Quonset Point (QP) in the Upper West Passage (UWP), Poppasquash Point (PP) and the T-Wharf (TW) in the Upper East Passage (UEP), Greenwich Bay Marina (GB) and Sally Rock (SR) in and near the Greenwich Bay embayment, and Mount Hope Bay (MH). A map showing all site locations is provided at <http://www.dem.ri.gov/programs/emergencyresponse/bart/stations.php#map> and Figure 1 of Chapter 15 of NBEP (2017) shows all stations except for PD.

The percent of time with valid measurement oxygen and chlorophyll values during 2018 and 2019 was comparable to or better than in past years; the general seasonal patterns, and short-term variability, during 2018 and 2019 for these parameters were comparable to past years (Table 3-1 and Figure 3-1 for near-bottom oxygen; Table 3-2 and Figure 3-2 for near-surface chlorophyll).

Table 3-1. Percent of time during mid-May to mid-October analysis period with valid near-bottom dissolved oxygen values, at each of the eleven sites during 2018 and 2019.

	PD	BR	CP	NP	MV	QP	PP	TW	GB	SR	MH
2018	100	85	93	92	86	76	77	96	100	93	92
2019	100	95	95	99	99	99	98	100	100	98	93

Table 3-2. Percent of time during mid-May to mid-October analysis period with valid surface chlorophyll values, at each of the eleven sites during 2018 and 2019.

	PD	BR	CP	NP	MV	QP	PP	TW	GB	SR	MH
2018	100	81	90	93	93	83	93	100	100	93	87
2019	100	94	99	99	91	83	100	100	99	100	100

Figure 3-1. Near-bottom dissolved oxygen measurements (units mg L⁻¹) from 2018 and 2019 at the 11 NBFSMN sites. The percent time with valid measurements is shown at upper right in each frame (and in Table 3-1).

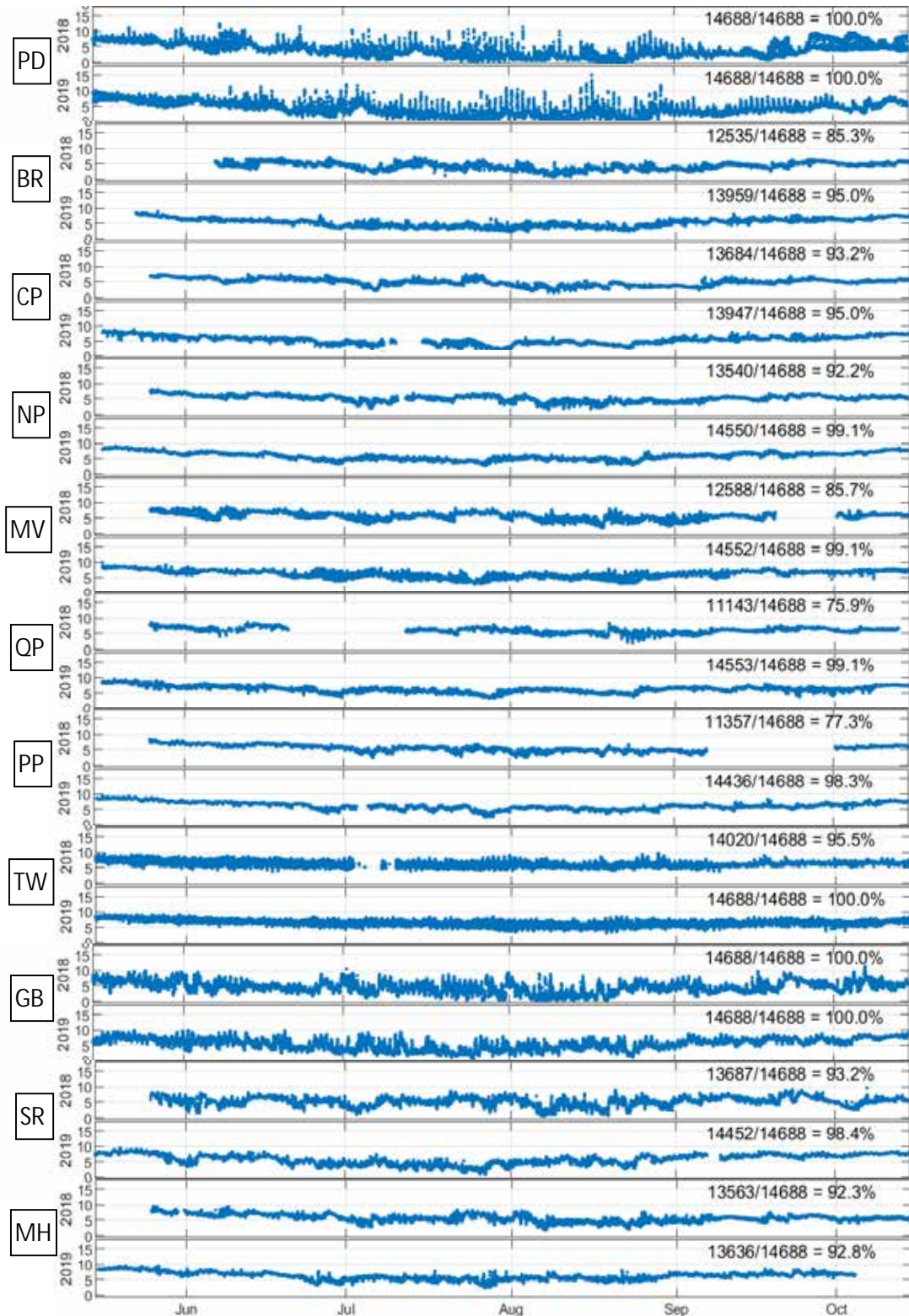
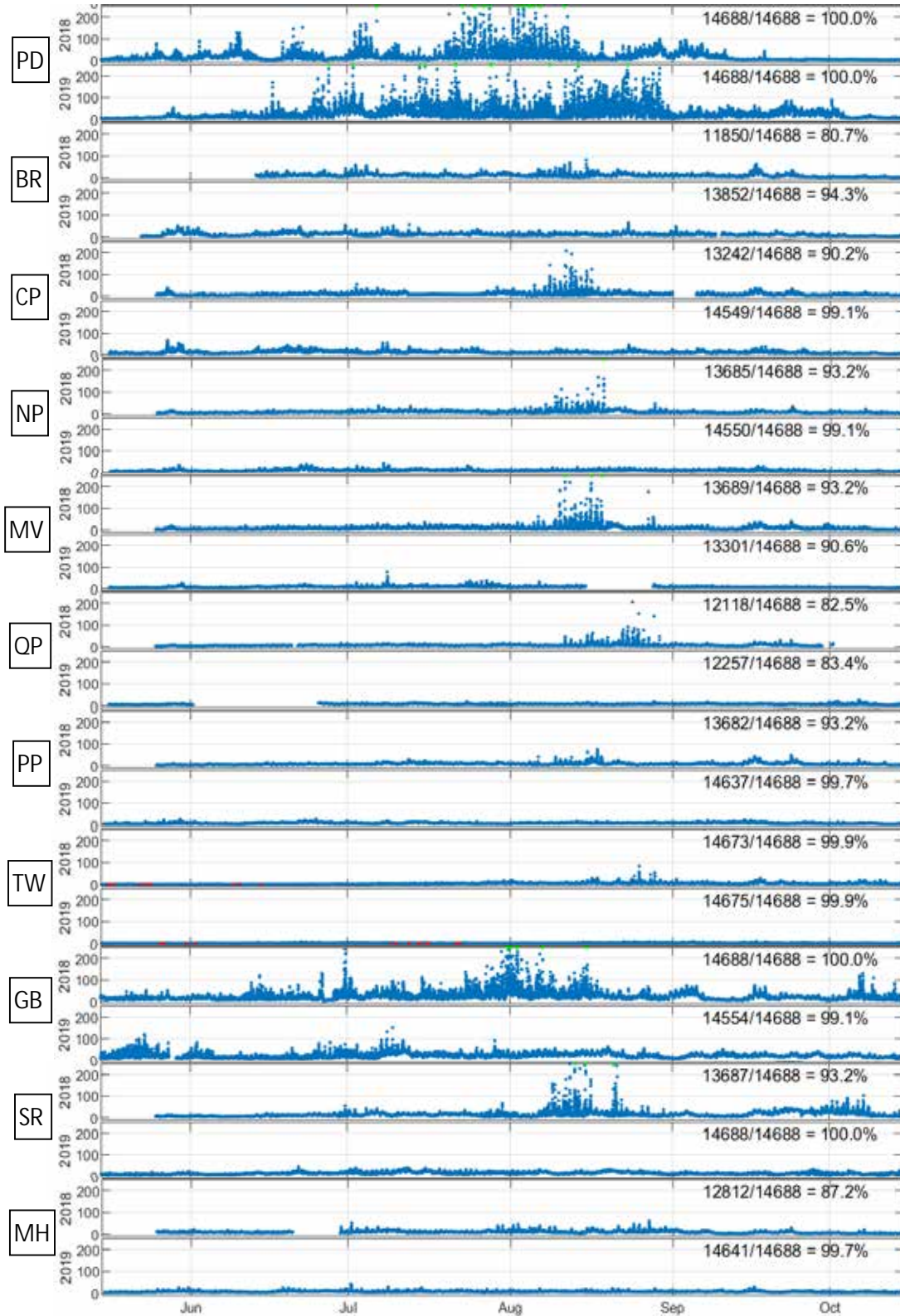


Figure 3-2. Near-surface chlorophyll measurements (mg L^{-1}) from 2018 and 2019 at the 11 NBFSMN sites. The percent time with valid measurements is shown at upper right in each frame (and in Table 3-2). Values higher than the vertical axis maximum, 250 mg L^{-1} , are green.



Task 4 Fixed-Site Monitoring Network: Hypoxia Index

4.1 Scope

Update the Hypoxia Index analysis in Codiga (2020a), which extended through 2017, by computing and appending results for 2018 and 2019.

4.2 Methods

Methods are as explained in NBEP (2017, Chapter 15) and Codiga (2020a). The metric for hypoxia is the Hypoxia Index, defined as the season-cumulative deficit-duration relative to a constant threshold.

As explained in NBEP (2017; Chapter 15, see its Figure 2 on p282), the deficit-duration is the area swept out below the threshold concentration by the measured oxygen concentration time series curve during a hypoxic event (defined as a period when the measured concentration is below the threshold concentration). Deficit-duration, and therefore Hypoxia Index, has units $\text{mg L}^{-1} \text{ day}$; for example if the measured concentration is 2 mg L^{-1} lower than the threshold (a deficit of 2 mg L^{-1}) for a duration of 3 days, then the deficit-duration of the event is $6 \text{ mg L}^{-1} \text{ day}$.

The season-cumulative deficit-duration (Hypoxia Index) is the summed deficit-duration of all hypoxic events between mid-May and mid-October.

The deficit-duration and Hypoxia Index results are computed independently using three thresholds (4.8 mg L^{-1} , 2.9 mg L^{-1} , and 1.4 mg L^{-1}) selected based on their regulatory relevance (as explained, for example, by Codiga et al 2009). Results for the 4.8 mg L^{-1} threshold are an indication of all relatively low oxygen conditions including the most mild hypoxia, the 2.9 mg L^{-1} threshold is used by regulators to designate impaired areas, and results for the 1.4 mg L^{-1} threshold are an indication of only the most severe hypoxic conditions.

The Hypoxia Index is computed at each of the 11 NBFSMN sites individually. The results are also averaged over station groups. The Providence River and Upper Bay (PRUB) station group includes the BR, CP, and NP sites. The Upper West Passage (UWP) group includes the MV and QP sites. The Upper East Passage (UEP) group includes the PP and TW sites. The Greenwich Bay group (GRBY) includes the GB and SR sites.

See page 118 for information about supporting code and data files, and page 121 for how to use them.

4.3 Results

Hypoxia Index results for all individual stations using the 4.8 mg L^{-1} , 2.9 mg L^{-1} and 1.4 mg L^{-1} thresholds are shown in Figure 4-1, and Figure 4-3, respectively. Each frame of each figure shows the station or stations in one of the station groups. Hypoxia Index results averaged over the station groups, for all three thresholds, are shown in Figure 4-4.

What follows here is a brief description of the 2018 and 2019 results in the context of earlier years. It makes reference to river flow designations (shown as background gray bars on the figures) as wet,

intermediate or dry calculated as explained in Task 1. For a more extensive synthesis and interpretation of other potential underlying processes see Task 6.

River flow conditions were designated intermediate in 2018 and wet in 2019. This means 2019 was the first year designated wet since 2013; three of the years following 2013 (2014-2016) were dry, and 2017 was intermediate. However, as noted in Task 1, although both 2019 and 2013 were classified as wet, 2019 was only slightly above the threshold between wet and intermediate (see Figure 1-2), whereas 2013 and all other prior wet years were far higher than it. In fact, from Figure 1-2 it is clear that 2019, although designated wet, is more similar to the intermediate years 2017 and 2018 (which were only slightly below the threshold between wet and intermediate) than it is to any earlier wet year. It is important to keep this in mind, when viewing the Hypoxia Index results figures, which show a darker gray background bar for 2019 (designated wet) than for 2017 and 2018 (designated intermediate); despite this visual distinction, the river flow during 2017, 2018, and 2019 were all quite similar and most closely comparable to the earlier intermediate years that fell high within the intermediate range (2001, 2008, and 2012).

Threshold 4.8 mg L⁻¹: All low-oxygen events including the most mild. For the highest threshold 4.8 mg L⁻¹, the Hypoxia Index results (Figure 4-1) are an indicator for all low-oxygen conditions including the most mild hypoxic events. The 2018 and 2019 results are most similar to the past several years since 2013, when nutrient load declines were mostly complete and the Index was notably lower than in many earlier years. In this sense they continue to support the interpretation that bay hypoxia has been notably lessened in severity by reduced nutrient loads.

However, all years since 2013 have been substantially drier than any year designated wet (2003, 2006, 2011, 2013) other than 2019 (which although designated wet is more similar to years with intermediate river flow as just noted). This suggests there remains some ambiguity as to whether the reduced nutrient loads or the drier conditions are most responsible for the lower Hypoxia Index. In addition, at some sites in and near embayments (PD, GB, and the PRUB group) the Index in 2018 was detectably higher than in 2014-2017.

As noted above, the years 2001, 2008, and 2012 from prior to when nutrient load declines had been substantially completed, had comparable river flow to 2017, 2018, and 2019 (Figure 1-2). From Figure 4-1 it can be seen that some sites (BR, CP, SR, PP, and to a limited extent MV and MH) have lower 2018-2019 Hypoxia Index than occurred in those earlier comparably wet years. This supports the interpretation that hypoxia in the bay has improved in recent years due to nutrient load reductions at least as much as due to the drier conditions.

However, there are other stations for which the 2018-2019 Hypoxia Index is about the same as the pre-2013 years with comparable river flow. Generally these are limited to the shallower embayment stations (PD, GB). This suggests the improvements are not bay-wide, when considering mild events with oxygen below the highest threshold.

Interestingly at nearly all stations the Hypoxia Index was higher in 2018 than in 2019. This is counter to the expectation based on 2019 being classified as wet and 2018 being classified as intermediate; in earlier years, especially prior to and during treatment facility upgrades which decreased nutrient loading to the bay over a period of several years and were mostly complete by 2012-2013, there was a strong relationship between higher Hypoxia Index and wetter conditions. However, as just explained, 2019 and 2018 river

flow were more similar to each other than any earlier wet year, and the amount by which 2018 Hypoxia Index results were higher than 2019 is generally modest or small. As a result, although the declines from 2018 to 2019 could be part of a long-term improvement in conditions, such an interpretation is not considered particularly robust.

Threshold 2.9 mg L⁻¹: Most-used by regulators. For the intermediate threshold 2.9 mg L⁻¹, the Hypoxia Index results (Figure 4-2) show many similarities to those just described for the 4.8 mg L⁻¹ threshold.

At stations other than the shallow embayments (PD, GB), the reductions during years 2014-2017 were to low levels, and 2018 and 2019 are as low as them (with a minor exception of BR in 2018).

Comparisons of 2018-2019 to the pre-2013 years with comparable river flow (2001, 2008, 2012) shows they generally have noticeably lower Hypoxia Index. For this threshold, more so than for 4.8 mg L⁻¹, a consistent interpretation is that nutrient load declines have improved hypoxic conditions bay-wide, excluding the shallowest embayment stations PD and GB, to a greater extent than the fact that recent years have not had particularly high river flow.

For PD, conditions in 2018-2019 were comparable to the year with the second-highest Hypoxia Index (2012). This contrasts its low Index values from 2014-2017 and strongly suggests this site has processes controlling hypoxia that are different from at other sites, and/or that nutrient load declines have not had sufficient impact on this site to lessen its hypoxia.

For GB, the 2018 Hypoxia Index results were higher than one earlier year (2012) with comparable river flow but lower than another such year (2008). Its results for 2019 were as low as 2012 and much lower than 2008. This supports the interpretation that GB hypoxia conditions are improving due to nutrient load declines, though not as strongly as other sites located in deeper water and/or farther down-bay.

Threshold 1.4 mg L⁻¹: Only the most severe hypoxic events. For the lowest threshold 1.4 mg L⁻¹, the Hypoxia Index results (Figure 4-3) since 2014 indicate almost no events at any station, including GB, except for PD. This remained the case during 2018 and 2019.

In sharp contrast, at the PD site, where the Hypoxia Index for this lowest threshold was very low from 2014-2017, during 2018-2019 it rose to a level comparable to the highest seen in any prior year. Results from 2018-2019 thus indicate PD is still subject to very severe events, unlike any other station including even GB. This reinforces the interpretation noted above, that processes influencing hypoxia at PD are very different from other stations and/or the nutrient load declines are not having as much impact on PD.

Station-group averages. In Figure 4-4, which shows station-group average Hypoxia Index for all three thresholds, all the main patterns just described for the prior three figures can be seen.

Further analysis and interpretation of these results is provide in Task 6.

Figure 4-1. Hypoxia Index relative to 4.8 mg L⁻¹ (highest of the three thresholds; a measure of all relatively low oxygen conditions including the most mild hypoxia) for individual sites (each frame showing a station group).

To improve clarity by reducing overlap of lines and symbols, symbols from each site are systematically offset a small distance horizontally relative to those of other sites in the frame. Error bars indicate uncertainties due to gaps in the time series because of sensor malfunction or data not meeting quality standards, and in most cases are smaller than the symbols. Years with bay-wide June to September river flow designated wet, intermediate, and dry (see Figure 1-2) are marked by gray vertical bars of three increasingly lighter shades, respectively.

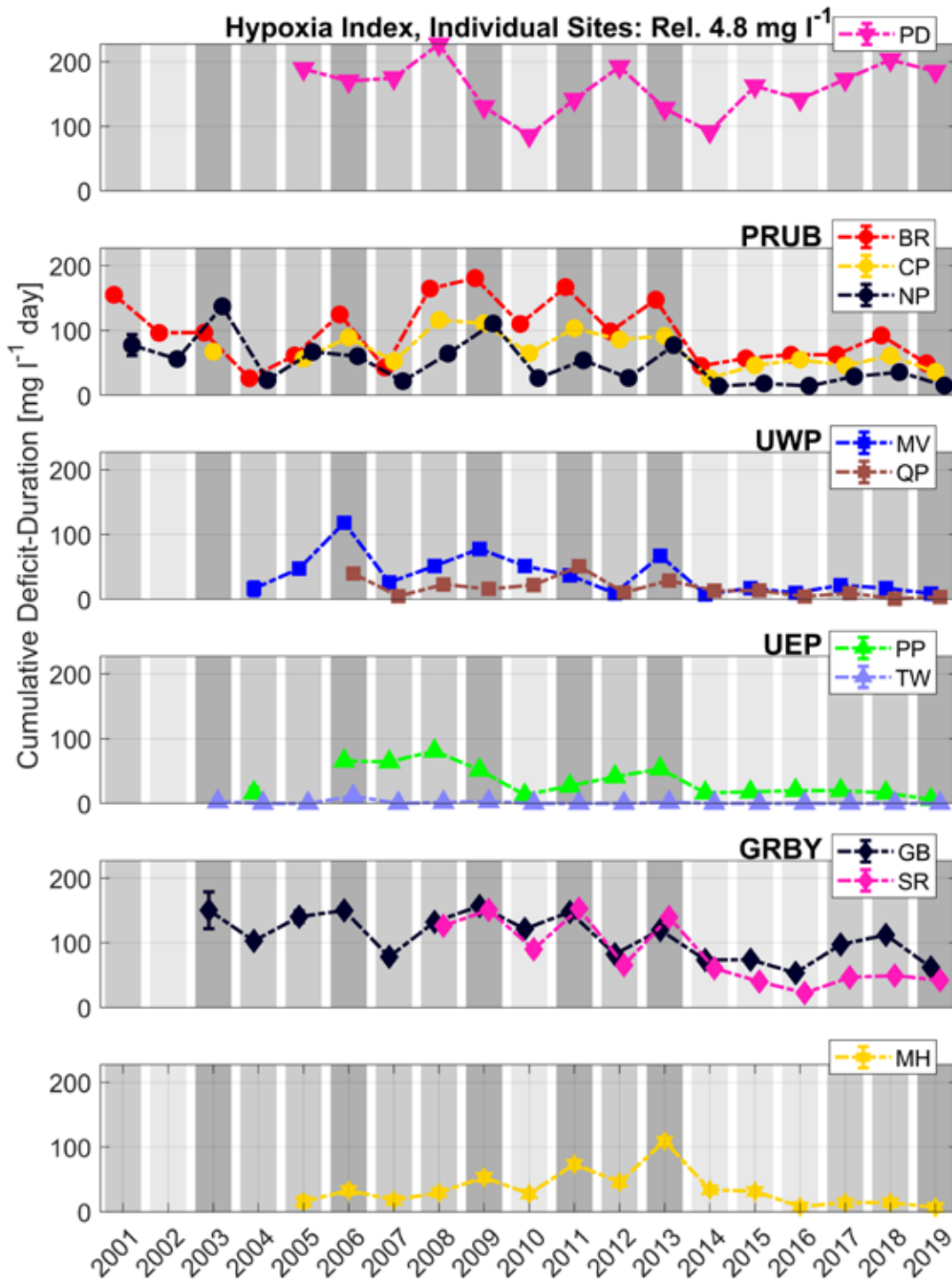


Figure 4-2. Hypoxia Index relative to 2.9 mg L⁻¹ (intermediate of the three thresholds; used by regulators to designate impaired areas), shown as in Figure 4-1.

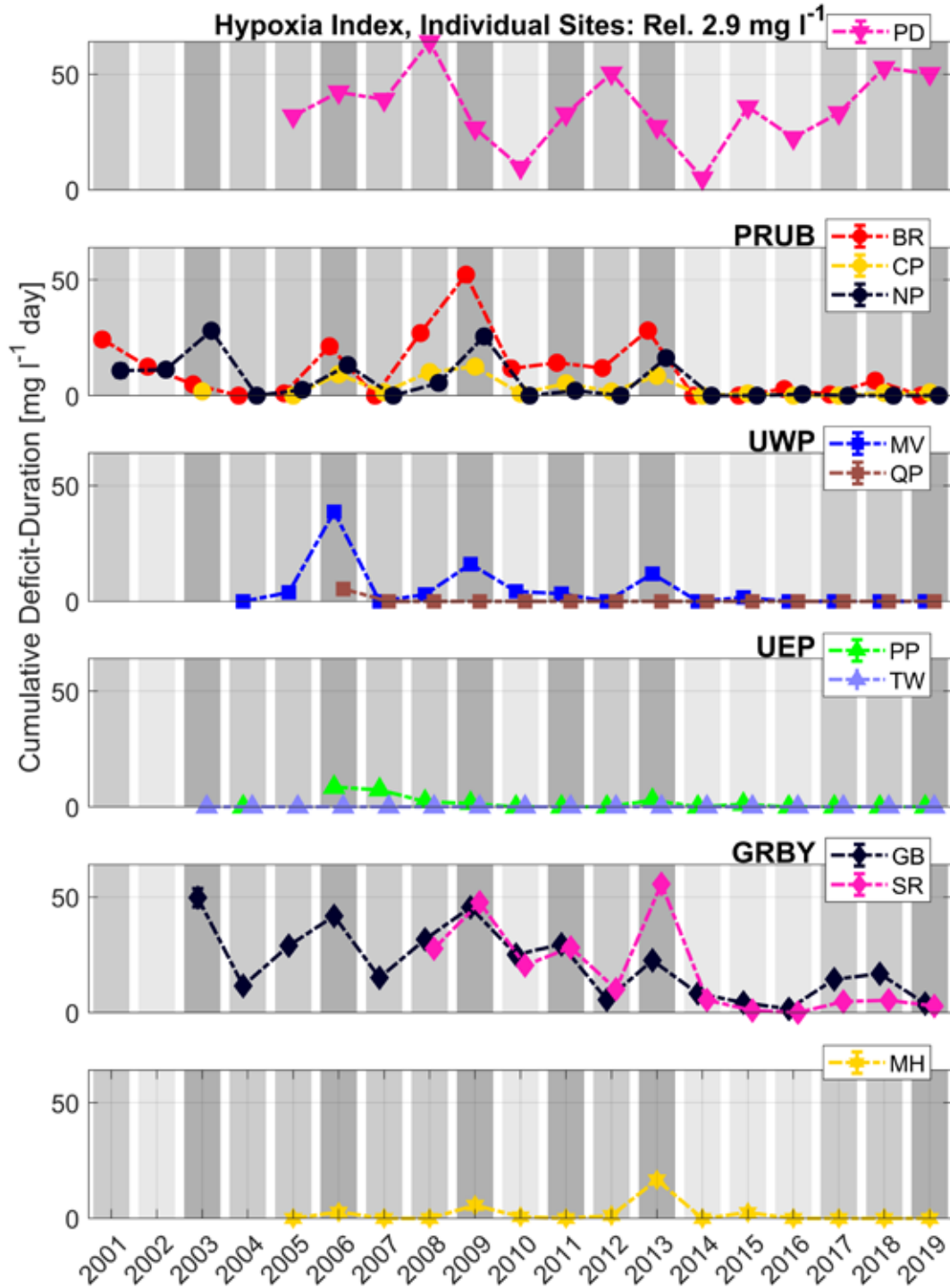


Figure 4-3. Hypoxia Index relative to 1.4 mg L^{-1} (lowest of the three thresholds; a measure of the most severe hypoxic conditions), shown as in Figure 4-1.

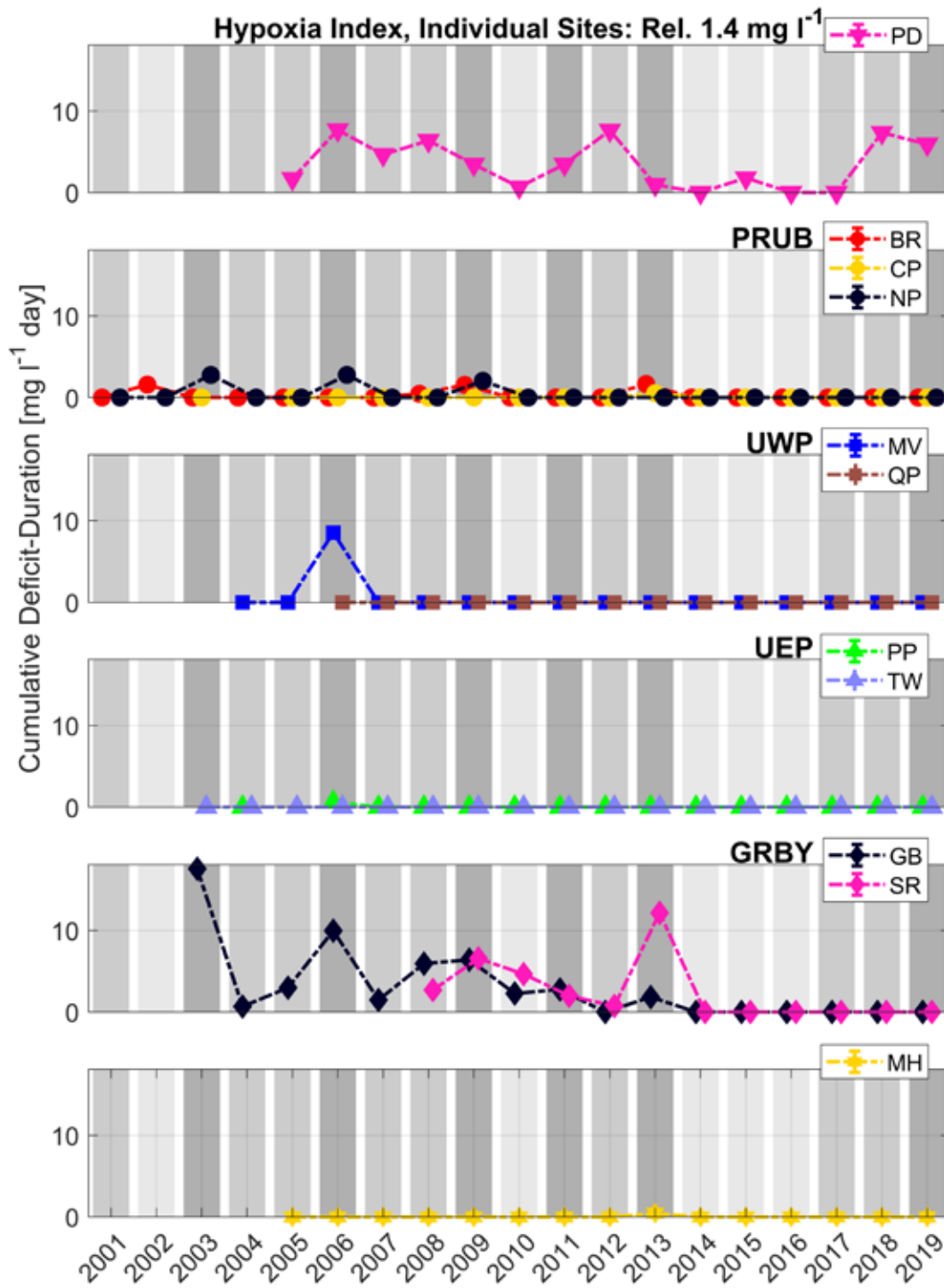
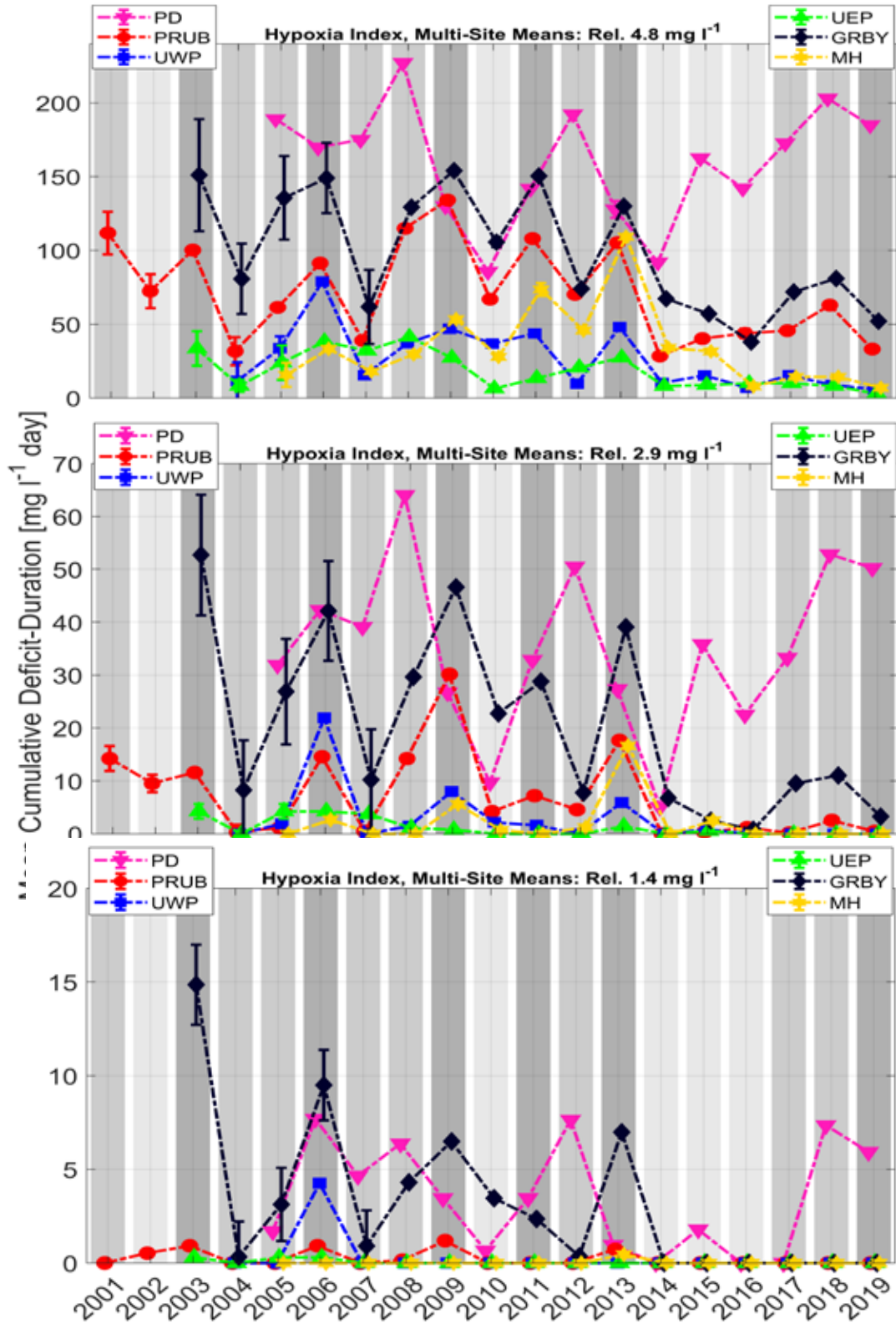


Figure 4-4. Hypoxia Index results, station-group averages. Threshold 4.8 mg L⁻¹, 2.9 mg L⁻¹, and 1.4 mg L⁻¹ are shown in the top, middle, and bottom panels respectively.



Task 5 Fixed-Site Monitoring Network: Chlorophyll Index

5.1 Scope

Update the Chlorophyll Index analysis using bay-wide thresholds in Codiga (2020a; Task 10), which extended through 2017, by computing and appending results for 2018 and 2019.

5.2 Methods

Methods are as explained in Task 10 (bay-wide thresholds; not Task 9 on site-specific thresholds) of Codiga (2020a). The metric for chlorophyll is the Chlorophyll Index, defined as the season-cumulative surplus-duration relative to a constant threshold.

As explained in NBEP (2017; Chapter 16, see its Figure 3 on p304), the surplus-duration is the area swept out above the threshold concentration by the measured chlorophyll concentration time series curve during a high-chlorophyll event (defined as a period when the measured concentration is above the threshold concentration). The term “high-chlorophyll event” is used, instead of “bloom”, as the latter is not defined as quantitatively and often is identified using context that varies from site to site and based on its particular conditions (time of year, typical background concentration, etc). Surplus-duration, and therefore Chlorophyll Index, has units $\text{mg L}^{-1} \text{ day}$; for example if the measured concentration is 10 mg L^{-1} higher than the threshold (a surplus of 10 mg L^{-1}) for a duration of 3 days, then the surplus-duration of the event is $30 \text{ mg L}^{-1} \text{ day}$.

The season-cumulative surplus-duration (Chlorophyll Index) is the summed surplus-duration of all high-chlorophyll events between mid-May and mid-October.

The surplus-duration and Chlorophyll Index results are computed independently using three thresholds (4.9 mg L^{-1} , 9.4 mg L^{-1} , and 17.6 mg L^{-1}). These thresholds were computed (Codiga, 2020a) as the 20th, 50th, and 80th percentile of all mid-May to mid-October chlorophyll time series measurements at all 11 NBFSMN sites bay-wide through the year 2017, and the same thresholds are applied to the records from all sites bay-wide.

As discussed in Codiga (2020a), the thresholds (4.9 mg L^{-1} , 9.4 mg L^{-1} , and 17.6 mg L^{-1}) are in a similar range to those used to assess water quality conditions in a national evaluation across many waterbodies (Table 2-5 in USEPA, 2015). In that evaluation, for the northeast US region, surface chlorophyll concentrations were designated Good, Fair, or Poor when $< 5 \text{ ug/L}$, between 5 and 20 ug/L , and greater than 20 ug/L , respectively.

Results for the lowest 4.9 mg L^{-1} threshold are indicative of all high-chlorophyll events, including the most mild. Results for the highest 17.6 mg L^{-1} threshold are indicative of only the most severe high-chlorophyll events.

The same thresholds are applied at all stations bay-wide, as is useful to help identify patterns and trends across the bay. (In contrast, site-specific thresholds, which were used in NBEP (2017; Chapter 16) and Task 9 of Codiga (2020a) but are not used here, are best-suited when the goal is application to any individual site including those with anomalously high or low ranges of typical values.)

Note that the thresholds used were not re-computed using all years including 2018-2019 (such thresholds are 17.4, 9.3, and 4.9 mg L^{-1} which differ by very small amounts from the thresholds computed using years through 2017, used here). This is so that the results shown here can be compared to those in Codiga (2020a) with equivalence. This avoids results from earlier years being different in Codiga (2020a) as compared to here. It is suggested that consideration be given to computing and using new thresholds only after 5 or more years of additional measurements beyond 2017 are available. Of course this also makes sense because doing so prior to such a time means such a small number of additional years will be added that is unlikely to result in meaningfully different thresholds in any case. (The same approach, using thresholds based on years up through 2017 and not recomputing them with inclusion of 2018-2019, was taken for the thresholds used to define bay-wide river flow conditions wet, intermediate, or dry; see Task 1).

The Chlorophyll Index is computed at each of the 11 NBFSMN sites individually. The results are also averaged over the same station groups as for the Hypoxia Index (see Task 4).

See page 118 for information about supporting code and data files, and page 122 for how to use them.

Meeting of group of phytoplankton/chlorophyll experts. This meeting was held on 3/31/2021. The agenda and meeting notes, which were circulated in draft form after the meeting and updated with input from the attendees, are included here:

Agenda

1. *Follow up discussion on work completed in 2020 (see Codiga 2020A report)*
 - a. *Chlorophyll Index: Bay-wide thresholds (Task 10), site-specific thresholds (Task 9)*
 - i. *Consensus to assess chlorophyll mainly with bay-wide thresholds results?*
 - b. *Potential post-deployment recalibration of fixed site dataset (based on Task 8)*
 - i. *Consensus this would not be sufficiently fruitful to carry out, correct?*
 - ii. *If this was pursued, what would be the expected goal or improvement?*
2. *New results, for current project, with 2018 and 2019 included*
 - a. *Chlorophyll Index results for individual stations and regional station groups*
 - i. *Uses bay-wide thresholds computed in 2020 report, based on period through 2017*
 - ii. *Changes to thresholds are inconsequential if use period through 2019*
 - b. *Basin-wide Chlorophyll Index results*
 - i. *Average over 8 of 11 sites—exclude PD, GB, SR because they have higher index and also have inter-annual variability different from other stations*
 - c. *Broader topics*
 - i. *Variability in summer chlorophyll metrics tied to basin-wide TN load variations*
 1. *Pronounced inter-annual swings, linked to river flow*
 2. *Long-term declines, due to plant upgrades, are becoming clearer*
 - ii. *Long-term variability in river flow and nutrient load during 6 month periods centered on summer & winter, compared to whole year*
 1. *Possible consideration to expand sampling to year-round (instead of May-Oct) at some additional stations in fixed-site network?*

Meeting Notes

Attendees: Courtney Schmidt, NBEP; Candace Oviatt, Kristin Huizenga, URI/GSO; David Borkman, DEM; Warren Prell, David Murray, Brown; Eliza Moore, Molly Welsh, Luis Cruz, NBC; Chris Deacutis, DEM (ret.)

Draft figures were briefly reviewed and explained. These suggestions were made:

- For the shaded gray bars indicating wet/intermediate/dry river conditions in the background of the Chlorophyll and Hypoxia Index plots, use shades with sharper contrast (including possibly white for the dry years) so they are more easily distinguished from each other.
- Use metric units (not lbs) for nitrogen loads (or show both; or make 2 versions of each figure, one with metric).
- For chlorophyll thresholds use 5, 10, and 20 ug/L (instead of 17.6, 9.4, and 4.9 ug/L, which are the 80th, 50th, and 20th percentiles)
- In addition to plots of the Chlorophyll Index and Hypoxia Index (area swept out by curve when it crosses the threshold), make additional plots showing days over threshold (duration that the curve remains across the threshold), so that the units are easier to understand.
- In the figure showing summed annual (12-month) TN load and river flow together with sums over summer-centered (May-Oct) and winter-centered (Nov-Apr) 6-month periods, try to use an average instead of a sum, and/or some other representation so that different units can be used.

On the following points there was consensus support:

- For the purpose of “bay-wide” analyses, it is best to use the “bay-wide thresholds” (computed, for example, as the 80th, 50th, 20th percentile of data from all sites combined) and not the “site-specific thresholds” originally used in the 2017 State of Narragansett Bay and Its Watershed. This is the approach taken in the ongoing analysis.
- Due to the inherently large range of variability in chlorophyll from both the fixed-site fluorometer time series dataset and the grab samples dataset, as demonstrated in Codiga 2020a, it will not be fruitful to pursue a post-deployment recalibration of the former using the latter. This should be explained in the upcoming report.
- With respect to tabulating flow to the bay, the present method based on river inputs is sufficient without adding treatment plant flows—because the latter vary less from year to year than rivers and likely will change flows, very crudely, as effectively a near-constant offset.
- For analysis of bay-wide conditions it is justified to omit the PD, GB, and SR stations from the fixed-site dataset, because they include inter-annual variability that is larger than that of the other 8 stations; their inter-annual variability is also independent from each other, and independent from that of the other 8 stations, which are more coherent with each other and representative of the bay as a whole.

Other topics discussed:

- Variability at and near the PD station should be analyzed in light of CSO flows, which changed in 2006 (upgraded wet weather facilities at Bucklin). (In 2008, 50% of stormwater diverted to plant affected mainly the Moshassuck, Woonasquatucket, and Providence Rivers.) Studying the salinity in that area should be useful to understand its inter-annual variations, which are different from the rest of the bay and can be counter-intuitive, likely because it is so narrow and responds to large pulses of flow differently than other more open parts of the bay.
- There have been rust tides (cochlodinium) during roughly Jul-Sep in Greenwich Bay in many of the last several years, likely in association with warming temperatures, and this species is high in chlorophyll so could explain higher values if observed.
- Macroalgae may have changed due to increased water clarity, but few quantitative measurements have been made. Some areas seeing increases, others decreases. Macroalgae is a weak spot in terms of monitoring and regulations. It could be important to overall bay phytoplankton, as it takes up nutrients, and to hypoxia as well; however, many studies in other

systems have looked at this and concluded it generally is secondary to water column phytoplankton.

- *The percent area high-chlorophyll and percent area hypoxic, from the spatial surveys, for 2018 and 2019 have yet to be calculated but this can be done by Brown using the GIS-based method they developed. The possibility to develop a non-GIS (i.e. matlab-script based) method was mentioned—perhaps objective mapping with two orthogonal covariance lengthscales, with masking using the coastline or 4-m isobath; or something similar/equivalent.*
- *A number of ideas for how to improve the calibration of the fixed-site fluorometers were raised. For example for the NBC stations PD and BR, pre-2016 data are from YSI 6000 series sondes; during 2016-2017 this continued but with YSI EXO sondes were also used as transition comparison period; in 2018 BR was converted to EXO and in 2019 PD was converted. These changes, and similar ones for URI/GSO sites which also have transitioned from 6000 series to EXO sondes in recent years, should be borne in mind when analyzing the results. At high concentrations some differences have been noted between the two sensors. The calibration method currently is “one-point” at zero, so improving this to a two-point method (second point at high concentrations) could lead to better agreement.*

5.3 Results

Chlorophyll Index results for all individual stations using the 4.9 mg L^{-1} , 9.4 mg L^{-1} and 17.6 mg L^{-1} thresholds are shown in Figure 5-1, Figure 5-2, and Figure 5-3, respectively. Each frame of each figure shows the station or stations in one of the station groups. Chlorophyll Index results averaged over the station groups, for all three thresholds, are shown in Figure 5-4.

What follows here is a brief description of the 2018 and 2019 results in the context of earlier years. For a more extensive synthesis and interpretation of other potential underlying processes see Task 6.

For the lowest threshold 4.9 mg L^{-1} , the Chlorophyll Index results (Figure 5-1) are an indicator for all increased-chlorophyll conditions including the most mild.

The 2018 and 2019 results for nearly all sites (excluding shallower embayment sites PD, GB, and SR) are comparable to, and some cases slightly lower than, the several years since 2013 (when nutrient load reductions were mostly completed). During these several years, the Chlorophyll Index results were quite similar to most or all earlier years, with a weak indication that long-term declines are occurring. This weak decline could be interpreted as a response to the reduced nutrient loads. At these deeper non-embayment sites inter-annual variability is generally quite weak (far less than for hypoxia and river flow; see Task 4). As discussed by Codiga (2020a) the most prominent spatial pattern is the down-bay gradient, with concentrations and Chlorophyll Index results that are higher to the north nearer the riverine inputs and decrease in the down-bay direction generally toward the south. In addition, the Chlorophyll Index is generally slightly higher in 2018 than in 2019, though the amount by which 2019 is lower is typically not as large as inter-annual variability in earlier years.

In contrast, for the shallow embayment stations PD, GB, and SR the results for 2018 and 2019 are higher than the most recent several years. For GB and SR the increases are modest, and higher in 2018 than 2019. For PD the increases are large, though not inconsistent with inter-annual variability that has occurred since 2013, and the 2019 result is higher than 2018.

For the intermediate threshold 9.4 mg L^{-1} , the Chlorophyll Index results (Figure 5-2) the main characteristics are quite similar to those just described for the 4.9 mg L^{-1} threshold. Small differences include that at CP there was a modest increase in 2019 relative to 2018, and at MH the index declined sharply in 2019 compared to 2018, which itself was notable lower than 2017.

For the highest threshold 17.6 mg L^{-1} , corresponding to only the most severe high-chlorophyll events, Chlorophyll Index results (Figure 5-3) include zero or near-zero results at many more stations (as expected because it is a measure of only the less common, very sharply increased, concentrations). In 2018 and 2019 the only sites with Chlorophyll Index notably higher than zero included PD, BR, CP, GB, and SR. For these stations the patterns are very similar to those described above, for the lower threshold results.

In Figure 5-4, which shows station-group average Chlorophyll Index for all three thresholds, all the patterns just described can be seen.

Further analysis and interpretation of these results is provide in Task 6.

Figure 5-1. Chlorophyll Index relative to $4.9 \mu\text{g L}^{-1}$ (lowest of the three thresholds; a measure of all high-chlorophyll events including the most mild) for individual sites (each frame showing a station group). Shown as in Figure 4-1 for the Hypoxia Index.

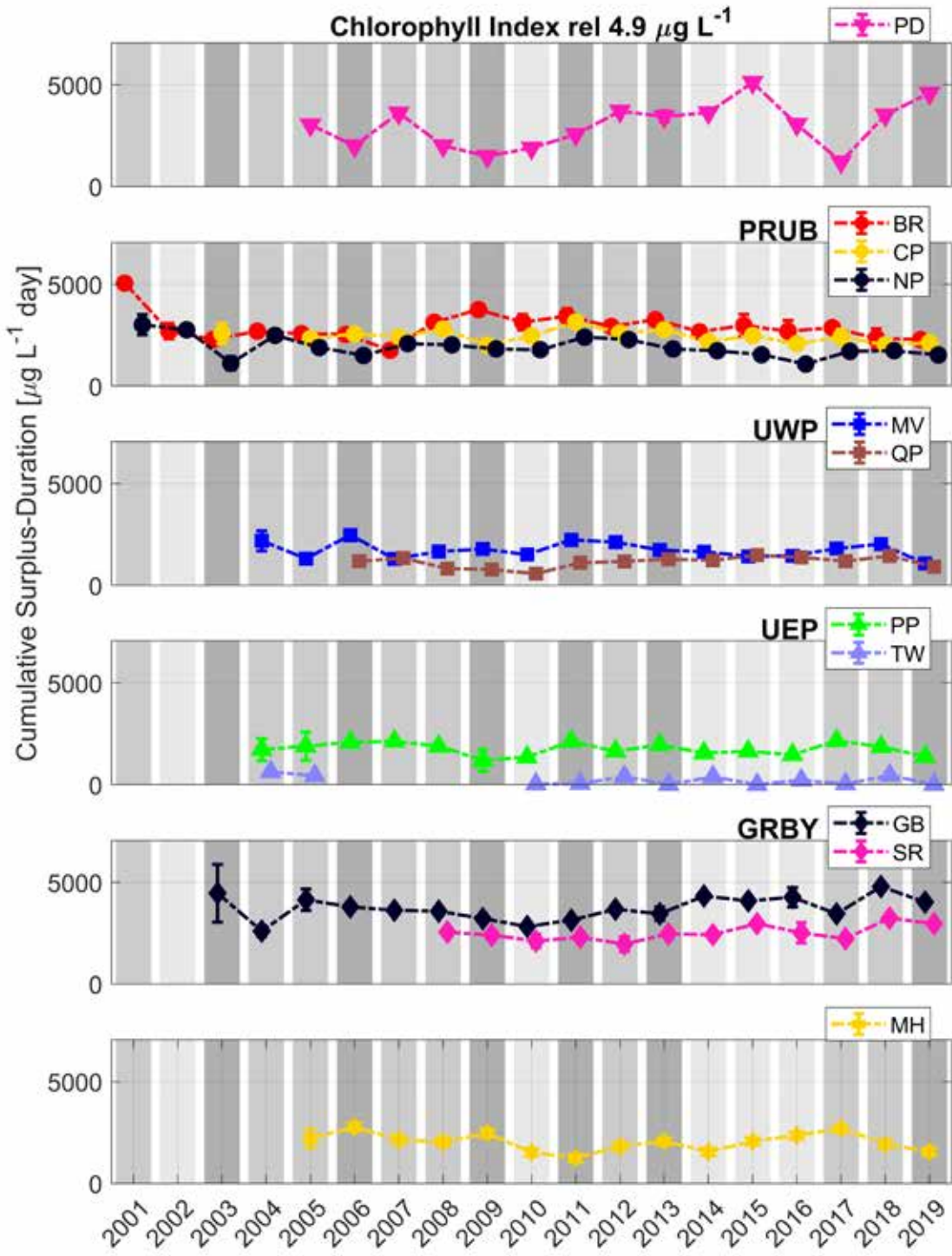


Figure 5-2. Chlorophyll Index relative to $9.4 \mu\text{g L}^{-1}$ (intermediate of the three thresholds), shown as in Figure 5-1.

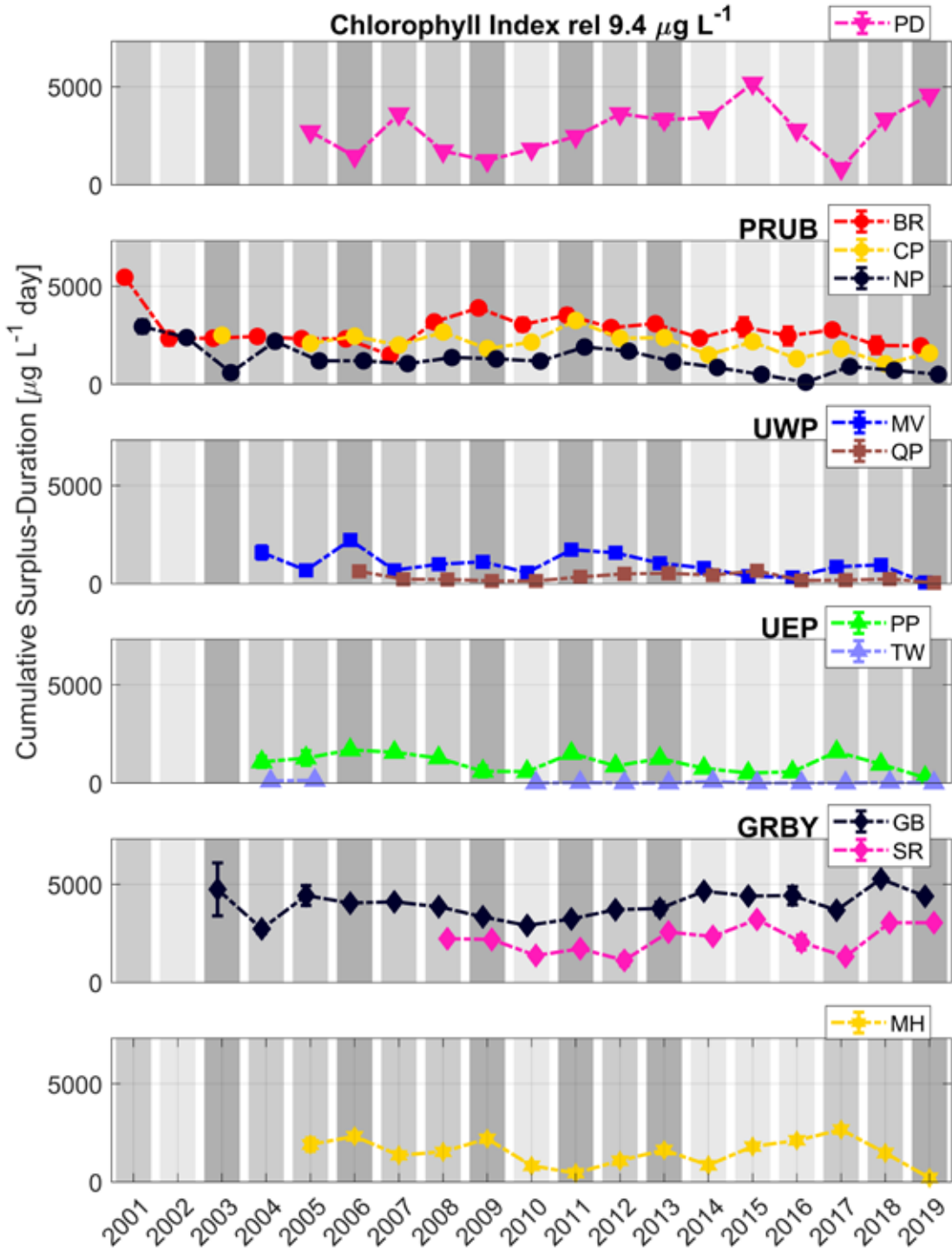


Figure 5-3. Chlorophyll Index relative to $17.6 \mu\text{g L}^{-1}$ (highest of the three thresholds; a measure of the most severe high-chlorophyll events), shown as in Figure 5-1.

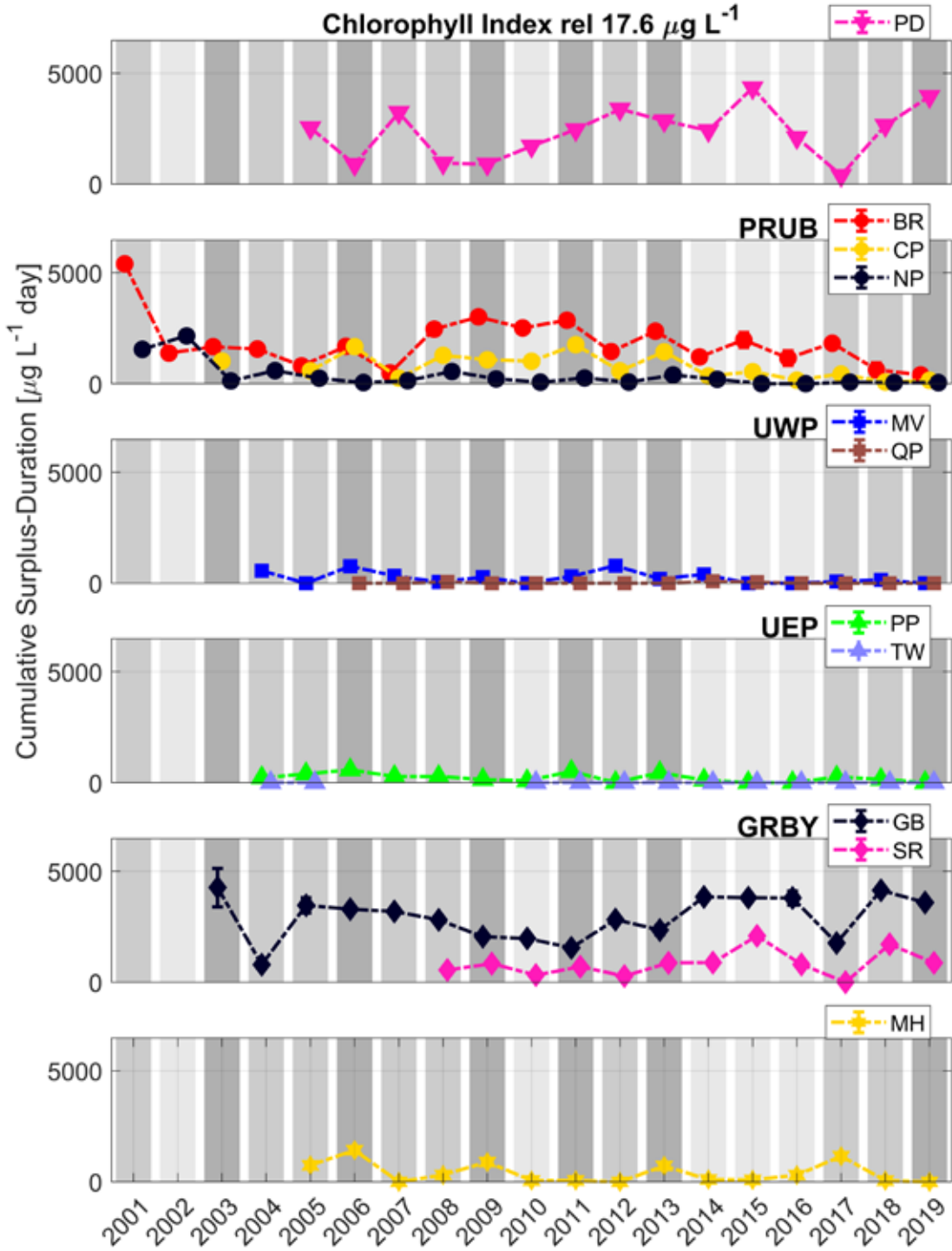
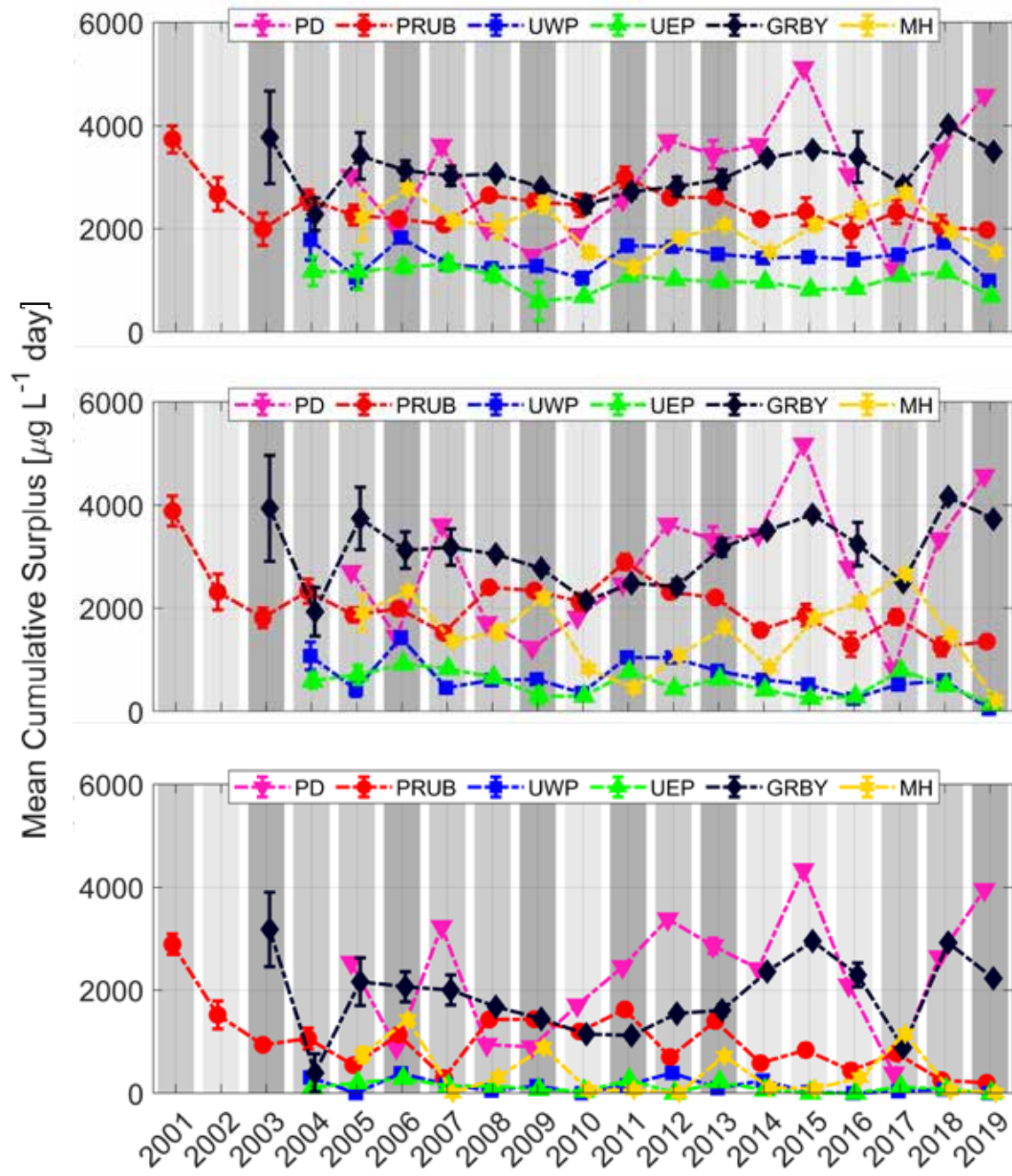


Figure 5-4. Chlorophyll Index results, station-group averages. Threshold 4.9 mg L^{-1} , 9.4 mg L^{-1} , and 17.6 mg L^{-1} are shown in the top, middle, and bottom panels respectively.



Task 6 Synthesis of Hypoxia, Chlorophyll, Nitrogen Load, Physical Drivers

6.1 Scope

Inter-annual variability in Hypoxia Index, Chlorophyll Index, bay-wide nitrogen load, river flow, and stratification are examined in context of temperature, wind, tidal range, and non-tidal sea level conditions using results of Tasks 1 to 5, with emphasis on identifying and interpreting patterns in the most recent several years. Earlier results suggested 2017 was the first year with little to no hypoxia when river flow and stratification were modest, and 2018-2019 are examined in this light. The original scope for this task was augmented during the project to include results from vessel-based spatial surveys, because they were made available by colleagues and are an independent dataset with metrics (percent area hypoxic, percent area high chlorophyll) complementary to those from the time series dataset.

6.2 Methods

See methods in Tasks 1 through 5. With appreciation to colleagues at Brown (Warren Prell and David Murray), results from the spatial surveys for percent area hypoxic and percent area high-chlorophyll (Prell et al 2015, 2016; methods described in Codiga 2020a) are included in this analysis, even though they were not in the scope of this project as originally planned.

About the term “bay-wide”. When referring to river flow and nitrogen load, the term “bay-wide” is used to mean the sum of all inputs to the bay; when referring to the in situ datasets (fixed site monitoring network, vessel-based spatial surveys) the term “bay-wide” is used to refer to the area spanned by the sampling. Note that the latter is an inaccurate use of “bay-wide” to the extent that the sampled area, which extends across roughly the northern half of the bay, does not span the entire bay. However the sampled area does span well beyond the area impacted by eutrophication and in this sense the term “bay-wide” is not inappropriate given the focus of the project. In addition, in the case of the fixed-site monitoring dataset the term “bay-wide” is applied to the group of 8 deeper sites, excluding 3 sites that are in shallow embayments; the latter are excluded because they generally exhibit a higher level variability that is independent from that of the other 8 which have variability that is more coherent with each other (see above sections as well as, e.g., Codiga 2020a).

About units for TN load. In Task 2 above, for TN load both metric units (kg yr^{-1}) and American units (1000 lb yr^{-1}) were shown on figures (one on the left vertical axis, the other on the right vertical axis), enabling the interested reader to explicitly see the proportionality between the two units. In this task the figures show only metric; at the end of this task a second set of figures is provided which shows American units instead.

See page 118 for information about supporting code and data files, and page 122 for how to use them.

6.3 Results

In the past few years the capabilities to define and tabulate indicators of bay-wide conditions, using multiple monitoring datasets, have advanced. There now are established methods to compute both river flow and nitrogen load that are representative of bay-wide conditions at daily resolution. In

addition, there are two key independent and complementary monitoring programs for in situ chlorophyll and oxygen, each spanning a large portion of the bay encompassing well more than the most eutrophication-prone regions, from which metrics for bay-wide conditions using a range of thresholds (mild, moderate, severe) have been defined: the fixed-site network with excellent temporal sampling characteristics, and the spatial surveys with excellent spatial sampling characteristics. In this section explorations of the various datasets are furthered and synthesized, to provide improved understanding of how bay eutrophication is responding to the long-term managed nitrogen reductions. The framework for the discussion is the conceptual model that eutrophication is driven by nitrogen inputs causing overabundant growth of phytoplankton and high chlorophyll levels, bringing hypoxia as a result of oxygen consumption during decay. Thus the discussion proceeds from nitrogen loads to chlorophyll and then hypoxia. The role of physical drivers including temperature, winds, tidal range, and non-tidal sea level gradients is taken up last.

6.3.1 Nitrogen load by source

An expansion of the prior analysis using the daily timeseries of TN load (Codiga 2020a) from Task 2 is taken up first. Time series of loads from each of the 18 sources to the bay are examined individually (Figure 6-1). Recall, 11 sources are individual wastewater treatment facilities (WWTFs) discharging directly to the bay, 5 sources are rivers which include load from WWTFs discharging into them upstream, one source is a river with no upstream treatment facilities (Moshassuck River), and one source is ungauged runoff from areas adjacent to the bay outside of the riversheds.

To help highlight the nature of long-term changes to loads over time, the sum of loads over the May to October period is presented. This is generally the time of year when upgraded treatment plant nitrogen removal is most active, in order to comply with regulations. Loads are known to vary strongly inter-annually in close correlation with river flow, so they are shown with the summed May-Oct basin-wide river flow superposed (thick black line on Figure 6-1, right axis). The 18 sources are ordered in the plot legend based on their mean May-Oct load over the 19-year period, from highest to lowest; this order differs from that of the figures in Task 2, which was based on the mean over all 12 months of the year, but the differences are generally minor.

Year to year changes in river flow are clearly a dominant influence on the inter-annual variations in loads, but the secular long-term decline in loads due to treatment plant upgrades over the 19 year period is apparent as well. The largest individual source, the Taunton River and its upstream WWTFs, shows a tight correlation with river flow through the entire record, including the most recent years, with long-term declines not particularly apparent (blue curve). Load of the next largest source, the Blackstone River and its upstream WWTFs, is largely similar but with somewhat more clear evidence of a long-term decline, and with the 2018 and 2019 values notably lower (red curve). The third-largest source, Fields Point WWTF, shows weaker inter-annual changes, as expected because it is a WWTF not a river; it declined substantially from 2011 to 2013, with years 2011 and earlier essentially at a higher relatively constant level and years from 2013 onward at a much lower relatively constant level (light green curve). By 2012, when its upgrades were fully activated, it had declined more than halfway to its present low level, reached for the first time in 2013. The fourth-largest source, the Fall River WWTF, also shows the expected weaker inter-annual variability, but with a long-term secular change that is absent or weakly increasing (black curve). The fifth-largest source is the Pawtuxet River and its WWTFs, which shows a slow and persistent long-term decline from about 2008 to present (pink curve). The sixth-largest source, the Bucklin Point WWTF shows a sharp decline from 2004-2006 and further smaller declines in years since 2006. The remaining sources all have loads well below the levels of the Fall River WWTF, the

Pawtuxet River and its WWTFs, and the Bucklin Point WWTF prior to its 2004-2006 decline; this includes the next-largest source, ungauged runoff direct to the bay from ungauged areas outside the river watersheds (dark green curve), which by definition is directly proportional to river flow.

Hypoxia in Narraganset Bay has been shown generally to be most prevalent and severe in the upper bay and areas to the north and west of it (e.g., Codiga et al 2009). It is of interest then to divide the loads from the 18 sources in to two portions, one which is delivered directly to those waters and second which is delivered to Mount Hope Bay. The sources are grouped based on whether they are located to the west or east of the Mount Hope Bridge, at the western edge of Mount Hope Bay; load from ungauged runoff direct to the bay, from areas outside the river watersheds, is assigned half to each of the two groups, as this reflects the rough proportion of runoff draining to waters east and west of the Mount Hope Bridge (Figure 2-1). The group of sources to the east of the Mount Hope Bridge includes the Taunton River and its upstream WWTFs, the Fall River WWTF, and the Somerset WWTF; the group to the west of the bridge includes all other sources. Results make clear that long-term declines in TN load are more pronounced for sources to the west of the bridge, and notably weaker for sources entering Mount Hope Bay (Figure 6-2). In addition, this figure makes clear that the 2004-2006 decline at Bucklin Point and the 2011-2013 decline at Fields Point (see Figure 6-1) each were major contributors to the decline of load from sources west of the Mount Hope Bridge during those year ranges.

6.3.2 Nitrogen load and river flow: long-term changes, seasonality

From here forward the bay-wide TN load is the focus. A scatter plot of TN load vs river flow is instructive because it facilitates comparisons of loads before and after the main declines due to plant upgrades, in effect grouping years based on river flow (Figure 6-3). The months June to September, same as are used to designate years as wet/intermediate/dry (Task 1), are used in Figure 6-3 but the results are similar for other periods that include the summer, such as May to October (not shown). From 2013 onward (triangles) the load for a year of given river flow is notably lower than during earlier years (circles) of similar flow. The one year from 2013 onward with relatively high flow was 2013 (triangle in right half of figure). All subsequent years (2014-2019) have had low or intermediate flow (six triangles in left half of figure), and corresponding loads that are all less than any prior year in the record, with the exception of 2017 which is on par with the lowest prior year. Of note is that during 2012, when plant upgrades were mostly complete (as explained in the prior section), there was already evidence, though not as pronounced as in years to follow, of the load decline relative to earlier years with similar river flow.

Some clarifications about the use of the term “post-reduction” by Codiga 2020a should be made. In that report the first “post-reduction” year was taken to be 2014. This is not unreasonable with respect to hypoxia, which was as severe in 2013 as in prior comparably wet years. However, as Figure 6-3 makes particularly clear, the TN load had in fact declined in 2013 relative to years with comparable river flow. Consequently, with respect to TN load specifically, if there was a need to identify a first “post-reduction” year then 2013 could be a more suitable choice than 2014. However, for both the load declines and response of hypoxia the changes span multiple years, so there is a limit to how meaningful it is to identify a single year as “post-reduction”. In any case, more important than attempting to designate when the a first “post-reduction” year occurred is the fact that in 2013, when TN load had declined, hypoxia did not decline, making clear that there is a lag of at least a year in the response of the bay. Further discussion of this topic is taken up in section 6.3.6 below.

To examine seasonality of long-term variability in loads and river flow, rather than focusing on the summer only as above, the sums over the 6-month summer-centered May-Oct period for each year and the prior winter-centered Nov-Apr period are compared to their sum, the annual totals (Figure 6-4).

Consider first the river flow (dashed lines, right axis). As expected, the winter-centered period contributes substantially more to the 12-month result than does the summer-centered period. In addition, a prominent feature of all three curves is a period of markedly lower flow from 2012-2016. Following that dry period, in 2017 the summer-centered flow rose modestly to a level nearer to normal and winter-centered flow was still very low so the 12-month flow increased modestly; then in 2018-2019 the summer-centered flow remained similar to 2017 but there were substantial increases in winter-centered flow and therefore in the 12-month flow. A prominent feature of the whole record for summer-centered flow is that from 2002 to 2011 about half of the years were local maxima with runoff substantially higher than the long-term mean, but from 2012 onward no year has been comparably as wet. In contrast, for winter-centered and 12-month flow, conditions following the dry period have returned to be comparably as wet as the wetter earlier years.

The TN load results (solid lines, left axis) can be viewed in context of the river flows. Load parallels river flow sufficiently tightly that it is higher during the winter-centered period than the summer-centered period by a factor comparable to the increases of winter-centered flow over summer-centered flow. The dry period 2012-2016 had reduced flows and loads during all periods of the year. The difference between these lower flows and loads and the higher levels during the pre-2012 part of the record is larger than the long-term secular changes, making the latter more difficult to identify.

Nonetheless the long-term secular declines in loads due to plant upgrades are clear, as described in the previous subsection, in the summer-centered results; as noted, the May-Oct summer-centered period is when treatment plants apply nitrogen removal to comply with regulatory requirements. In contrast, for the winter-centered load there have been larger increases in the last few years of the record, paralleling river flow, and a long-term secular trend is not as apparent. Because the winter-centered load is so much larger than the summer-centered load, the long-term secular trend in the 12-month load also is only weakly apparent. In this context the summer-centered treatment plant TN load reductions, although substantial and apparently leading to declines in indicators for eutrophication (chlorophyll, oxygen) as discussed below, can be noted to have relatively small influence on the annual total loads.

6.3.3 Role of stratification

It has long been recognized that inter-annual variations in hypoxia severity are linked strongly to river flow variations. However, as discussed by Codiga (2020a), river flow variations drive variations in both nutrient loads and density stratification (Codiga, 2012), so it has been challenging to determine which of these two is most tightly linked to hypoxia. One hypothesis is that nutrient loads are always high enough to drive hypoxia but only when stratification is sufficiently strong does it occur; another hypothesis is that hypoxia is driven by nutrient loads primarily, with stratification a secondary influence. Codiga (2020a) suggested that to resolve this would require new approaches that better isolate specific mechanisms. However, with the additional two years 2018-2019 included in the record, it now has become clearer that the latter hypothesis (stratification secondary to nutrient load) is the more applicable interpretation.

As shown below, there is a relationship between nitrogen load and changes in chlorophyll and oxygen conditions, for both inter-annual variability and long-term declines. In addition, as shown above, long-

term declines in nitrogen load are due to treatment plant upgrades and are distinct from river flow in that the latter does not show a parallel long-term decline. This stands in contrast to the relationship between bay-wide June to September stratification and river flow, which are correlated tightly (Figure 6-5) for all years. Bay-wide stratification is the mean across 8 of the 11 fixed site stations, excluding the three (PD, GB, SR) shallow embayments where inter-annual variability is more pronounced and independent from that of the other 8 stations.

The tight relationship between river flow and stratification spans both years prior to 2013 and from 2013 onward, in contrast to the situation for nitrogen load shown in Figure 6-3 and described above; stratification during the recent years 2018-2019 was similar to 2017 and, importantly, comparable to stratification in earlier years with similar river flow. This supports the conclusion that stratification is sufficiently correlated to river flow that variability in this relationship is not strong enough to explain, better than nitrogen loads do, the long-term changes underway in chlorophyll and oxygen. Stratification likely is a necessary condition for hypoxia, but long-term changes in nitrogen load are primarily responsible for the corresponding reductions of chlorophyll levels and hypoxia.

6.3.4 Changes in chlorophyll and hypoxia due to nitrogen load reductions

It is informative to examine the time series of mean June to September conditions over all years of the record for bay-wide river flow and nitrogen load, together with bay-wide metrics for severe and moderate surface chlorophyll and hypoxia conditions from the fixed-site and spatial survey monitoring (Figure 6-6). The top frame in the figure shows the river flow and nitrogen load results described in detail above, to provide context for the chlorophyll and hypoxia results in frames below. The chlorophyll results are grouped by severe (second frame) and moderate (third frame) thresholds, defined as the 80th and 50th percentile concentrations for the respective monitoring datasets: the Chlorophyll Index from fixed-site time series (dark green, left axes) relative to 17.6 ug/L and 9.4 mg/L thresholds, and the percent area from the spatial surveys (light green, right axes) above 27.5 ug/L and 14.0 ug/L. Similarly, the hypoxia results are grouped by severe (fourth frame) and moderate (bottom frame) thresholds of 1.4 mg L⁻¹ and 2.9 mg L⁻¹ respectively (same thresholds for time series and spatial surveys). The Chlorophyll Index and Hypoxia Index results are averages across 8 of the 11 fixed site locations, excluding the three (PD, GB, SR) shallow embayments where inter-annual variability is more pronounced and independent from that of other stations across the bay. The percent area metrics from the spatial surveys are computed as the mean across the 5-7 one-day surveys each summer.

The chlorophyll results show similar evidence of long-term declines in both the fixed site and spatial survey datasets, that are comparable for both the severe and moderate thresholds. The severe thresholds are the 80th percentiles of all values in each dataset: 17.6 mg L⁻¹ for the fixed site time series and 27.4 mg L⁻¹ for the spatial surveys. The moderate thresholds are the 50th percentiles: 9.4 mg L⁻¹ for the fixed sites and 14.0 mg L⁻¹ for the spatial surveys. The fixed site concentrations at a given percentile are lower than those of the spatial surveys because the fixed site stations are generally located in deeper areas, on or near the channels, and therefore unlike the spatial surveys do not sample shallower off-channel locations where chlorophyll reaches higher concentrations.

The visual similarity between the Chlorophyll Index results (both severe and moderate thresholds; dark green in second and third frames) and the nitrogen load (purple in top frame) is clear for both the inter-annual changes over 1-3 year periods and also the long-term declines over the full duration of sampling. In 5 of the most recent 6 years (after major nitrogen load declines had occurred) the Chlorophyll Index is

equal to or less than all prior years except 2007 (severe threshold) or less than all prior years (moderate threshold). A scatterplot illuminates the nature of the relationship (Figure 6-7). One of the most pronounced differences between the Chlorophyll Index variations and those of nitrogen load was during 2018-2019, when the former declined much more than the latter (Figure 6-6). The reason for this is not yet understood.

As noted, the spatial surveys sample both shallow and deep areas of the bay, but are infrequent so may be less representative of season-long conditions, whereas the fixed site results on which the Chlorophyll Index is based are representative mainly of deeper areas. Despite these underlying differences in the metrics, in Figure 6-6 the percent high-chlorophyll area from spatial surveys (light green) and the Chlorophyll Index (dark green) show similar year-to-year variability and long-term declines (second and third frames). There are some differences, for example the percent high-chlorophyll area for the severe threshold had somewhat larger declines earlier (2012) while the percent high-chlorophyll area for the moderate threshold had somewhat larger declines later (2015-2017). However these differences are not pronounced, and may be associated with the contrasting natures of the two metrics, which is expected to cause differences between them. Overall, these independent datasets are indicating quite similar results, reinforcing confidence in them.

Hypoxia results (Figure 6-6: dark red, left axes for Hypoxia Index from fixed site time series; light red, right axes for percent area oxygen below threshold from spatial surveys) for the severe 1.4 mg L^{-1} threshold (fourth frame) and moderate 2.9 mg L^{-1} threshold (bottom frame) show long-term declines at least as substantial as seen in chlorophyll. From 2014 onward the Hypoxia Index relative to both the severe and moderate thresholds was zero or less than all non-zero years prior to 2014.

The Hypoxia Index relative to the severe threshold (dark red, fourth frame), an indicator of the lowest oxygen conditions, was meaningfully higher than zero in 3 years, the most recent of which was 2013. It seems likely, based on this Hypoxia Index result, that severe hypoxia has become extremely rare. The Hypoxia Index relative to the moderate threshold (dark red, bottom frame), as expected, is non-zero more often, but from 2014 onward it has been zero or lower than in all prior years. Moderate hypoxia has become more uncommon during the period after the main nitrogen load declines.

The spatial survey percent area hypoxic metrics (light red) also show long-term declines, with values since 2014 lower than or comparable to the lowest values in earlier years. The inter-annual variability of the percent hypoxic area differs from that of the Hypoxia Index more so than the percent high-chlorophyll area differs from that of the Chlorophyll Index. This is somewhat surprising because the deeper areas of the bay where hypoxia is more prevalent are sampled more similarly by the spatial surveys and fixed site locations than is the case for surface chlorophyll.

Scatterplots show the relation between hypoxia metrics and nitrogen loads (Figure 6-8). For the severe threshold (upper frame) the high number of zeros, as noted above, limits potential for a tightly correlated linear relationship. This is not as much of a limitation for the moderate threshold results (lower frame), for which a correlation is apparent.

Considering all the evidence, the various bay-wide eutrophication-related conditions examined lend support to the interpretation that the response of Narragansett Bay to managed nitrogen load reductions consists of declines in both chlorophyll levels and the frequency and severity of hypoxic events. This interpretation could not be made as confidently before the inclusion here of 2018-2019 results, because the decline has occurred gradually over several years and is superposed on larger year-

to-year variations. However, it is supported by the agreement of metrics from both fixed-site time series and spatial surveys, two complementary and independent monitoring programs.

This interpretation of the bay response aligns well with the consensus or conventional wisdom from research on eutrophication in estuaries, that by reducing nutrient loads the associated excess chlorophyll can be reduced sufficiently that the hypoxia driven by its decay will also become less severe. By this reasoning load reductions affect chlorophyll directly and affect hypoxia indirectly through their effects on chlorophyll. Hypoxia responds not only to changes in chlorophyll but also other processes. As noted above, in the 6 years since the main decline in load, there has not been a summer that is comparably as wet as the summers of 2006 and 2009 when chlorophyll levels and hypoxia metrics peaked. In some future year when such a wet summer occurs, the difference between its chlorophyll and hypoxia conditions and those during 2006 and 2009 should provide more definitive information as to how much managed reductions of nitrogen loads have changed the bay. However, even lacking such a wet summer, based on the entire record—more than 15 years, with at least 6 years since the main nitrogen load decline occurred, some of which had intermediate to strong river flow—with the inclusion of 2018-2019, it is clear that chlorophyll and hypoxia have decreased substantially and that the declines are linked to the nitrogen load reductions.

6.3.5 Physical drivers: temperature, wind, tidal range, sea level differences

The interpretation supported in the above discussion is that long-term changes in chlorophyll and hypoxia metrics are tied to nitrogen load declines, with substantial inter-annual variability superposed due to the dominant role of river flow on nitrogen load. It suggests that the role of physical drivers other than river flow (temperature, winds, tidal range, sea level differences) are secondary in importance. This is consistent with some earlier initial explorations (e.g. Codiga 2020a) of the potential that physical drivers could explain some of the variability in hypoxia.

Here, we briefly reexamine physical drivers to see if any relationships between them and the variability in chlorophyll and/or hypoxia might be strong enough to be considered of primary importance. For each physical driver there are plausible hypotheses relating it to chlorophyll and/or hypoxia. Temperature sets rates of metabolic processes, and reduces solubility of oxygen, so warmer conditions can be expected to be associated with higher chlorophyll levels and more severe hypoxia. Winds drive aeration through the air-sea interface, which can alleviate hypoxia, and also have major impact on the strength and direction of currents which influence chlorophyll and hypoxia through advection. The power available for tidal mixing, which can break up stratification to change the vertical distribution chlorophyll and end near-seafloor hypoxic events, is proportional to the cube of the tidal range, an indicator of spring-neap tidal variations. Finally, the non-tidal sea level difference between Providence and Newport is a measure of large-scale pressure differences that affect weather-band variability in the circulation and flushing time of the estuary, a potentially major influence chlorophyll and hypoxia.

It is informative to examine the physical drivers averaged over the same June to September period used for river flow and TN load (Figure 6-9). For context the top two frames of the figure show river flow, TN load, and the moderate-threshold Chlorophyll Index and Hypoxia Index results repeated from Figure 6-6. Visual inspection suggests that none of the physical drivers are characterized by inter-annual peaks and valleys that parallel those in the Chlorophyll Index and Hypoxia Index as closely as do the TN load.

The temperature (3rd frame of figure) results show a long-term trend for warming (further explored in Task 7). The interpretation made above, that long-term declines in TN load are responsible for long-term

declines in chlorophyll and hypoxia, implies that the latter are occurring despite the opposing influence of warming temperatures increasing metabolic rates. The influence of temperature on stratification has been shown to be minor (see Task 7; also Codiga, 2020a). Stratification has been shown earlier in this task to be more strongly correlated to river flow, and thus less tightly associated with chlorophyll and hypoxia, than nitrogen load.

The wind speed and wind direction results (4th frame of figure) show little evidence of a systematic relationship to the trends or year-to-year variability in the Chlorophyll Index and Hypoxia Index results. They may be important in an individual year, on occasion, but are considered to be of at most secondary importance to the year-to-year and long-term patterns in chlorophyll and hypoxia.

A long-term increase in tidal range cubed (bottom frame of figure, left) seems clear, which potentially supports the hypothesis that it drives the long-term decline in hypoxia. However, there is no clear corresponding long-term trend in stratification (e.g., top frame, Figure 6-6), which suggests that the magnitude of tidal range changes is not large enough to have impact. In addition, although an earlier study using the first few years of fixed-site observations suggested that hypoxic events were associated with weaker tidal mixing during neap tides (Bergondo et al, 2004), later investigations based on a longer period of measurements showed that tidal range is not linked to hypoxic events (Codiga et al., 2009). It follows that tidal range is only of secondary importance.

Like wind speed and direction, the non-tidal Providence-Newport sea level difference (bottom frame of figure, right) varies in characteristically different ways than the chlorophyll and hypoxia results. So it is considered of secondary importance at most, except possibly during an individual year.

The overall conclusion remains that chlorophyll and hypoxia variability (both year-to-year extrema, and long-term trends) is primarily the result of variations in TN load. Physical drivers may potentially be important during an individual year, on occasion, but are at most secondary in importance. These conclusions are based on examining the mean of selected parameters over the June to September period; investigations of other parameters, and/or other averaging periods or methods, might lead to different conclusions, but this analysis makes this seem less likely.

6.3.6 Additional discussion

Delays of a year or more between nutrient load changes and chlorophyll/hypoxia responses. It is important to note that the response of bay chlorophyll and hypoxia to nitrogen load declines was not apparent during 2013 (Figure 6-6), despite that this was the first summer when the most prominent load reductions were effectively completed (Figure 6-3 and Figure 6-6). This result does not fit the above-described narrative of how the bay has responded to load reductions (with chlorophyll relatively tightly correlated to nitrogen loads each summer i.e., on timescales shorter than a year): there was a lag of at least a year before chlorophyll and hypoxia responses to the 2013 load decline were meaningful. Given that the flushing time of the bay is on the order of days to weeks, this implies a process acting on a longer timescale is important.

The 2018-2019 results also suggest processes acting on a timescale longer than a year are playing a role. As noted above, during 2018-2019 river flow was moderate to strong and nitrogen loads rose correspondingly compared to the prior few dry years, but chlorophyll and hypoxia remained lower than prior years with comparable nitrogen load.

In order to better understand these aspects of the system, processes that can potentially influence bay eutrophication on timescales of a year or longer deserve further investigation. There are many such processes. A prominent possibility is sediment fluxes. The physical drivers explored above also could be important, as could flux of nitrogen into the system from offshore, discussed next.

Influence on bay nitrogen budget of exchange with offshore waters. Rosa (2020) studied exchange processes between the bay and offshore waters using field observations and hydrodynamic simulations, and applied the results to revise the bay nitrogen budget of Nixon et al (2008). A conclusion drawn was that the input of nitrogen to the bay from offshore is a substantially larger fraction of the total than found by Nixon et al (2008). The increased role of offshore inputs was due to two changes made by Rosa (2020) in estimating the budget: the input from wastewater was reduced by 50% based on treatment plant upgrades that have occurred since the Nixon budget, and the input from offshore was increased by a factor of 3.6, based on use of an offshore nutrient concentration almost twice as high together with a volume transport in to the bay from offshore almost twice as high.

While the result is provocative, results detailed in this report suggest that the influence of offshore nutrient fluxes on eutrophication in the bay is of secondary importance. The main evidence for this conclusion is that both the year-to-year variability and long-term declines of chlorophyll metrics follow nitrogen loads from the watershed (Figure 6-6 and Figure 6-7).

In addition, the possibility that offshore inputs of nitrogen have a primary impact on eutrophication, which occurs in the far northern reaches of the bay, also seems unlikely given the north-south gradients in the bay. These gradients are prominent and well understood characteristics of observed concentrations of nutrients and chlorophyll in the bay. The highest concentrations are in the northern areas most distant from offshore inputs.

There are at least a couple ways to resolve the apparent disagreement between the results here, that watershed nitrogen loads are dominant, and the Rosa (2020) result that offshore inputs of nitrogen are important. First, the updated offshore flux estimates are highly uncertain because they are the product of the offshore concentration and the volume transport in to the bay, both of which are very poorly known. In addition the fluxes have been shown to vary substantially on short timescales, but are estimated based on infrequent sampling. So the estimate by Rosa (2020), which is for the long-term mean, may be at the high end within the range of uncertainty, which itself is very large, and the actual long-term mean contribution may be much lower.

Secondly, even presuming that the Rosa (2020) result for higher offshore nitrogen flux in to the bay is accurate, it does not necessarily follow that nitrogen concentrations in the northern portions of the bay would be influenced by the offshore flux. This is because nitrogen from offshore enters the bay mainly at the southern end of the lower East Passage. The ultimate destination of this nitrogen is determined by complex circulation pathways and associated dispersion processes. At least a fraction of it can and likely does exit the bay by advection before reaching northern areas where it could affect chlorophyll important to eutrophication.

Offshore waters entering the bay are part of the estuarine exchange flow, which is fundamentally driven by freshwater inputs and thus expected to have year to year variations that parallel those of river flow, to the extent other processes (such as the influence of wind) are less important. This basic dynamic implies that nitrogen flux in to the bay in the deep incoming limb of estuarine exchange would increase during a wet summer, when nitrogen loads from the watershed also increase, and vice-versa. Therefore,

while considered unlikely based on the above discussion, it is possible that nitrogen loads to the northern portions of the bay where excess chlorophyll and hypoxia occur do include a large portion coming from offshore. If so, the treatment plant load reductions are a smaller fraction of the total inputs than if offshore inputs are ignored, but nonetheless their influence appears responsible for the declines in chlorophyll and hypoxia, as shown above.

Based on the results of Rosa (2020), nitrogen flux in to the southern end of the bay from offshore is sensitive to the direction of local winds. However, in the above exploration of the potential relationship between wind direction and chlorophyll and hypoxia no strong relationship was seen, consistent with offshore shore having a minor influence at most. Nonetheless it is possible offshore inputs of nitrogen may have some effects in certain individual years. For example, an unusually high or low offshore input may contribute to apparent lags (discussed above) that occur between watershed nutrient load changes and changes in chlorophyll or hypoxia.

Figure 6-1. TN load timeseries for 18 individual sources to the bay (left axis), with bay-wide river flow superposed as thick black line (right axis); both are the mean over the May-Oct period.

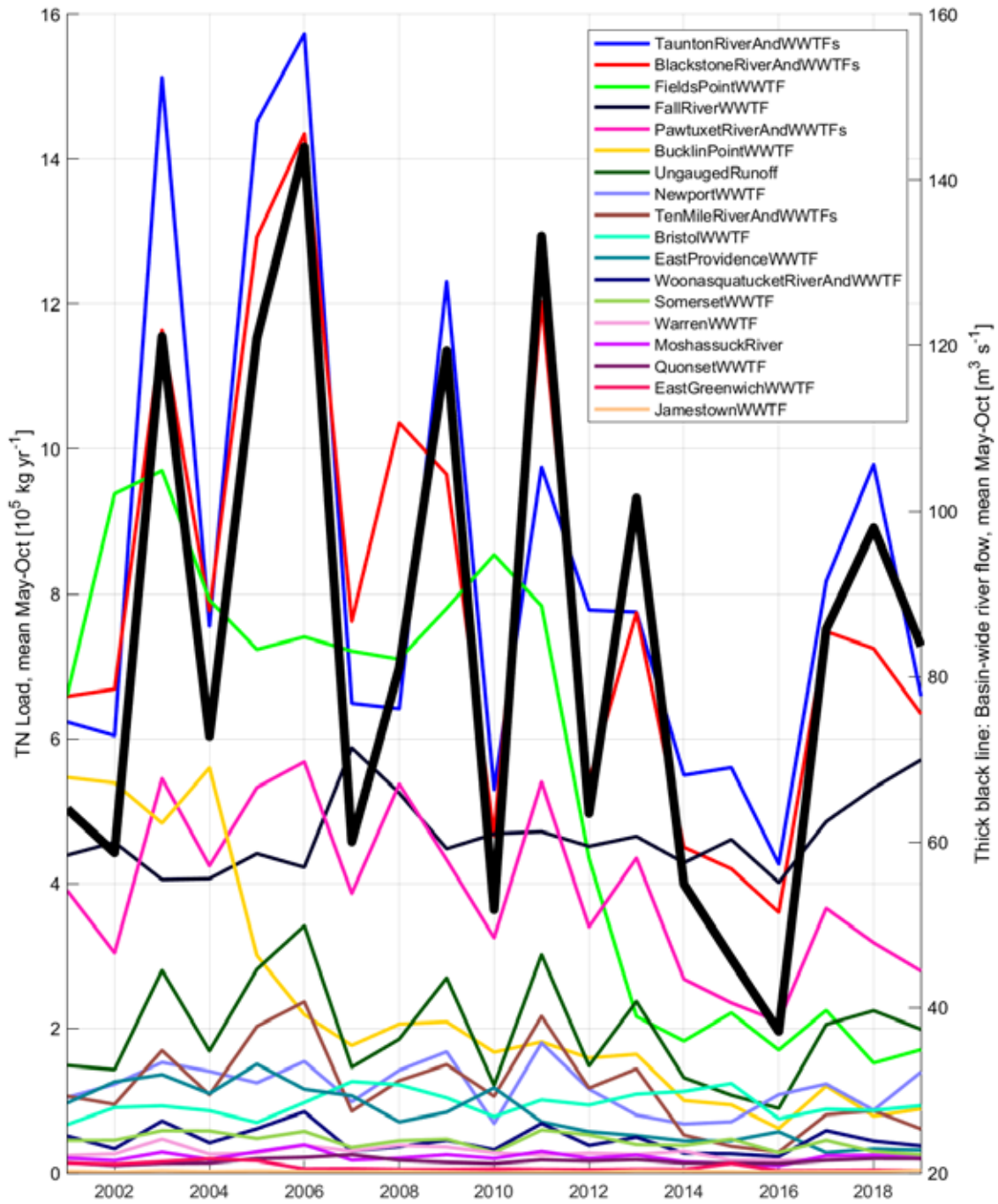


Figure 6-2. TN load from sources to the east and west of the Mt Hope bridge, May-Oct, with river flow superposed.

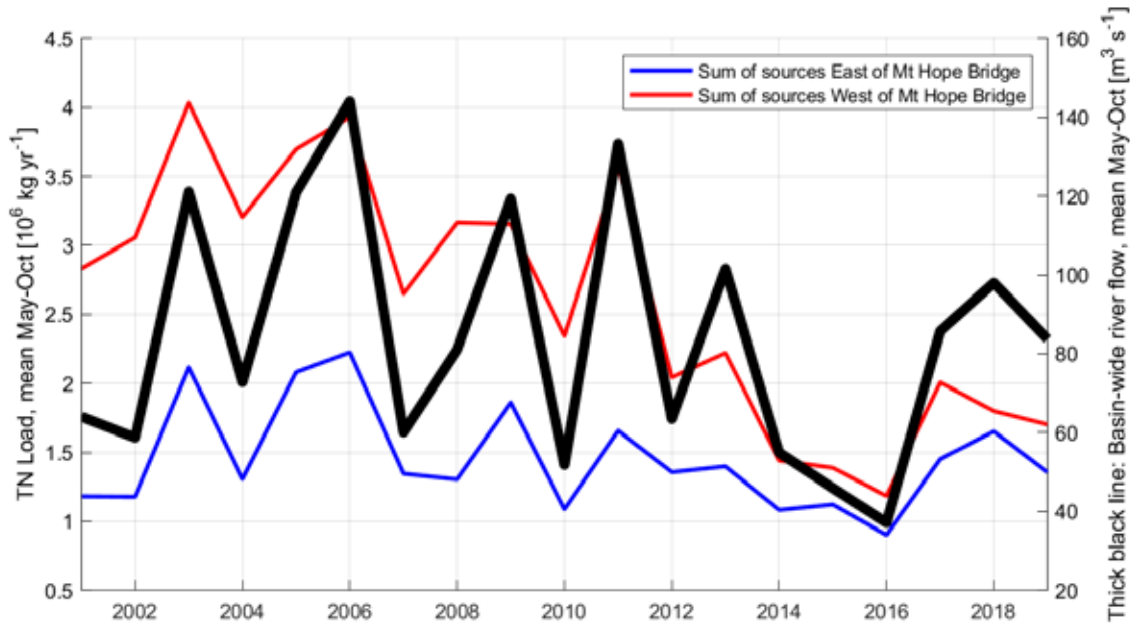


Figure 6-3. Scatter plot of bay-wide TN load vs bay-wide river flow, means over the June-September period. Years prior to 2013 are circles and years from 2013 onward are triangles. The latter are all notably lower, for each range of river flow, which quantifies the extent to which treatment plant upgrades have reduced loads. Linear regressions to the two year ranges have r^2 values 0.94 and 0.98, respectively (both $p < 0.05$).

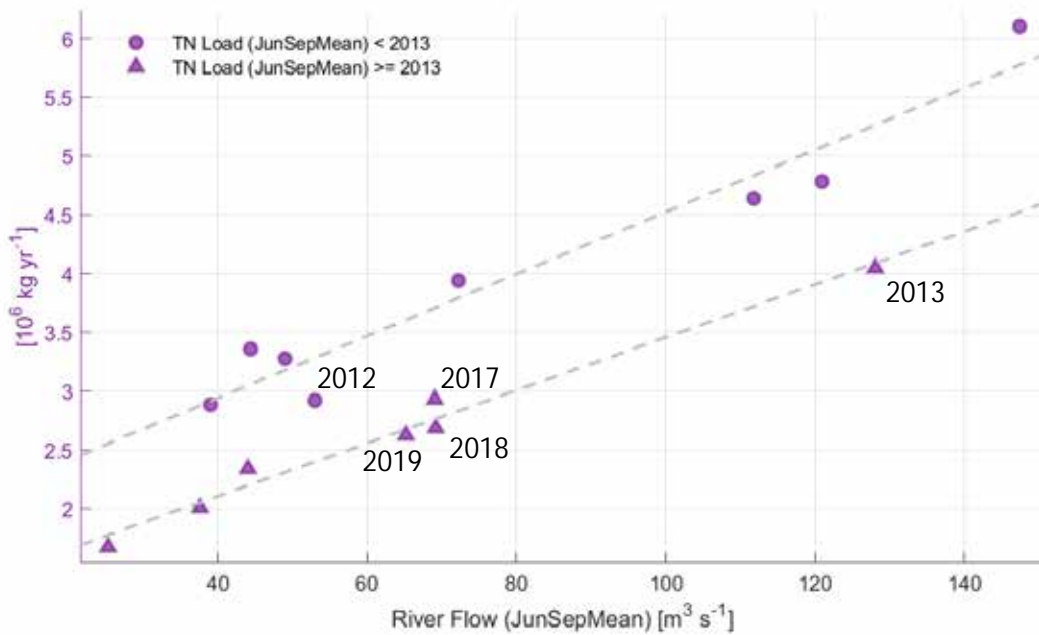


Figure 6-4. Bay-wide TN load (left axis, solid curves) and river flow (right axis, dashed curves) sums (TN load in lb; river flow in m³) broken out by time of year: all 12 months (red); Nov-Apr, the 6 months centered on winter (blue), and May-Oct, the 6 months centered on summer (black). Note scale factor at top of each y-axis.

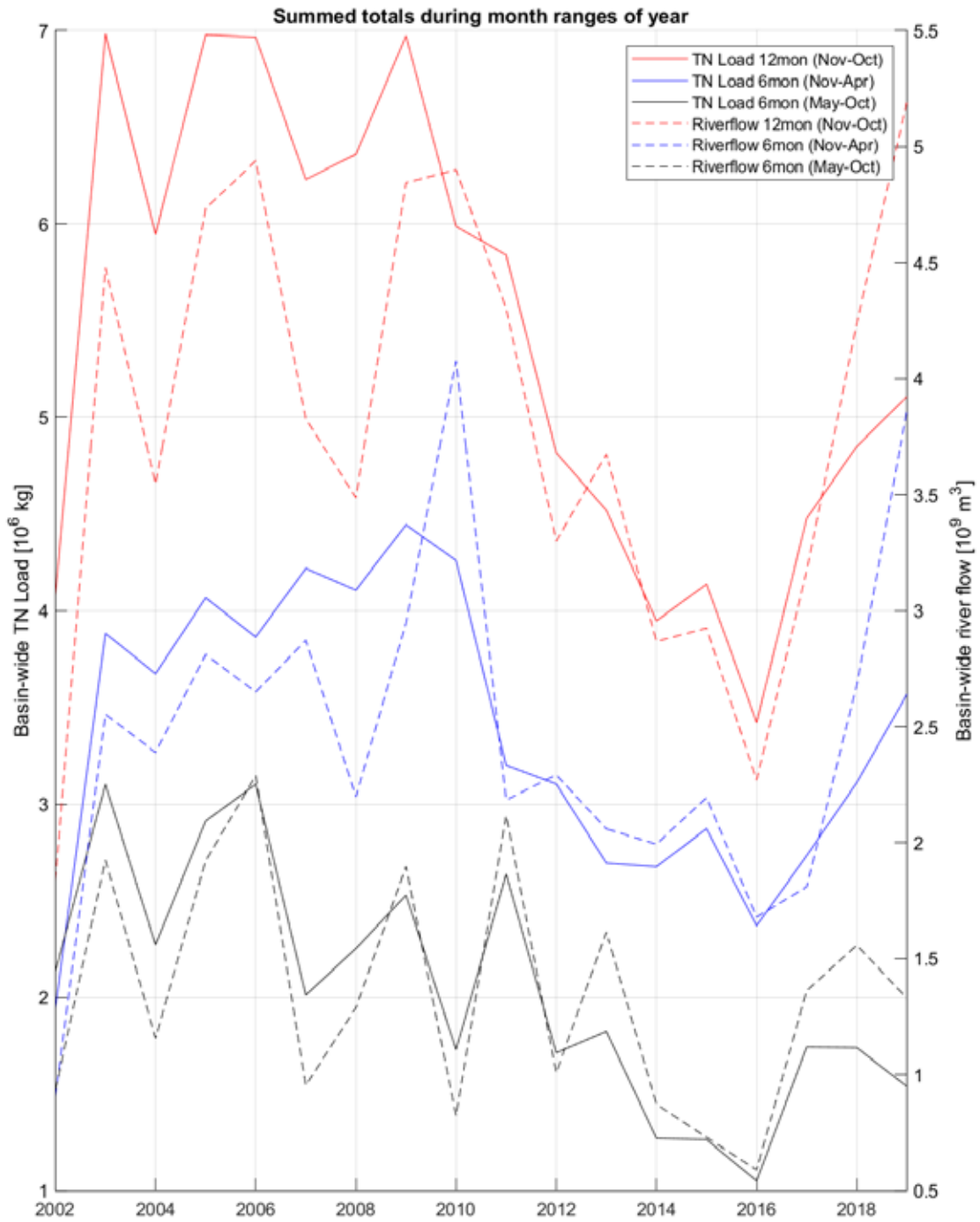


Figure 6-5. Bay-wide stratification vs bay-wide river flow, June to September mean. Linear regression in scatterplot is based on all years and has r^2 value 0.94 with $p < 0.05$.

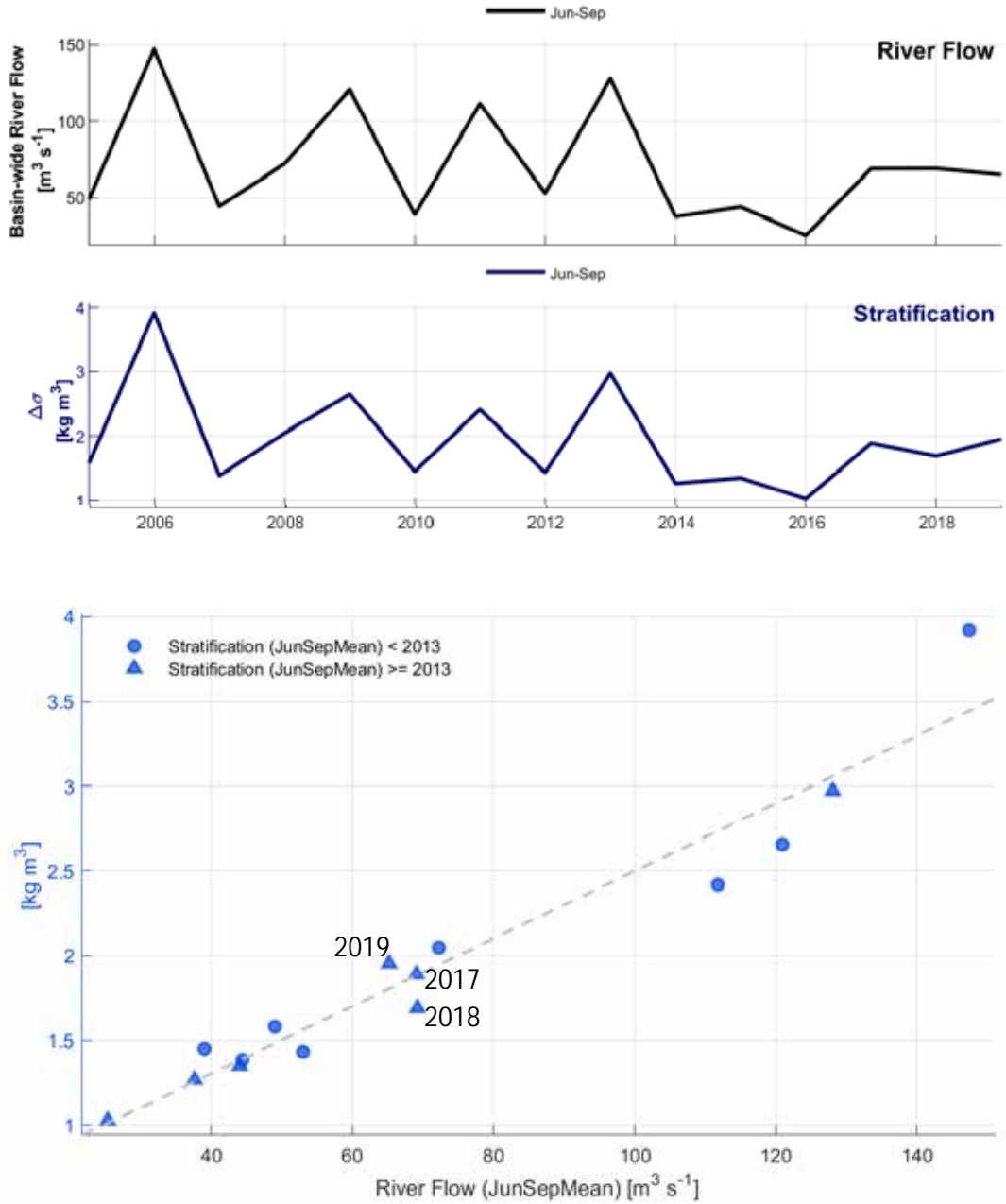


Figure 6-6. Time series 2005-2019 of bay-wide eutrophication-related summer conditions in relation to river flow and TN load.

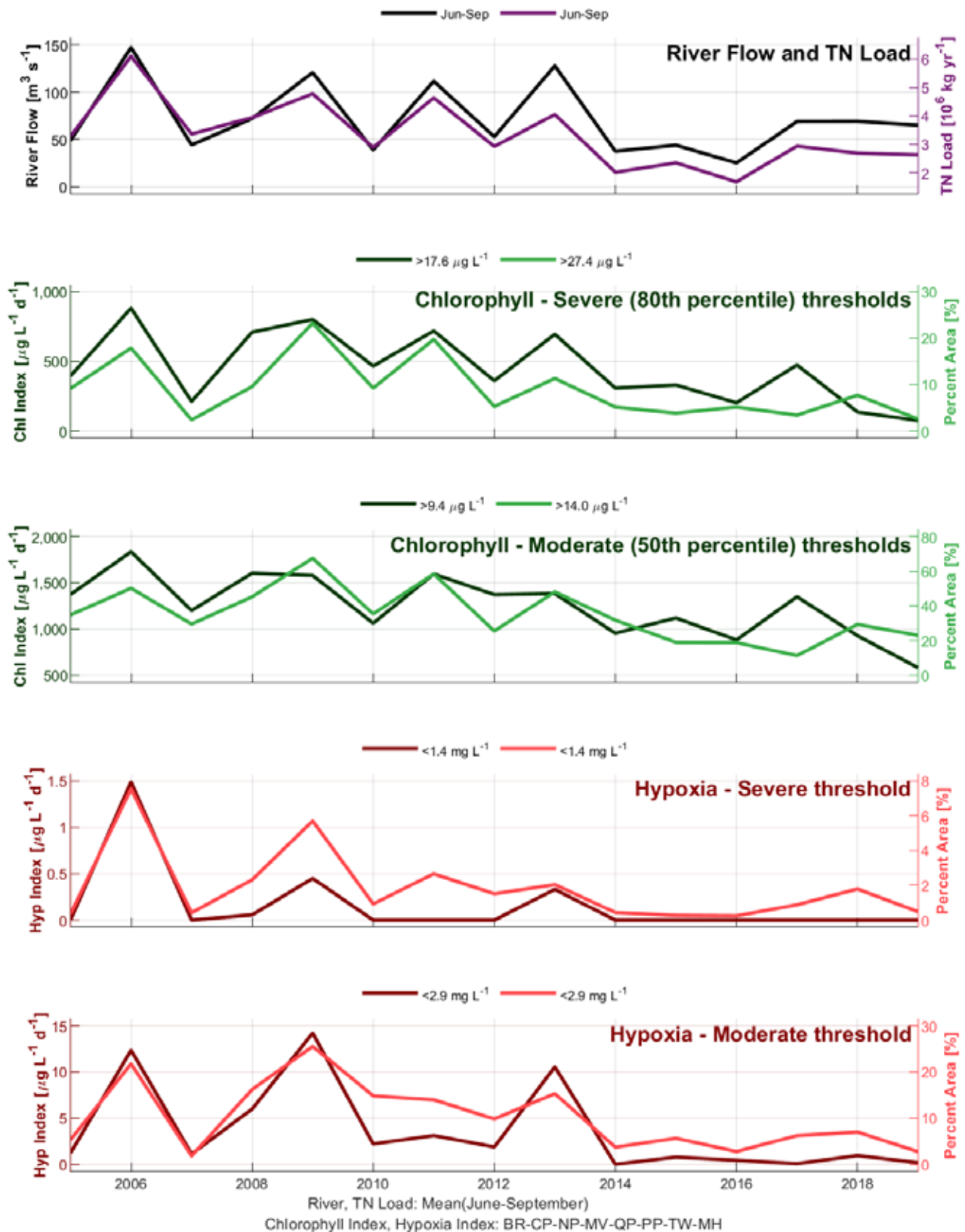


Figure 6-7. Bay-wide chlorophyll metrics vs June to September mean bay-wide TN load. Upper frame: severe thresholds. The r^2 values for Chlorophyll Index and percent high-chlorophyll area are 0.73 and 0.66 respectively (both $p < 0.05$). Lower frame: moderate thresholds. The r^2 values for Chlorophyll Index and percent high-chlorophyll area are 0.71 and 0.64 respectively (both $p < 0.05$).

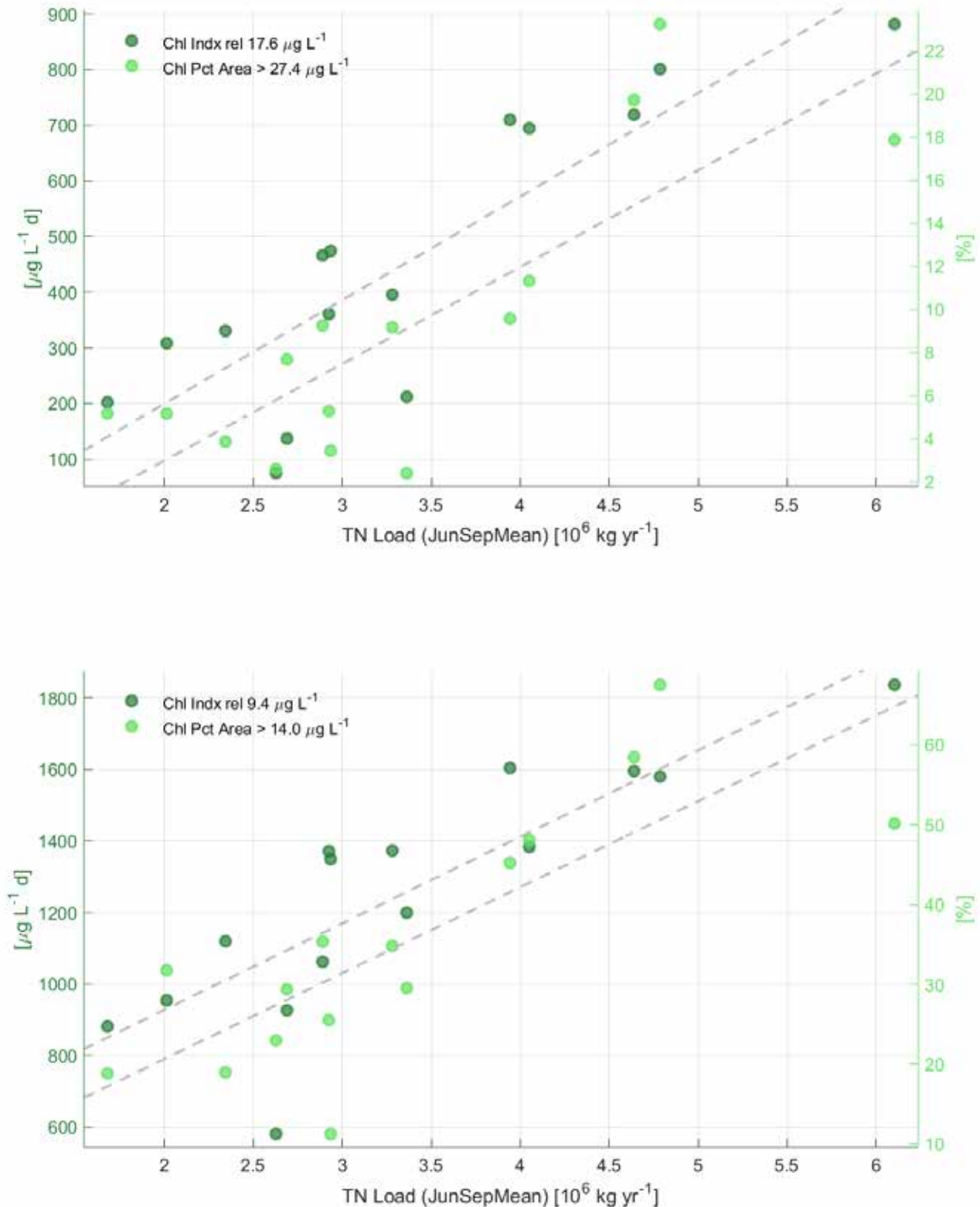


Figure 6-8. Bay-wide hypoxia metrics vs June to September mean bay-wide TN load. Upper frame: severe threshold. (No regression lines because of the high fractions of zero values.) Lower frame: moderate threshold. Regression lines for Hypoxia Index and percent hypoxic area have r^2 values 0.68 and 0.67 respectively (both $n < 0.05$).

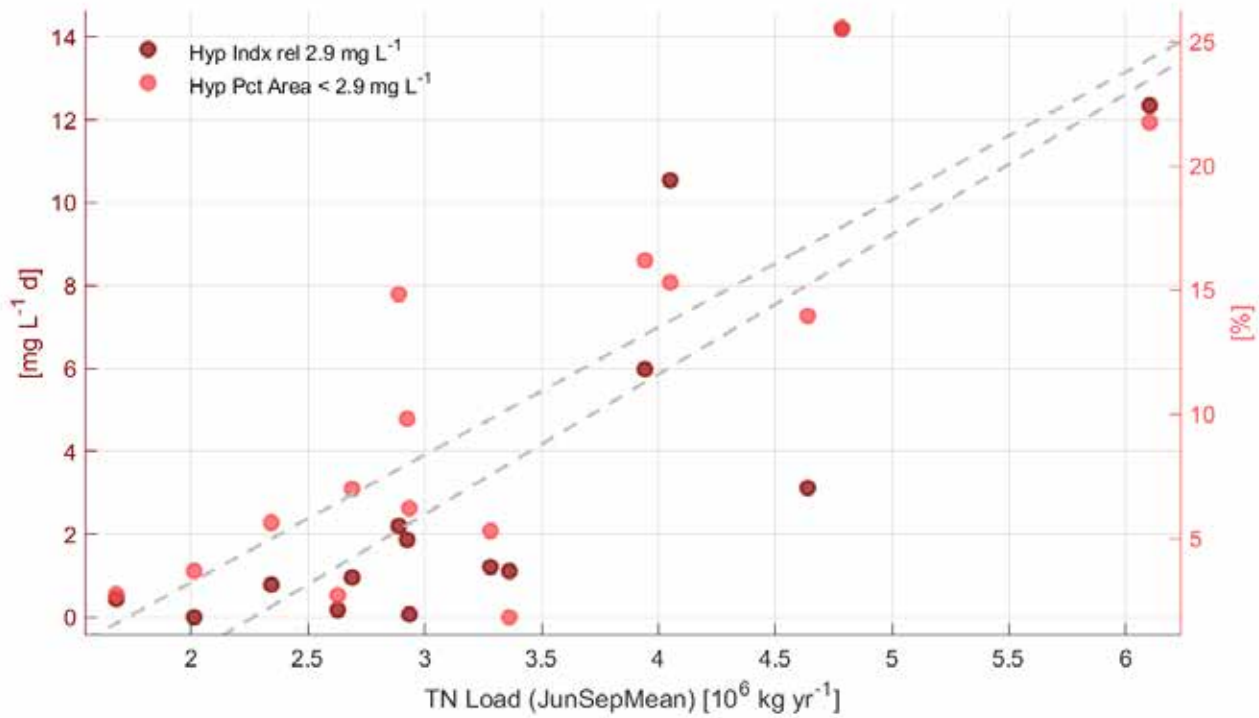
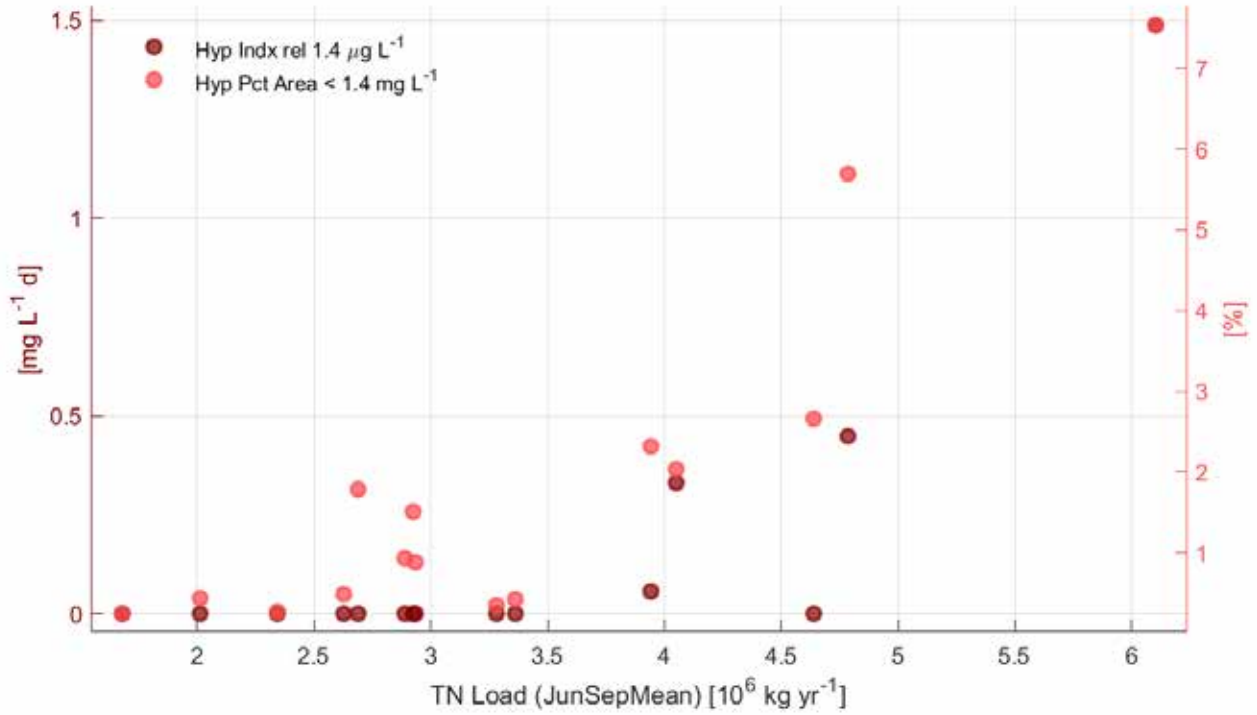
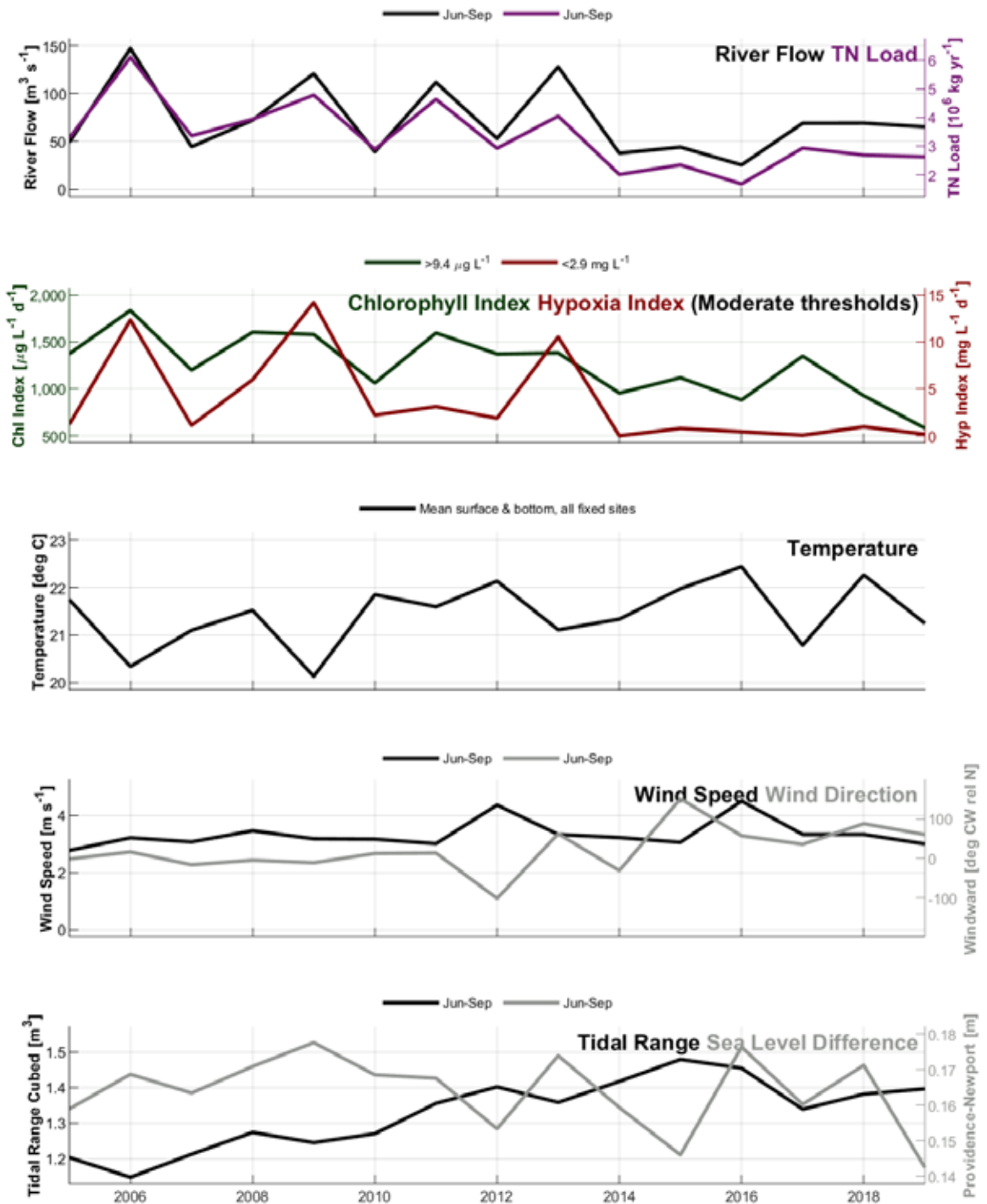


Figure 6-9. Physical drivers, mean June to September: temperature (frame 3), wind speed and direction (frame 4), tidal range (frame 5 left), and Providence less Newport non-tidal sea level (frame 5 right). To provide context, in frames 1 and 2 the river flow, TN load, Chlorophyll Index, and Hypoxia Index results from Figure 6-6 are shown.



Figures with American units for TN Load (designated by "A" prefix to figure number).

Figure A6-1.

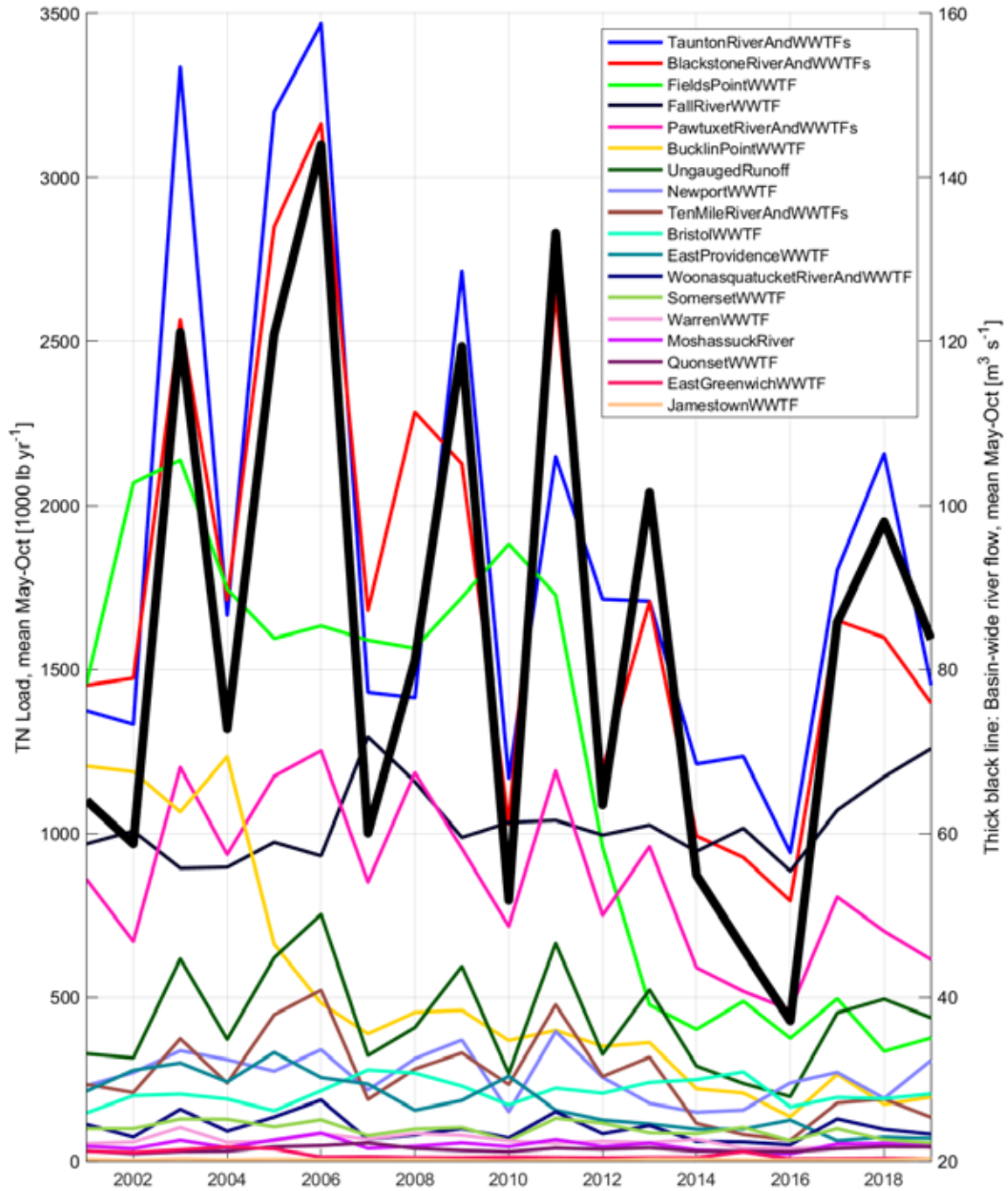


Figure A6-2.

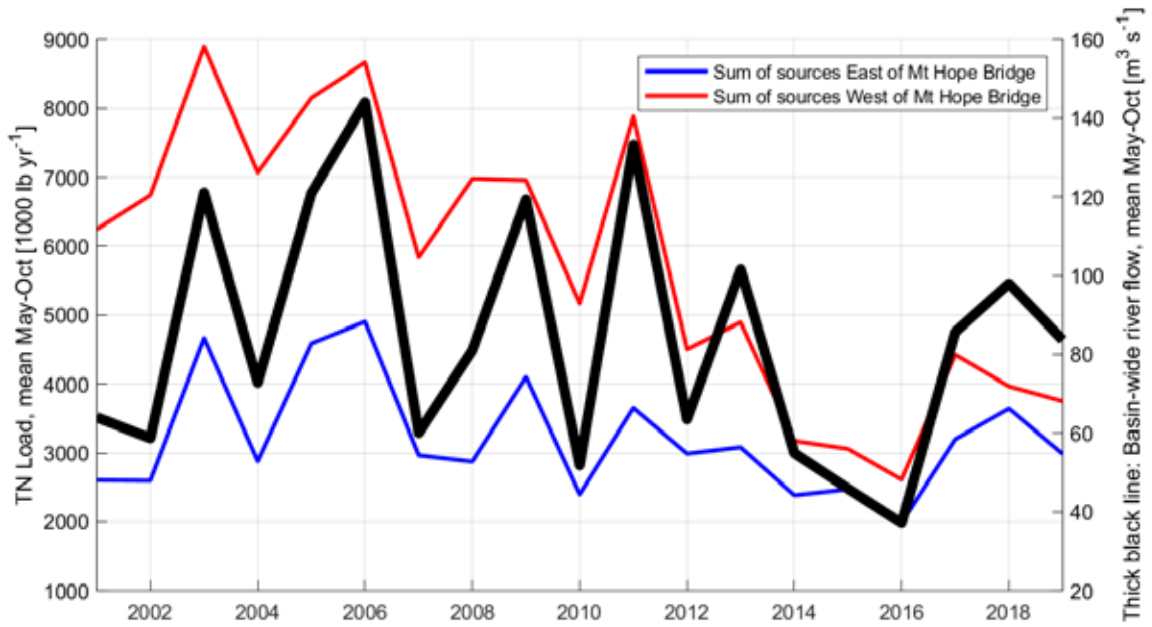


Figure A6-3.

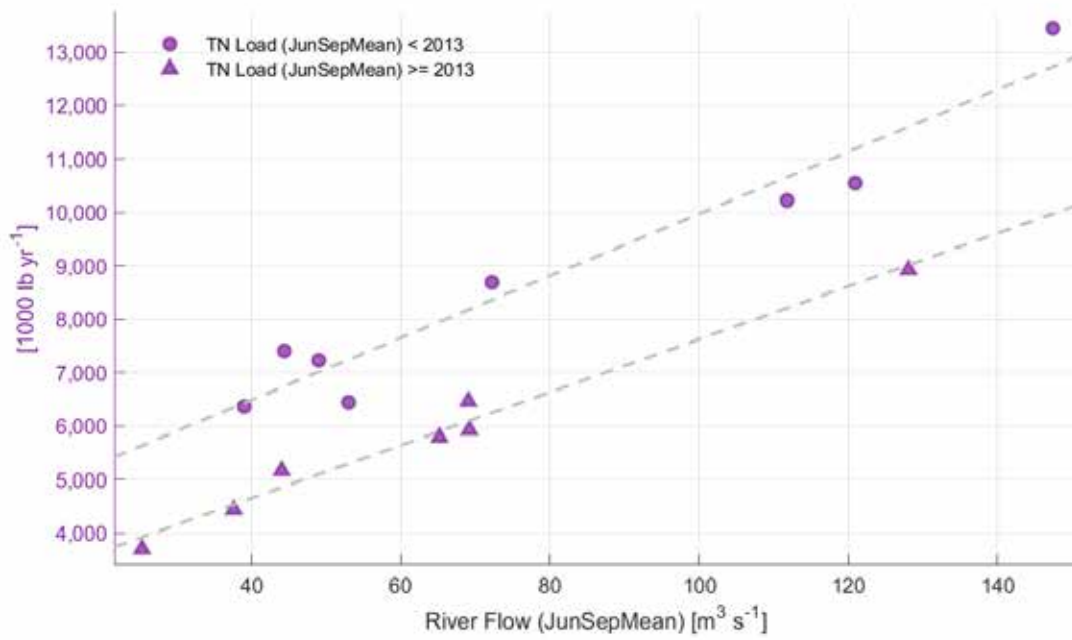


Figure A6-4.

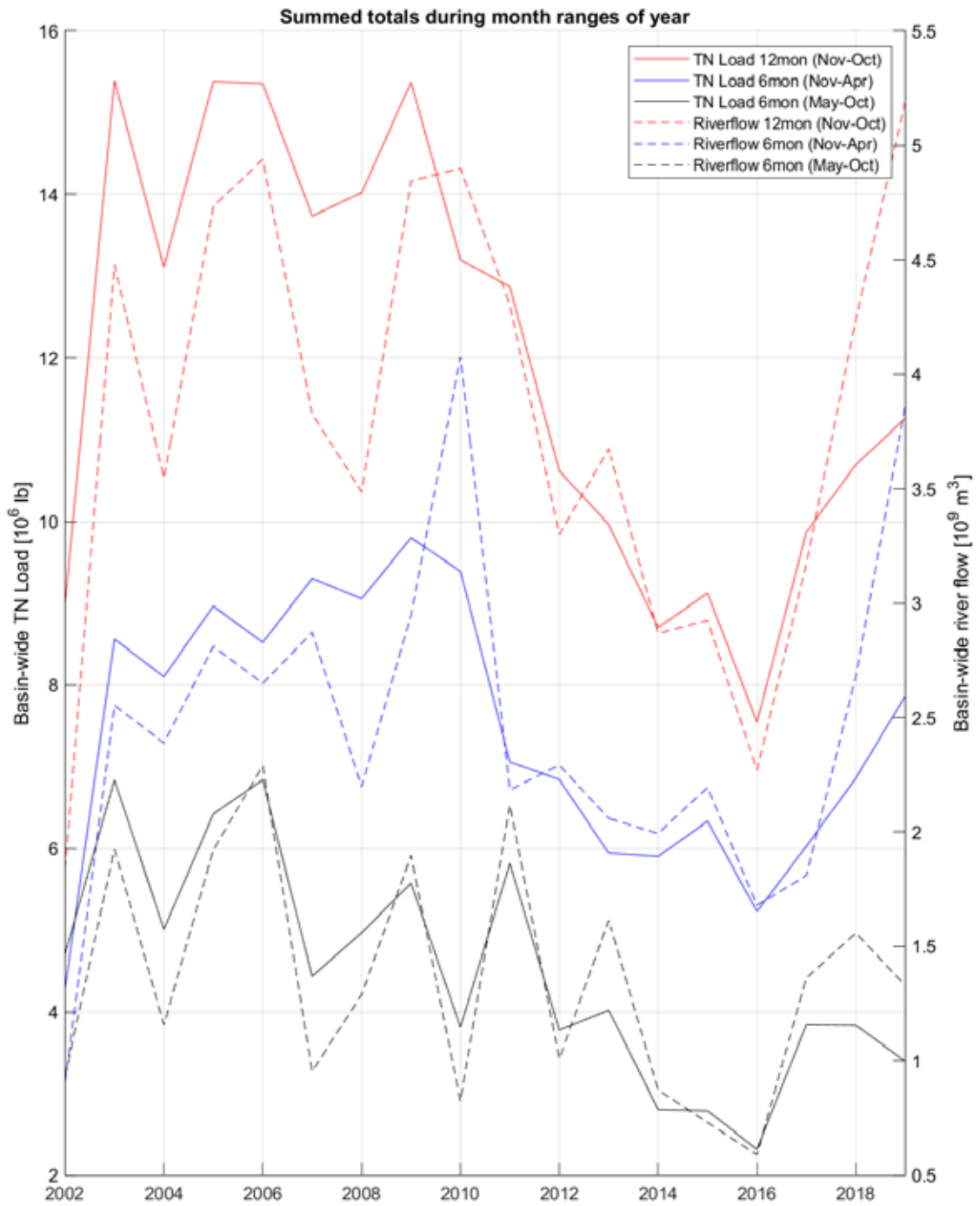


Figure A6-6.

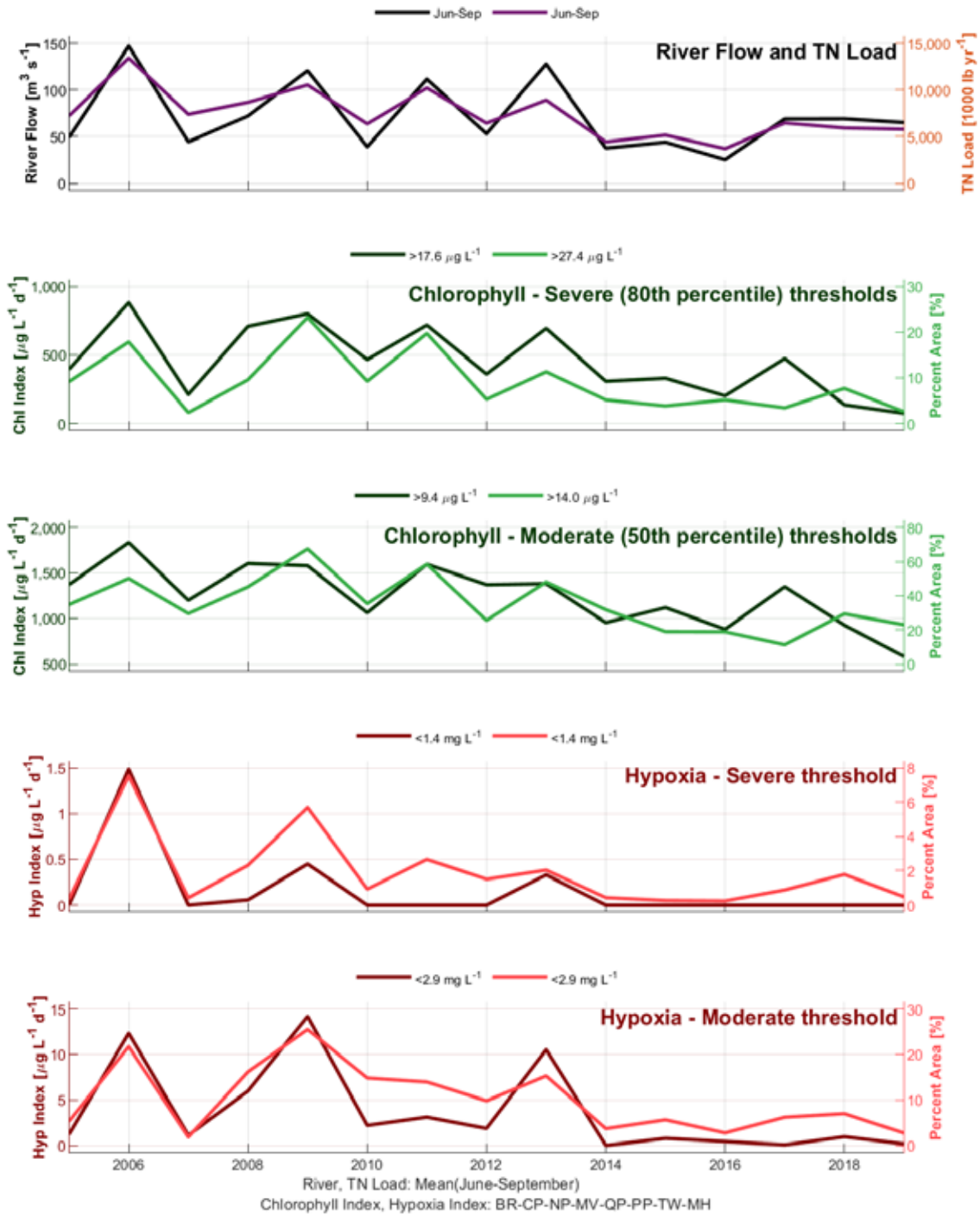


Figure A6-7.

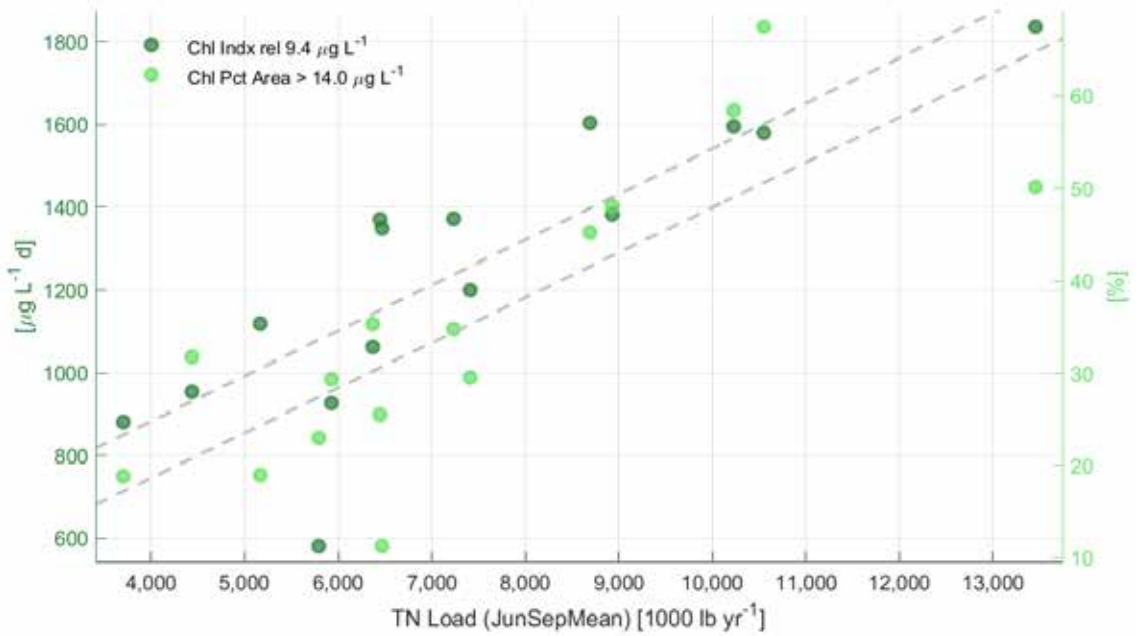
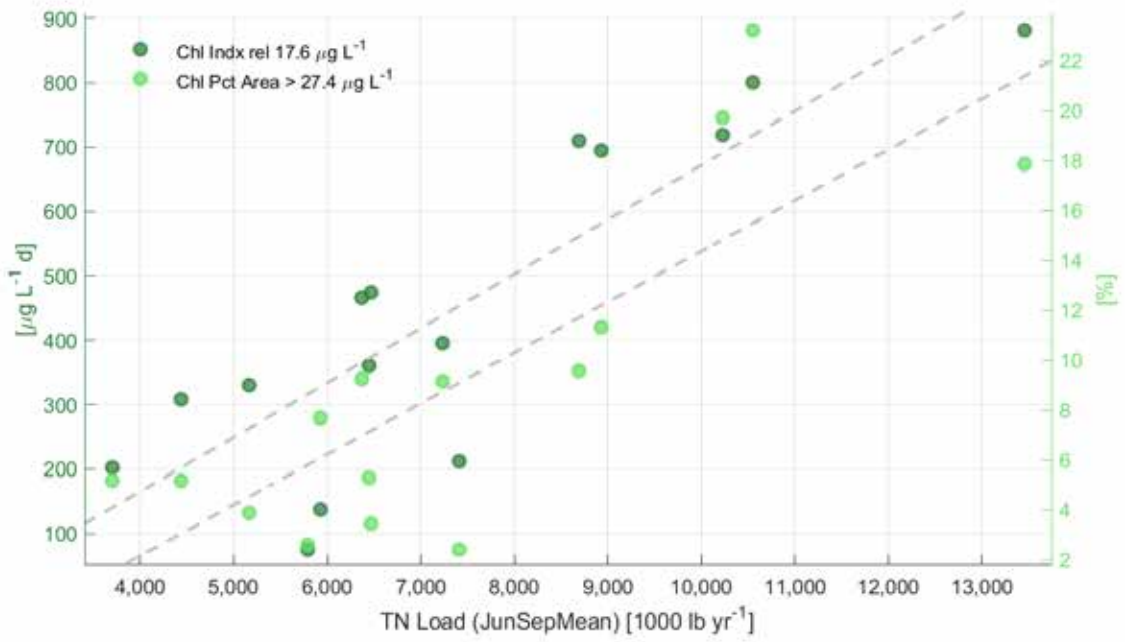


Figure A6-8.

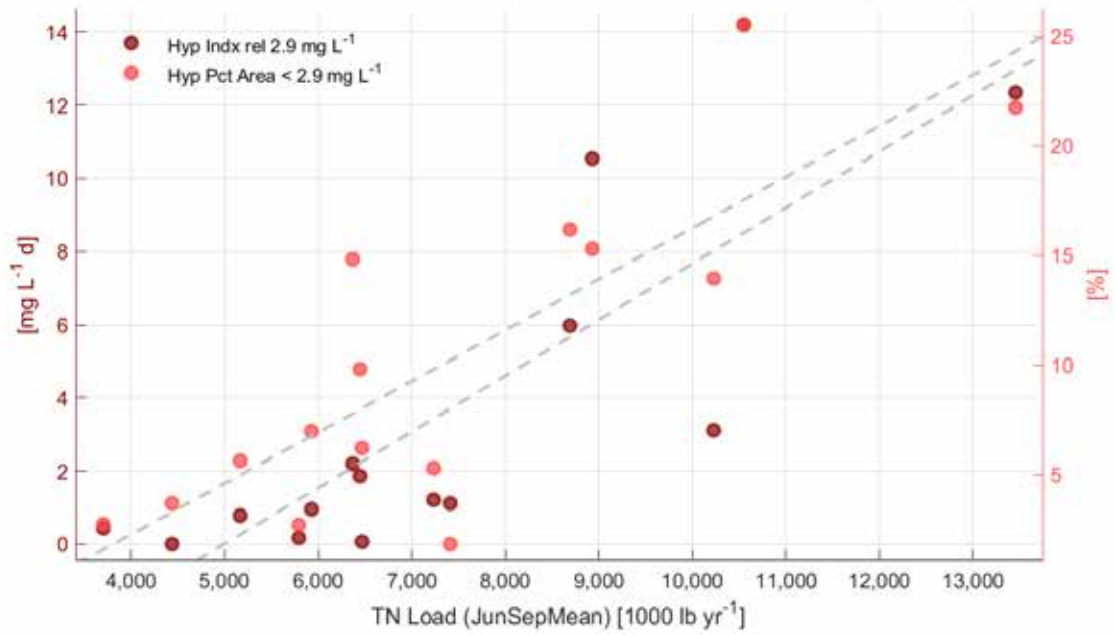
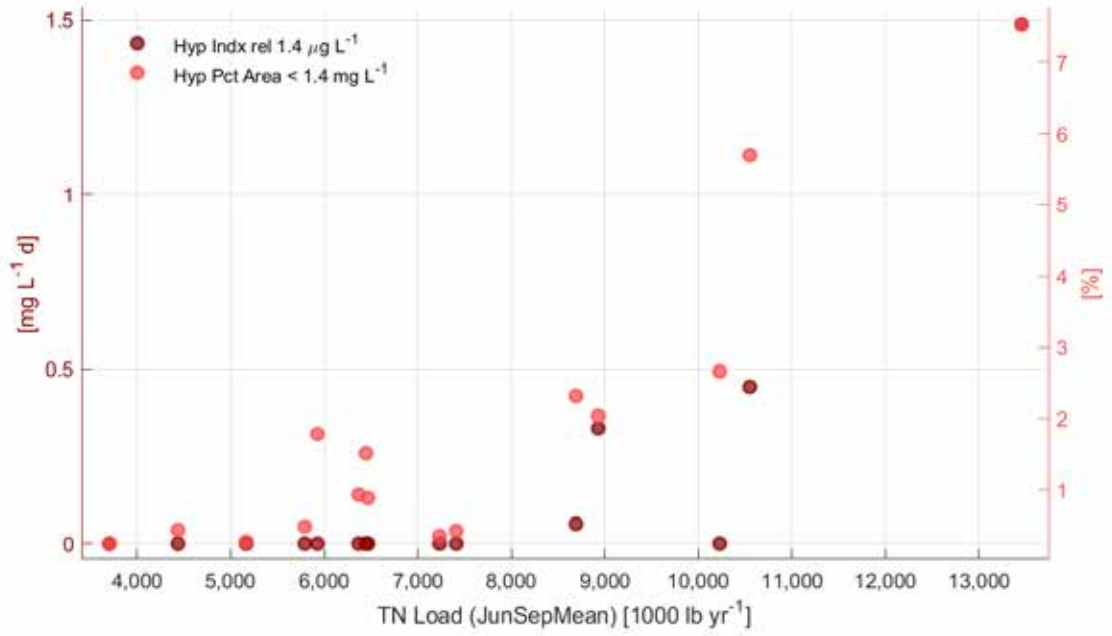
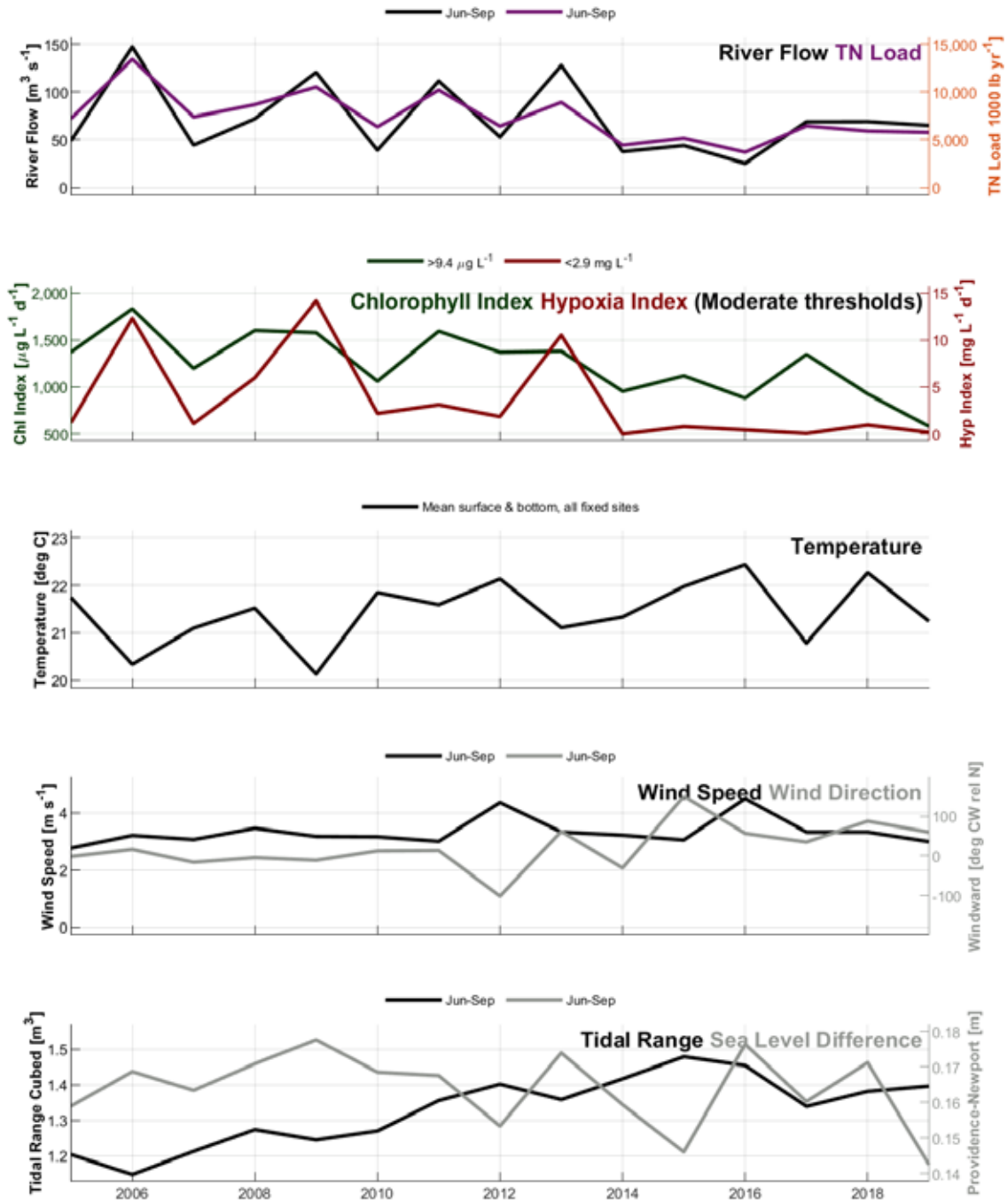


Figure A6-9.



Task 7 Long-Term Trends in Temperature, Salinity, and Stratification

7.1 Scope

An analysis of long-term trends in temperature, salinity, and density stratification during the May-October period was completed by Codiga (2020a) using NBFSMN observations through 2017. Here the analysis is extended to include NBFSMN records from 2018-2019, and from one additional NBFSMN station, GSO Dock. In addition, observations from four independent measurement programs (GSO Fish Trawl, GSO Long-term Plankton, RIDEM Coastal Trawl Survey, NOAA Newport) are used to examine trends. For sites where 12 months of the year are sampled, the trend analysis is applied to summer and winter periods individually, in addition to all months.

7.2 Methods

A summary of the variables sampled, and the spatial locations and temporal characteristics of the sampling, for each of the datasets (Table 7-1, Figure 7-1) gives informative context for their complementary strengths and weaknesses. The NBFSMN sites have the most frequent temporal sampling, at 15 minutes, and 12 sites spanning northern/central portions of the bay (the 11 sites used in prior analyses, plus the GSO Dock, where only surface sampling occurs). However, except at a few sites, NBFSMN sites are sampled from mid-May to mid-October, whereas the other datasets have year-round sampling. The GSO Fish Trawl (2 sites) and GSO Long-term Plankton (1 site) datasets have weekly sampling and, like the 11 NBFSMN sites other than GSO Dock, sample both temperature and salinity at both near-surface and near-seafloor depths as required in order to compute stratification. The RIDEM Coastal Fish Trawl dataset includes 13 stations spanning central/southern portions of the bay, but measures temperature only. The Newport site has frequent sampling, at least hourly, but samples only at the surface.

It is important also to note that temperature and salinity are variables of primary interest for the NBFSMN and Newport datasets; in contrast, for the GSO Fish Trawl, GSO Long-term Plankton, and RIDEM Coastal Trawl datasets temperature and salinity are auxiliary variables, and can therefore be expected to potentially be characterized by less complete sampling and more frequent data quality issues. In addition, NBFSMN and Newport are the only datasets that do not involve vessel-based sampling, so their sampling cannot be subject to a potential “fair weather” bias (e.g., Fulweiler et al 2015) in which wintertime samples might preferentially be collected during milder weather and sea state conditions.

For simplicity a single year range is treated, 2006 to 2019, the longest range suitable for all datasets (Table 7-1). This has the disadvantage that measurements from years earlier than 2006, which are available for some datasets, are not used. However, for the dataset of central interest, the NBFSMN, for nearly all stations earlier data only goes back to 2004 or 2005 so only 1-2 years are excluded (the earliest is 2001, for just two stations). In addition, for at least some of the other datasets the field methods earlier than 2006 used less modern equipment so may be of lower quality. Use of the year range 2006-2019 throughout the analysis ensures direct comparability of all results across datasets and stations.

To explore the nature of long-term trends for different times of the year, which is possible for the datasets with year-round sampling, the analysis is applied not only using all 12 months but also using only 6-month intervals centered on summer and winter. The summer-centered month range is May

through October, to align with the summer-only NBFSMN sampling from mid-May to mid-Oct, and the winter-centered month range is November through April. The full-year analysis treats periods from November through October, to keep aligned with paired winter-centered and summer-centered month ranges. Thus for a given year, for example 2010, the results for the full-year analysis correspond to Nov 2009 through Oct 2010 with results for the winter-centered and summer-centered analyses corresponding to Nov 2009 through Apr 2010 and May 2010 through Oct 2010, respectively.

Methods for data reduction for all datasets are described next, then methods for trend analysis.

7.2.1 Data reduction

For datasets that sample density stratification (NBFSMN, GSO Fish Trawl, and GSO Long-term Plankton), density was computed using the seawater equation of state and stratification was computed as the difference between the near-bottom and near-surface densities.

NBFSMN (“Fixed sites”). See Task 3 above for reduction of 15-min resolution time series.

GSO Fish Trawl. Files were obtained from the project website (<https://web.uri.edu/fishtrawl/>) and from Jeremy Collie and Nina Santos. They include temperature and salinity measurements, from near-surface and near-bottom depths, at two stations (Figure 7-1): Fox Island, in water about 7m deep in lower east passage, and Whale Rock, in water about 21 m deep outside the bay to the south, in northwestern Rhode Island Sound. The measurements are collected nominally once per week, year-round. For temperature the record extends back to 1959 and for salinity it begins, with a partial year, in 2006. In this analysis only the record from 2006 onward (through 2019) is used, because it includes salinity, was collected using a modern water quality sonde (YSI Model 6920 V2), and has fewer gaps. Outliers were identified as temperatures outside the range -4 to 26 deg C, and salinity outside the range 15 to 34 PSU, and removed. A small number of dates had more than one value and these were averaged. Diagnostic plots of the reduced values for Fox Island and Whale Rock are shown in Figure 7-2 and Figure 7-3, respectively. There are important gaps in sampling during 2007 and gaps are generally minor from 2008 onward.

GSO Long-term Plankton. The data file was obtained from the project website (<https://web.uri.edu/gso/research/plankton/>), with background information from Tatiana Rynearson, Tricia Thibodeau, and Jacob Strock. Near-surface and near-bottom temperature and salinity measurements are used from one location, station S2 (Figure 7-1) in the lower east passage with water depth about 8 m. Sampling is nominally weekly year-round. The record goes back to the 1950s but here only 1999 onward (through 2019) was obtained. Prior to 2009 the sensors were a hand-held mercury thermometer and refractometer, and since 2009 a water quality sonde (YSI 6000 series) has been used. A small number of dates had more than one value and these were averaged. Outliers were identified as temperatures outside the range -4 to 30 deg C, surface salinities outside the range 10 to 35 PSU, and bottom salinities outside the range 20 to 35 PSU, and removed. In addition, bottom salinity measurements, which were considered the most uncertain, were designated outliers and removed when the resulting stratification ($\Delta \sigma_t$, bottom minus surface) was negative and less than -1 kg/m^3 . A diagnostic plot of the reduced values is shown in Figure 7-4. There are important gaps in sampling during late 2011 and all of 2012, and otherwise gaps are generally minor. During some of the earlier years, and 2013, the salinities have coarse resolution (0.5 PSU).

RIDEM Coastal Trawl Survey. Data files and information were obtained from Chris Parkins and Scott Olszewski, with some background information also from the project website (<http://www.dem.ri.gov/programs/marine-fisheries/surveys-pubs/coastal-trawl.php>) and a recent RIDEM report (Parkins and Olszewski, 2019). The measurements include near-surface and near-bottom temperature (not salinity). The survey occurs year-round and has two components, “monthly” and “seasonal”. Only data from sites regularly sampled during the once-monthly surveys, or combined monthly-seasonal surveys, were used. The sampling began in 1990 and all years through 2019 are used. Temperature at near-surface and near-bottom depths is measured by a thermometer in Niskin bottle samples prior to each trawl. The 13 sites are located (Figure 7-1) through the bay, with one in Rhode Island Sound, at a range of bathymetric depths. The site locations shown in Figure 7-1 are as computed by averaging the latitude-longitude values for all data from each station, and are near the target locations for survey sampling. Data from station 1 stratum 2, and from station 26 stratum 2 are not part of the 13 core stations and were excluded. About 30 outliers, mostly zero values, were identified and removed. A diagnostic plot of the reduced values is shown in Figure 7-5. Stations 161 and 205 are missing data prior to 2004. There are other gaps but they are generally minor.

NOAA Newport tidal station. Temperature and conductivity measurements, only available at the near-surface depth, from NOAA station 8452660 in Newport (Figure 7-1) were downloaded from the NOAA ERDDAP server using TableDAP. Records from 2000 onward (through 2019) were treated to data reduction (though as noted above only 2006-2019 were used). There is a mixture of temporal sampling, hourly in most of the early years and 6-minute more recently. Therefore daily averages were used, for dates on which there are at least 12 measurements that span at least a 12 hour duration. Outliers were identified as temperatures outside the range -3 to 27 deg C and conductivities lower than 10 mS/cm, and removed. In addition, temperature on 2004-05-24 and 2007-07-04 were identified as outliers by visual inspection and removed. Salinity was computed from conductivity by the seawater equation of state using the associated temperature value or a linearly interpolated value from the nearest available temperature measurements. Salinities higher than 34 PSU were removed as outliers, and salinities from 2004-05-29 to 2004-06-09 were identified as outliers by visual inspection and removed. A diagnostic plot of the reduced values is shown in Figure 7-6. There are numerous important gaps, from a few days to a few months long, throughout the temperature record. The salinity record is essentially missing prior to 2002, and has gaps at least as serious as those in the temperature record.

7.2.2 Trend analysis

Records from individual depths (near-surface or near-bottom), at each site, from each dataset, are treated independently.

For each trend analysis the data were first averaged over monthly intervals. The monthly intervals were either from the first to the last day of the month or from the 15th day of the month to the 14th day of the following month. The latter choice is to match treatment of NBFSMN measurements in earlier analyses (e.g. Codiga 2020a), used to maximize coverage because the most common start and end dates of NBFSMN sampling are roughly mid-May and mid-October.

For each trend analysis the given month-range (for example, May-Oct; or all 12 months Nov-Oct) for 2006-2019 is treated. From the monthly-mean values, for the month range of interest, the mean seasonal cycle across all years is computed. A de-seasoned record is created by subtracting this mean

seasonal cycle from the monthly means (Figure 7-7 shows an example). A Theil-Sen regression (Theil, 1950; Sen, 1968; Gilbert 1987) is carried out on the de-seasoned values to determine the slope of the linear trend spanning the years treated, and its 95% confidence interval, with a p-value.

The Thiel-Sen method is non-parametric and more robust to outliers than standard (parametric) linear regression. Calculations were also done using standard regression (not shown) and differences of the trend magnitudes from the Theil-Sen were minor in all cases. Confidence intervals from the Theil-Sen method are slightly larger than the standard method. This is apparent on comparing confidence intervals presented here to those from linear regression as presented in Codiga 2020a.

The Mann-Kendall test (Mann 1945; Kendall 1975; Gilbert 1987) for presence of a trend was applied to the de-seasoned values, so there was no need to use a seasonal Kendall test also.

In all cases a confidence interval range that does not include zero, a p-value less than 0.05, and a positive Mann-Kendall test result occurred together; similarly, a confidence interval range that includes zero, a p-value greater than 0.05, and a negative Mann-Kendall test result occurred together. For this reason it is sufficient to present only the confidence intervals, without explicitly indicating the Mann-Kendall test or p-value results; if zero falls within the confidence intervals the Mann-Kendall test is negative and the p-value is > 0.05 , and vice versa. This approach has the advantage of simplifying the presentation of the results. Furthermore, the size of the confidence interval range (in addition to whether zero falls within it) is a useful continuous measure of the statistical strength of the trend as opposed to the binary results of the Mann-Kendall test and comparison of p-value to 0.05.

A second measure used to gauge the statistical strength of trends is the years duration of sampling required in order to correctly detect, with probability 0.9, a trend that is at least twice as large as the noise in the record. To the extent this “years duration statistic” (Tiao et al. 1990, Weatherhead et al 1998, Leroy et al 2008, Phojanamongkolkij et al, 2014) is longer than the 14 years sampled from 2006-2019, the trend is more meaningful statistically in comparison to the noise. The method uses the autocorrelation of the unexplained variance or noise, computed as the de-seasoned values minus the trend from the Theil-Sen regression (Figure 7-7). It was originally developed by Tiao (1990), and both Weatherhead et al (1998) and Leroy et al (2008) developed improved variants, as explained by Phojanamongkolkij et al (2014), which provides enhancements to the Leroy et al method. Because it makes no assumptions about the structure of the autocorrelation, the enhanced Leroy et al method is more general than the Weatherhead et al method. However, when applying these methods to data from a limited range of months (for example May-Oct) instead of all months of the year, missing values in the autocorrelation function are problematic. In this analysis both the Weatherhead et al and enhanced Leroy et al methods were applied, but only to records with data from all months of the year. They generally gave similar results, within about 10-20% of each other with few exceptions. No conclusions of the analysis depend on which method is used and for simplicity the results from one of them are presented, the Leroy et al method as enhanced by Phojanamongkolkij et al.

In summary, the results of trend analyses are presented graphically with uncertainty bars indicating the confidence interval range, from which the p-value relative to 0.05 and the Mann-Kendall trend test results can be inferred based on whether zero falls within it. In addition, for analyses that treat measurements from all months of the year, results are presented for years duration sampling required to meet a specific statistical trend detection standard.

7.2.3 Bootstrap: weekly/monthly vs 15-minute sampling

For NBFSMN each monthly-mean value is an average over a large number (typically more than 2800) of individual values, each from a 15-min sampling interval, and is therefore genuinely representative of conditions throughout the month. In contrast, for the GSO Fish Trawl and GSO Long-term Plankton datasets, the sampling frequency is weekly, so each monthly value is an average over 4 values; and for the RIDEM Coastal Trawl dataset, with monthly sampling frequency, the monthly value is a single sample. Monthly means computed from such a small number of samples (4 or 1) will be more uncertain, relative to the true monthly mean, than means computed from the dense temporal sampling at NBFSMN sites. To quantify the associated increase in trend confidence intervals, and in the years duration statistic, a bootstrap resampling method (e.g. Efron and Gong, 1983) was applied to the NBFSMN records.

Trend calculations were carried out using monthly values computed as a mean over four samples (weekly sampling), or using one sample (monthly sampling), randomly selected from all the 15-minute samples that month. For each weekly (monthly) interval, the random sample was selected using a Gaussian probability function with peak in the center of the week (month) and probability at the start and end of the week (month) half as high as at the peak. Results are the averages across 50 replicates of such calculations.

See page 118 for information about supporting code and data files, and page 122 for how to use them.

7.3 Results

7.3.1 Fixed site monitoring network

7.3.1.1 All fixed sites: mid-May to mid-Oct results with 2018-2019 included

As a starting point the period from mid-May to mid-Oct is treated as in the prior analysis (Codiga 2020a), but here the years 2006-2019 are treated at all stations, and the GSO Dock site is included (Figure 7-8).

Surface temperatures (solid orange bars, Figure 7-8) are warming at between about 0.3 and 0.8 deg C per decade, with the exception of the MH station, where there is a cooling trend due to decommissioning of a power plant that influenced the heat budget of Mount Hope Bay about midway through the analysis period (Codiga, 2020a). The rate of near-surface warming is consistent with results from prior analyses (Oviatt, 2004; Pilson, 2008; NBEP 2009; Nixon et al, 2009; Smith et al, 2010; Fulwieler et al, 2015; NBEP, 2017).

Deep temperatures (open orange bars, Figure 7-8) are warming at between about 0.5 and 1.0 deg C per decade. Among a range of potential reasons for the stronger warming at depth, the most likely (Codiga 2020a) is the influence of subsurface offshore conditions, which results from advection in to the bay by the deep up-estuary limb of the estuarine exchange flow. The mixed layer is typically about 3-4 m deep (e.g. Prell et al, 2015), so stations at sites with bathymetric depth shallower than that would not be expected to be as strongly influenced by the deep inflow. Results from the three stations (PD, GB, SR) that shallow are not inconsistent with this; two of them are the only stations that do not show faster warming at depth (GB, SR), while the other (PD) is anomalous in a number of ways due to its far up-

estuary and substantially more riverine shallow location, including with respect to salinity trends as described below.

To quantify the difference between the warming at shallow and deeper depths, trends were averaged across stations with bathymetric depth greater than 4 m and both near-surface and near-seafloor sampling (MH, BR, TW, CP, MV, QP, PP, NP). For surface warming, the average trend at these stations, excluding MH for reasons noted above, is 0.43 deg C per decade; for deep warming the average is 0.79 deg C per decade, which is 84% higher. While not larger than the confidence intervals, the difference is systematic across all these stations.

It is important to note that only the temperature trends with larger magnitudes exceed the 95% confidence intervals. Trends that do not exceed confidence intervals, despite being suspect in the strict statistical sense, are interpreted here to have some meaning, in particular where patterns are consistent across multiple stations.

Near-surface salinities (solid purple bars, Figure 7-8) are increasing, at between about 0.2 and 1.8 PSU per decade at all stations except PD. At PD in the Seekonk River, the shallowest station, which is located farthest up-estuary, distant from all other stations and in a markedly more riverine setting, the increase approaches 3 PSU per decade. Near-seafloor salinities (open purple bars, Figure 7-8) are also increasing but generally more slowly, at between about 0.1 and 0.9 PSU per decade (at PD, about 1.1 PSU per decade). Averaged across stations deeper than 4 m, the near-surface and near-seafloor salinities are increasing at 0.81 and 0.27 PSU per decade, respectively. The increasing salinities can be attributed to the relatively dry summer conditions during years since 2013, as noted in Task 6 above, due to weaker river flow. The higher rate of increasing salinity near the surface than near the seafloor is consistent with river flow having a stronger influence on near-surface conditions, due to stratification when it is present.

The patterns in the trends in density (violet bars, Figure 7-8), across the different stations and at near-surface and near-bottom depths, generally follow those of salinity. This is because, by the equation of state for seawater, a 1 kg m⁻³ change in density is caused by roughly a 1 PSU change in salinity or a 5 deg C change in temperature; trends in salinity, in the range of about 0.3-0.8 PSU per decade, therefore affect trends in density about 5 times more strongly than trends in temperature which are in the range of about 0.4-0.8 deg C per decade. Rates of density increase are up to about 0.9 kg m⁻³ per decade, except at PD where they approach 1.9 kg m⁻³ per decade. At some stations, near-seafloor densities are weakly decreasing, at rates as strong as about 0.2 kg m⁻³ per decade, because the warming is sufficiently strong to overcome the increasing salinity.

Density stratification (cyan bars, Figure 7-8) at stations deeper than 4 m is decreasing at rates between about 0.2 and 0.8 kg m⁻³ per decade. An exception is the MV station, where the trend is very small, the reason for which is not understood. As for density, trends in stratification are dominantly influenced by trends in salinity, due to the seawater equation of state. The average rate of stratification decrease for stations deeper than 4 m is -0.37 kg m⁻³ per decade. This is weak in the sense that it would take at least a few decades for it to result in meaningful changes, because the season-mean stratification averaged across all stations is in the range of 1-4 kg m⁻³ (see Task 6 above) and substantially stronger at stations in the north (Codiga, 2012).

A summary of the overall characteristics of trend results from the fixed-site time series dataset, with emphasis on bay-wide conditions and deeper stations, for the mid-May to mid-Oct period is as follows:

- Near-surface warming occurred at a rate of about 0.4-0.5 °C/decade; this is consistent with analyses of other datasets in the region, lending credence to the data quality and methods.
- At stations with bathymetric depth greater than the typical mixed layer depth, warming at near-seafloor depths is about 80% faster than the near-surface rate. This is most likely due to the influence of offshore waters advected into the bay by the deep limb of estuarine exchange flow.
- Salinities increased at both near-surface depths (stronger; average 0.81 PSU per decade) and near-seafloor depths (average 0.27 PSU per decade). This is most likely due to variations in river flow, and in particular the period of relatively dry summers since 2013.
- Stratification declined, by about 0.37 kg m⁻³ per decade averaged across deep stations; both temperature (faster warming at depth) and salinity (faster increase near surface) contribute to the decline, and the latter is about 5 times as important. The rate of declining stratification is slow, in the sense that it would require at least several decades to meaningfully decrease the typical magnitude of seasonal stratification.

These conclusions do not deviate substantially from the prior analysis (Codiga 2020a). The differences between this analysis and the earlier one can be summarized as follows:

- Here, 2018-2019 were added, and years prior to 2006 (available at a small number of stations) were omitted. This changed the results in minor ways, as expected because short durations relative to the total sampling period were affected.
- The GSO Dock results are included here; they are consistent with those from other stations.
- Confidence intervals here, based on the non-parametric Thiel-Sen method, are somewhat larger than from the standard method applied in the earlier analysis.

7.3.1.2 Summer, winter, year-round results: fixed sites with 12-month sampling

The four NBFSMN records (PD, GB, TW, GD) sampled year-round are used to explore if trends are different in the summer (all above results), winter, and all-year periods.

The temperature trends (orange bars, Figure 7-9) during the winter months (Nov to Apr) are cooling. The magnitudes of the cooling are smaller than those of the warming in summer months (May to Oct) so the year-round trend, which is effectively a mean of the winter and summer, is warming at less than half the summer rate. The confidence intervals on the winter trends are larger than on summer trends (particularly at the two shallow sites PD and GB), no winter trend is larger than the confidence interval, and except for one station the annual trends are smaller than the confidence intervals. However, the result of winter cooling is consistent across all four sites, and at both depths for the three sites where deep sampling occurs.

The salinity trends (purple bars, Figure 7-9) show weak differences between the winter and summer results, without clear patterns across multiple stations. This also is true for trends in density (violet bars, Figure 7-9), as they are mainly due to those in salinity, and for density stratification (cyan bars, Figure 7-9). At the only station deeper than 4 m, TW, the winter trend for stratification is a slightly weaker decline than in summer.

The years duration statistic can be computed using the 12-month records, unlike for the summer-only analysis. As explained in the methods section above, it is the years of sampling required in order to detect, with probability 0.9, a trend that is at least twice as large as the noise in the record (defined as

the raw monthly values, minus the mean seasonal cycle over the year range analyzed, minus the trend). The extent to which the years duration statistic is longer than 14 years (the duration of the sampling) is a measure of declining statistical confidence in the trend results. Values are mostly in the range of about 20 to 40 years (Table 7-2). Overall the results suggest the dataset is not long enough to detect trends at the specified level of statistical confidence. Together with the fact that trend magnitudes are mostly smaller than confidence intervals, as noted above, this implies the dataset duration is at best marginally long enough to support the trend analyses applied.

7.3.2 Bootstrap quantification of weaker statistics for weekly/monthly sampling

With the exception of Newport all the other datasets analyzed have weekly or monthly sampling frequency, so the results of the bootstrap analysis are presented next. For temperature, the differences between trend results using weekly sub-sampled values and using the full quarter-hour resolution dataset ("w" and "q" in Figure 7-10, respectively) are generally minor, 10-20% or less, with some exceptions of up to about 40% (e.g., surface BR). The confidence interval ranges are higher for the weekly sampling as well, but typically by small amounts. For monthly sampling ("m" in Figure 7-10), differences from the 15-minute trends are similar to the weekly sampling results, but confidence interval ranges increase substantially (typically a factor of 1.5 or more).

For salinity and density, the differences between results from using weekly/monthly sub-samples instead of full resolution data are generally more minor than for temperature, likely due to their less pronounced seasonality compared to temperature, which reduces within-month variability. Nonetheless, as expected the same pattern occurs: confidence interval ranges increase for weekly sampling over the 15-minute resolution results, and increase further for monthly sampling.

The years duration statistic generally increases for weekly sampling, with some exceptions, by modest amounts and increases substantially for monthly sampling (Table 7-3).

In sections that follow, results for weekly-sampled datasets (GSO Fish Trawl, GSO Long-term Plankton) and the monthly-sampled RIDEM Coastal Trawl dataset are presented, including confidence intervals and the years duration statistic. It should be borne in mind that, based on this bootstrap analysis, these results are underestimates. This is most important for temperature and less so for other parameters. For temperature, in the weekly datasets the effect is relatively minor (typically an increase of confidence intervals and years duration of roughly 10-20%) and for the monthly dataset it is larger (typically an increase in confidence intervals of roughly 50% and an increase in the years duration of 50-100%).

7.3.3 GSO Fish Trawl

At the Fox Island (FI) and Whale Rock (WR) stations of the GSO Fish Trawl dataset, near-surface temperature trends (solid orange bars, Figure 7-11, middle two columns) show warming in summer and cooling in winter, which is similar to the NBFSMN results. In addition, the rate of near-surface summer warming is comparable to that in the NBFSMN dataset. These aspects lend credence to the meaningfulness of the trends despite their small magnitudes compared to the confidence intervals, which based on the bootstrap analysis are modestly larger than shown. At FI the winter cooling magnitude weakly exceeds that of summer warming so the year-round trend is nearly zero, while at WR there is weaker winter cooling and the year-round trend is warming.

Near-seafloor temperatures (open orange bars, Figure 7-11, middle two columns) also are warming in summer and cooling in winter, at both FI and WR. The magnitude of winter cooling in near-seafloor temperatures is larger than summer warming so the year-round trend is weak cooling.

The rate of deep summer warming is notably weaker than the near-surface rate, in contrast to the results from NBFSMN stations described above. The FI station is near the QP station of the NBFSMN dataset and the reason for this discrepancy is not understood. The QP result can be considered more robust owing to the much higher-frequency 15-minute resolution of its sampling compared to the weekly sampling at FI, the fact that the QP results are consistent with other NBFSMN stations, and the smaller magnitudes of the FI trends relative to the confidence intervals.

The WR station is outside the bay to the south, where stronger warming at depth has been hypothesized to be responsible for deep warming within the bay (see Codiga 2020a, and above discussions of the NBFSMN results), but its results do not indicate stronger deep warming. A possible explanation of this apparent inconsistency is that WR in western Rhode Island Sound may be more representative of water exiting the bay than water entering it in the deep up-estuary portion of the estuarine exchange flow, which occurs mainly in lower East passage to the east (e.g. Rogers, 2008).

Trends in salinity (purple bars, Figure 7-11, middle two columns) show year-round increases, at a slightly higher rate in winter than in summer. The summer rate is comparable to that seen in the NBFSMN dataset, and all rates all exceed the confidence intervals. The increases are not weaker near the seafloor than near the surface, as is seen in the NBFSMN dataset. At WR, which is more distant from river forcing, this could be expected; at FI it is in contrast to the weaker near-seafloor increases than near the surface seen in the NBFSMN dataset, including the QP station near to FI. The reason for this discrepancy is not known, but as noted above there are reasons why the QP result can be considered more robust.

Density trends (violet bars, Figure 7-11, middle two columns) mainly parallel those of salinity. Stratification (cyan bars, Figure 7-11, middle two columns) is increasing at FI, most strongly in summer, and has weak trends at WR.

The years duration statistic results (Table 7-4), for year-round sampling and shown by the bootstrap results to be underestimates, are somewhat longer for temperature and shorter for salinity, relative to the NBFSMN results.

7.3.4 GSO Long-term Plankton

At station S2 of the GSO Long-term Plankton dataset the trends in temperature (orange bars, Figure 7-11, left column) are similar in nearly all ways to those at the nearby FI station of the GSO Long-term Trawl dataset. There is warming in summer and cooling in winter, both near the surface and near the seafloor. A difference from the FI results is that at S2 the winter cooling is not as strong, so the year-round trends are warming. Another difference from FI results is that near-seafloor warming is somewhat stronger than the near-surface warming (similar to QP). Trend magnitudes are less than the confidence intervals with one exception, the deep summer warming.

For salinity at S2 (purple bars, Figure 7-11, left column) the trends are increasing year-round, both near-surface and near-seafloor. The near-surface rate is slightly faster in summer than winter, and the near-seafloor rate is smaller than the near-surface rate in summer. Density (violet bars, Figure 7-11, left

column) and stratification (cyan bars, Figure 7-11, left column) are mainly influenced by salinity but also temperature; stratification is declining due to the stronger warming and weaker salinity increases near the seafloor.

Overall the S2 results are similar to those at FI except for summertime deep warming that is stronger and deep salinity increases that are weaker. Both differences make the S2 results match the fixed site results more closely than do results at FI.

The years duration statistic results (Table 7-4), for year-round sampling and shown by the bootstrap results to be underestimates, are also generally similar to the fixed-site results.

7.3.5 RIDEM Coastal Fish Trawl

The temperature-only RIDEM Coastal Fish Trawl dataset results at the near-surface depth (solid bars, Figure 7-12) show strong cooling in the range of about 0.8 to 2.75 deg C per decade at all stations, in both summer and winter, strongest in winter. The magnitude of the cooling is substantially larger than the warming seen in the other datasets, and in most cases exceeds the confidence intervals. The near-seafloor results (open bars, Figure 7-12) for the winter and year-round sampling also show cooling, though weaker than the near-surface rates, whereas the summer results show weaker cooling and warming at some stations.

Even though the station locations span a somewhat different, more southern area of the bay (Figure 7-1), the opposite sense and larger magnitude of these results cannot be reconciled with those of the other datasets treated here or in the previous analyses cited above. They suggest the sensor or sensors did not undergo calibration frequently enough over the years to accurately measure long-term trends; this outcome is not inconsistent with the objectives of the sampling, for which the focus is fish sampling and temperature is an auxiliary variable.

However, variations of results within the dataset—for summer vs winter time periods, and near-surface vs near-seafloor conditions—reinforce some key characteristics seen in the other datasets. Winter trends show stronger cooling, or equivalently, weaker warming than summer; near-seafloor trends show weaker cooling, or equivalently, stronger warming than near-surface. In addition, the strongest surface cooling is seen at C25 and C26, the two stations in Mount Hope Bay nearest to the MH fixed site where other datasets indicate anomalously strong surface cooling as noted above. Such within-dataset variations support the robustness of these characteristics of bay trends as identified in other datasets. They also point to the self-consistency of the RIDEM dataset and strengthen the interpretation, posited above, that its spatial and seasonal patterns are accurate despite that year-to-year calibrations are not accurate enough over long periods to successfully capture the sense and magnitude of long-term trends.

The years duration statistic results (Table 7-4), for year-round sampling and shown by the bootstrap results to be underestimates, are mostly in the range of about 15-30 years. This is relatively short compared to the other datasets and mainly the result of the relatively strong trend magnitudes.

7.3.6 NOAA Newport station

For the Newport station (rightmost column, Figure 7-11) the temperature trends are strong cooling. Because other datasets treated here do not sample the Newport location we cannot be certain from this analysis that the cooling is not real. However, given the data quality issues noted in methods above, the

most likely explanation is that it is an artifact due to year-to-year calibration issues with the temperature sensor. The cooling is stronger in winter and weaker in summer, a difference that is consistent with the winter-summer differences seen in the other datasets. The salinity results show increases with magnitude generally consistent with other datasets, and strongest in summer. The years duration statistic results (Table 7-4) for year-round results are 16 years and 49 years for temperature and salinity respectively.

7.3.7 Conclusions

This analysis focused on trends over the period from 2006 through 2019. In nearly all cases the magnitudes of the trends are not larger than the confidence intervals, and the years duration statistic is substantially longer than the 14 year sampling period. Thus from a strict statistical standpoint the datasets are at best marginally suitable for the trend analyses applied. However, the surface temperature trends are consistent with those reported in earlier published analyses, and there are clear patterns in differences from season to season and between near-surface and near-seafloor depths that are present across multiple sites and multiple datasets, lending credence to the meaningfulness of the results.

Trends identified using multiple datasets, that are applicable at the bay-wide scale and mainly for portions of the bay deeper than the typical mixed layer depth of 4m, include the following:

- Warming of near-surface summer temperatures at about 0.4-0.5 deg C per decade.
- Stronger warming of near-seafloor summer temperatures, about 80% faster than near-surface.
- Year-round trends for warming but at rates slower than in summer (by up to about 50%), with a smaller difference between near-surface and near-seafloor rates, because of winter temperatures that are cooling at similar near-surface and near-seafloor rates.
- Salinity increasing during summer at about 0.8 PSU per decade near the surface and about 0.3 PSU per decade near the seafloor, and at similar rates in winter.
- Density stratification decreasing at about 0.4 kg m⁻³ per decade in summer, with contributions from both temperature (faster warming at depth) and salinity (slower increases at depth), and the latter most important.

These findings are primarily from the fixed site dataset—which has the highest temporal frequency of sampling and generally the highest data quality, owing in part to its inclusion of temperature and salinity among the parameters of its primary focus—and are also supported by the other datasets. In particular, nearly all the above characteristics are apparent in the GSO Long-term Plankton dataset, as is true for the GSO Fish Trawl dataset except that it does not have comparably strong evidence for faster warming near the seafloor. The RIDEM Coastal Trawl dataset results can be interpreted to support the winter-summer and shallow-deep differences in temperature trends, despite that the sense and magnitude of its trends overall are not reconcilable with other datasets (likely due to sensor calibration issues, consistent with the auxiliary nature of temperature sampling in the context of trawl sampling). The Newport dataset has relatively poor data quality but supports the winter-summer differences in warming, and the increasing salinities.

In terms of processes leading to the identified trends, many aspects are understood reasonably well. Increasing temperatures are due to warming at the global scale, which has a strong regional signature. The faster warming at depth is most likely associated with the influence of offshore conditions through the deep inward limb of estuarine exchange flow. Increasing salinities are linked to relatively low river

inputs in years since 2013, the second half of the analyzed period, particularly during summer; increases are faster near the surface, because less-dense river flow influences the upper portion of the water column more strongly. Due to the seawater equation of state the dominant cause of the declining stratification is the difference in near-surface and near-seafloor salinity trends. The rate of decreasing stratification is weak, in the sense that it would take at least a few decades before it would substantially reduce the strength of stratification reached in a typical year.

Table 7-1. Summary of sampled variables (T = temperature, S = salinity), and spatial locations and temporal characteristics of the sampling, for each of the different datasets treated by the long-term trend analysis. Station locations are shown in Figure 7-1. The most recent year included in the analysis is 2019.

	Number stations	Shallow	Deep	Frequency	Months of year	First year	Notes
Fixed sites (NBFSMN)	9	T, S	T, S	15 min	May-Oct	2005	Some stations started earlier, 2001 earliest
	3 (PD, GB, TW)				Jan-Dec		
	1 (GD)	T, S	--				
GSO Fish Trawl	2 (FI, WR)	T, S	T, S	~1 week	Jan-Dec	T: 1959 S: 2006	Water quality sonde starting in 2006
GSO Long-term Plankton	1 (S2)					1999	Water quality sonde starting in 2009
RIDEM Coastal Trawl	13	T	T	~1 month	Jan-Dec	1990	
NOAA Newport	1	T, S	--	1 hour (6 min, recent years)	Jan-Dec	2002	T from 1996; S from 1999 but sparse pre-2002

Table 7-2. Years duration statistic, NBFSMN sites with 12-month sampling.

	Temperature		Salinity		Sigma		DSigma
	Sh	Dp	Sh	Dp	Sh	Dp	
PD	23	19	23	33	25	36	24
GB	37	29	32	34	41	41	39
TW	74	31	18	21	19	28	20
GD	24	-	19	-	-	-	-

Table 7-3. Same as Table 7-2 but showing bootstrap results for weekly ("w") and monthly ("m") sub-sampling of the 15-minute resolution measurements ("q" for quarter-hourly; values repeated from Table 7-2). Asterisks indicate the results were not finite.

	Sampling frequency	Temperature		Salinity		Sigma		DSigma
		Sh	Dp	Sh	Dp	Sh	Dp	
PD	q	23	19	23	33	25	36	24
	w	38	24	26	67	27	69	70
	m	74	47	35	61	41	52	57
GB	q	37	29	32	34	41	41	39
	w	40	28	33	33	40	42	84
	m	*	87	37	34	47	48	112
TW	q	74	31	18	21	19	28	20
	w	*	34	18	22	19	27	22
	m	*	58	20	23	22	32	39
GD	q	24	-	19	-	-	-	-
	w	27	-	20	-	-	-	-
	m	46	-	20	-	-	-	-

Table 7-4. Years duration statistic, for datasets other than NBFSMN. Based on the bootstrap results, results for these weekly- and monthly-sampled datasets are underestimates.

		Temperature		Salinity		Sigma		DSigma
		Sh	Dp	Sh	Dp	Sh	Dp	
GSO Trawl	FI	66	38	15	9	16	9	38
Weekly resolution	WR	32	41	18	12	19	10	120
GSO Long-term Plankton	S2	79	34	24	26	26	30	39
Weekly resolution								
DEM Coastal Trawl Monthly resolution	C26	14	14	-	-	-	-	-
	C13	22	52	-	-	-	-	-
	C138	23	22	-	-	-	-	-
	C89	21	35	-	-	-	-	-
	C132	23	40	-	-	-	-	-
	C161	22	25	-	-	-	-	-
	C25	15	16	-	-	-	-	-
	C197	20	40	-	-	-	-	-
	C194	19	22	-	-	-	-	-
	C158	23	19	-	-	-	-	-
	C2	25	64	-	-	-	-	-
	C1	22	25	-	-	-	-	-
	C205	24	26	-	-	-	-	-
Newport		16	-	49	-	-	-	-
Hourly (min) resolution								

Figure 7-1. Station location map of datasets used in trend analysis. See Table 7-1 for variables sampled, and characteristics of temporal sampling, for each dataset.

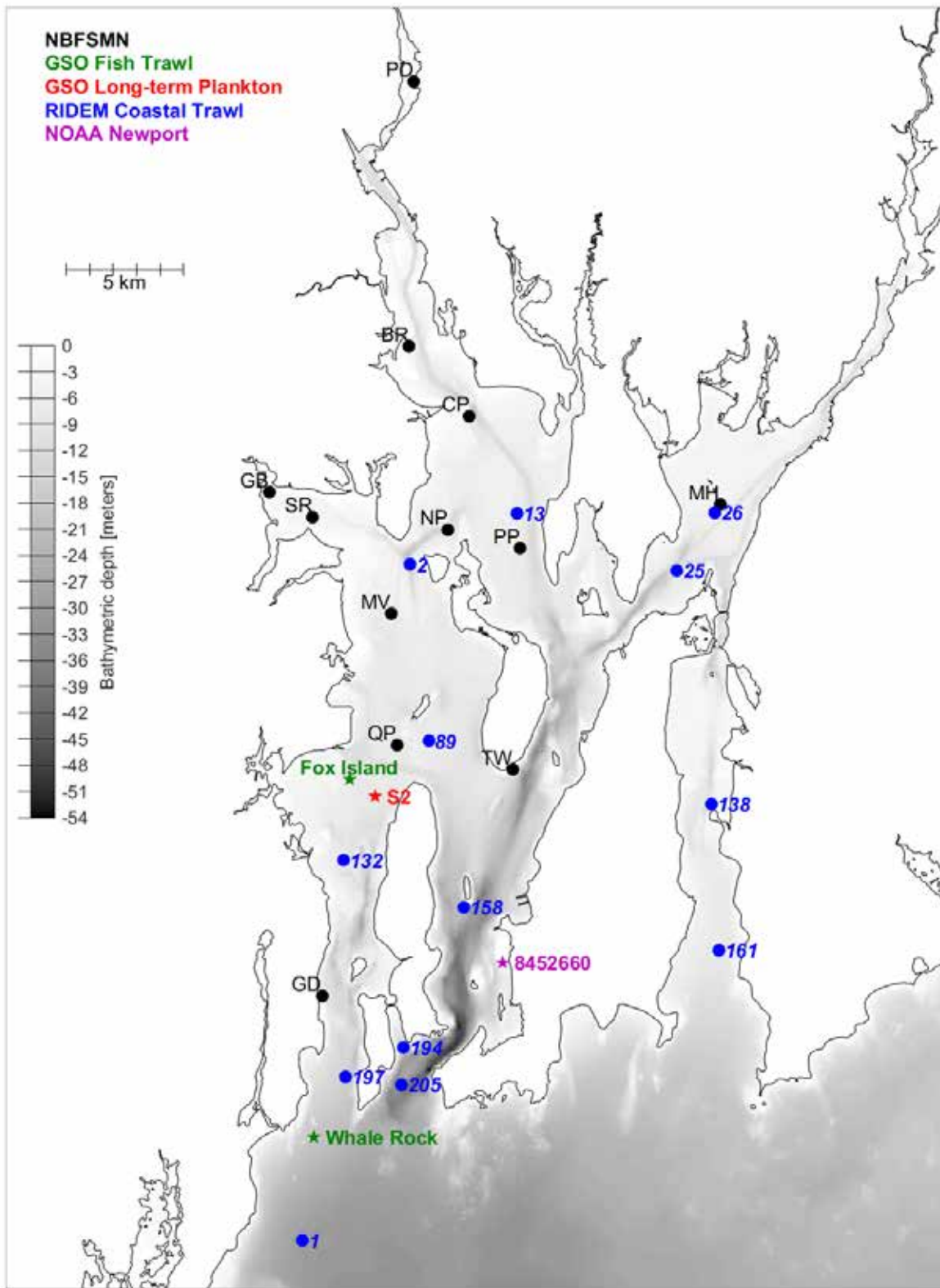


Figure 7-2. Post data-reduction GSO Fish Trawl measurements, Fox Island station.

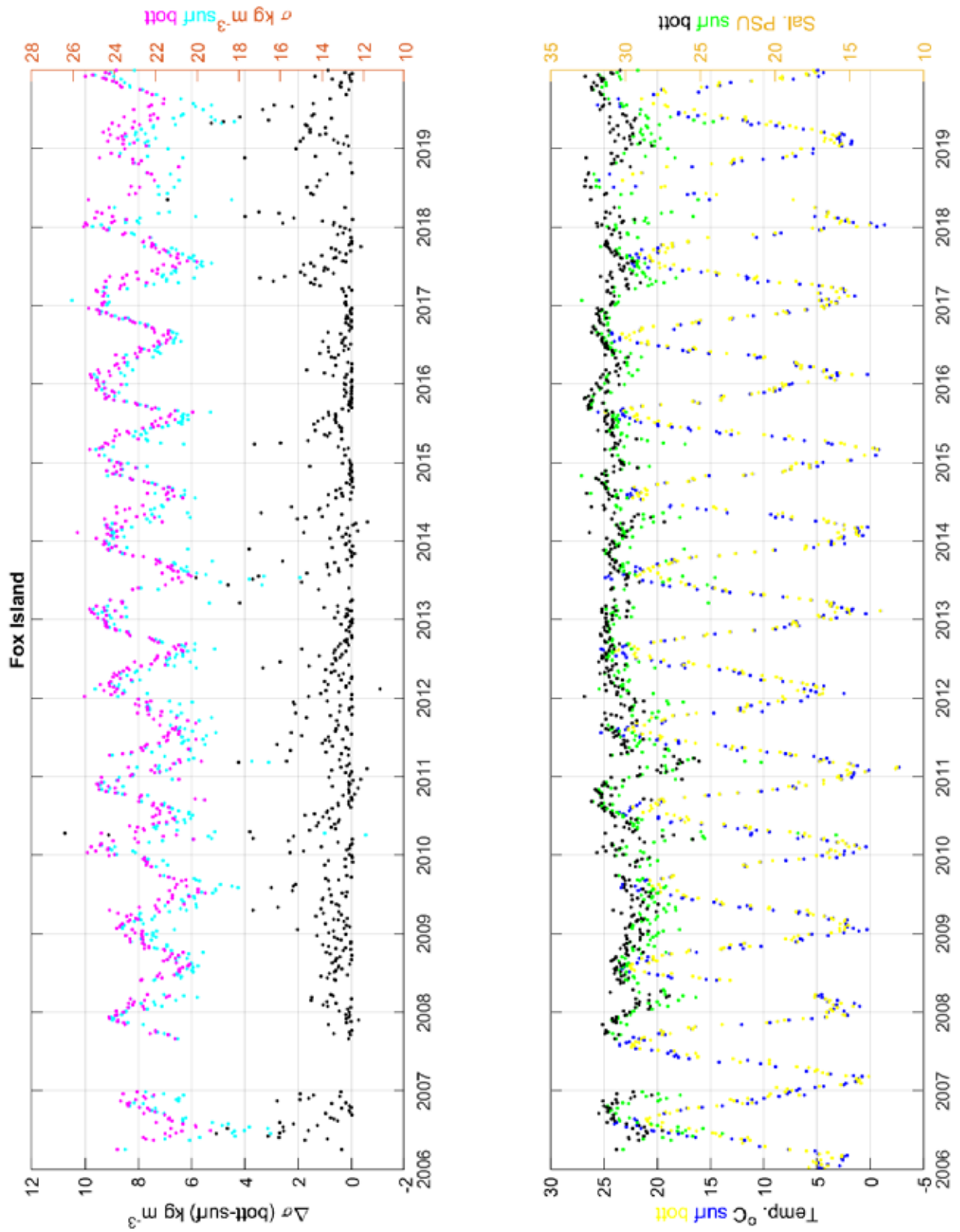


Figure 7-3. Post data-reduction GSO Fish Trawl measurements, Whale Rock station.

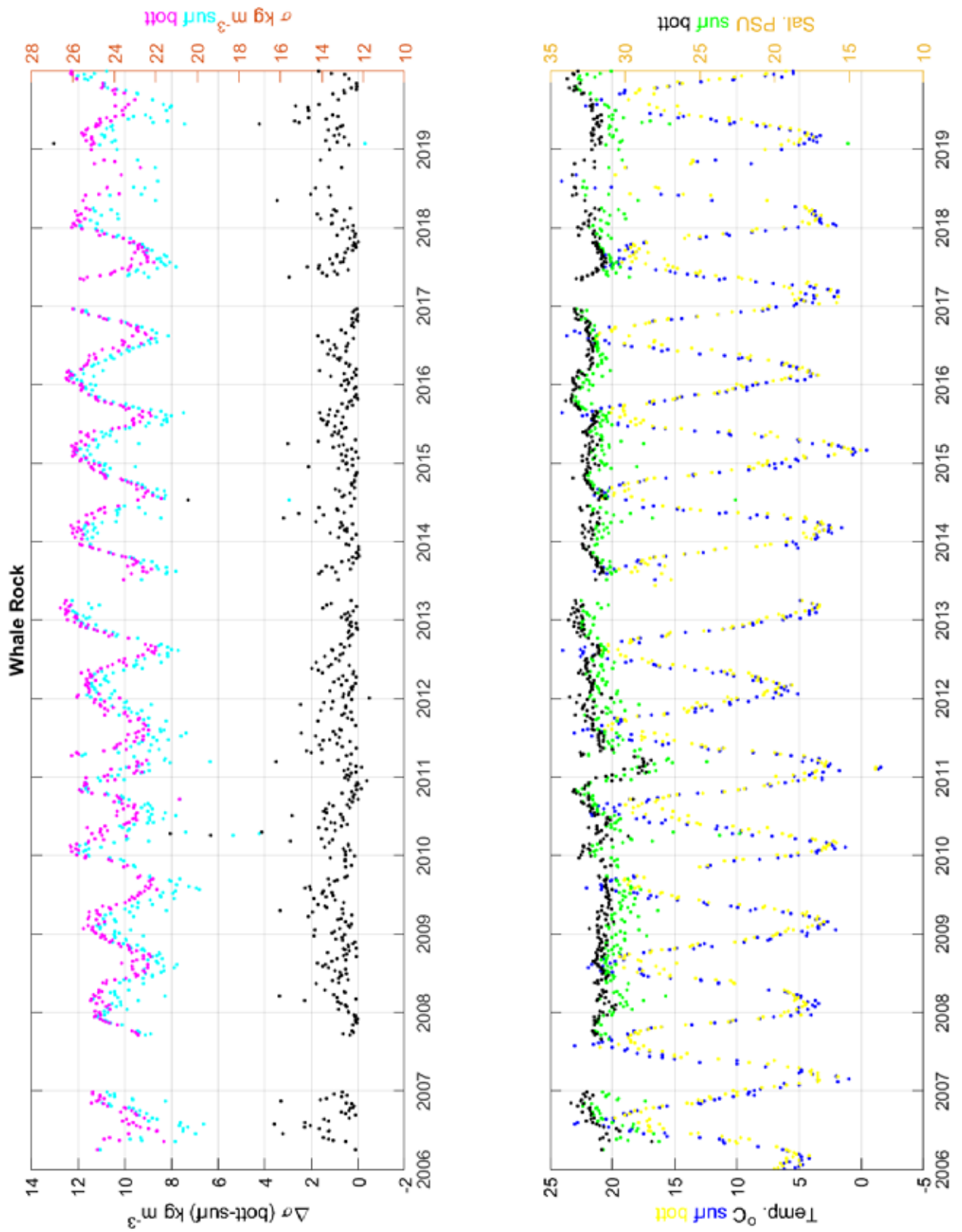


Figure 7-4. Post data-reduction GSO Long-term Plankton Time Series measurements.

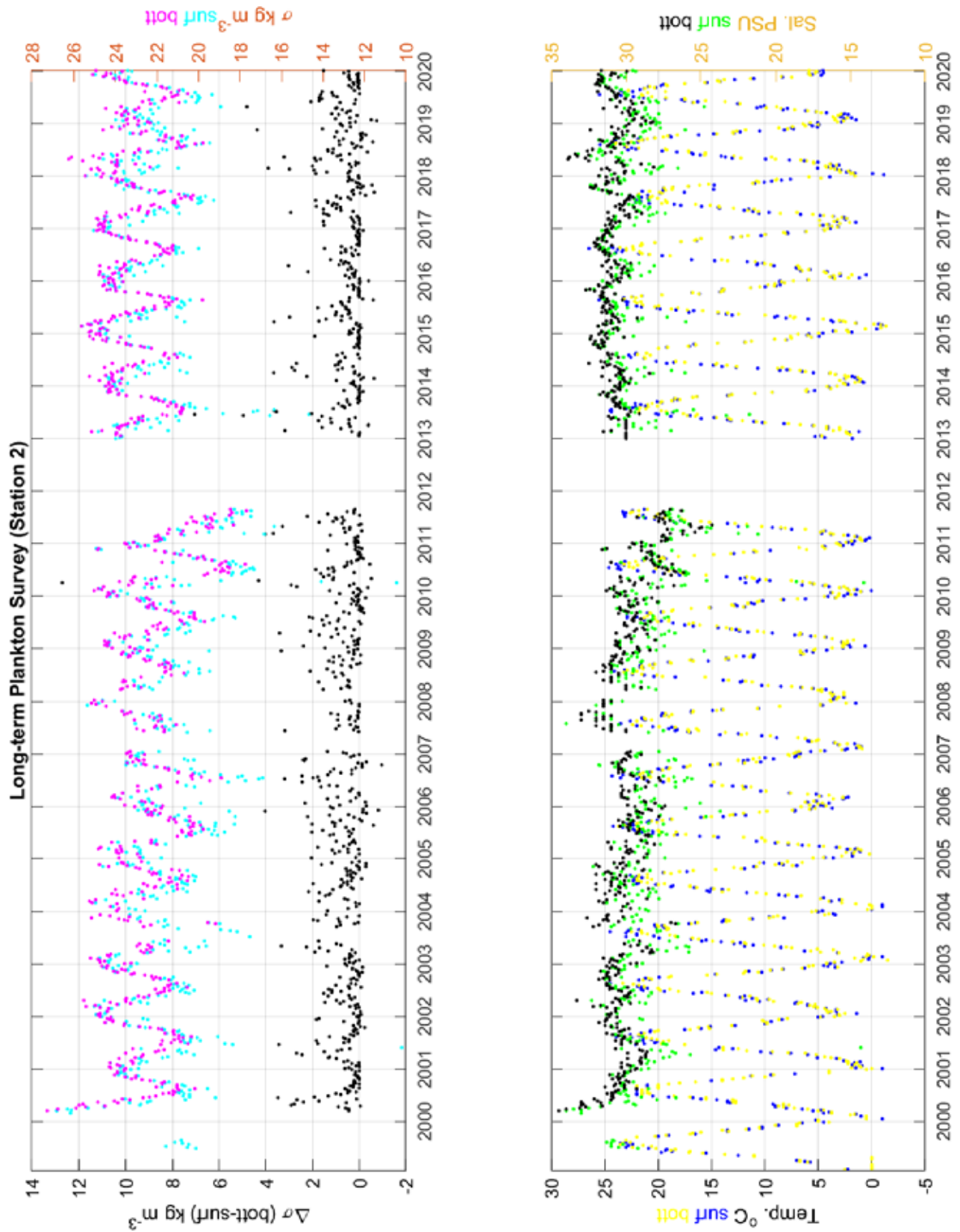


Figure 7-5. Post data-reduction RIDEM Coastal Trawl Survey measurements.

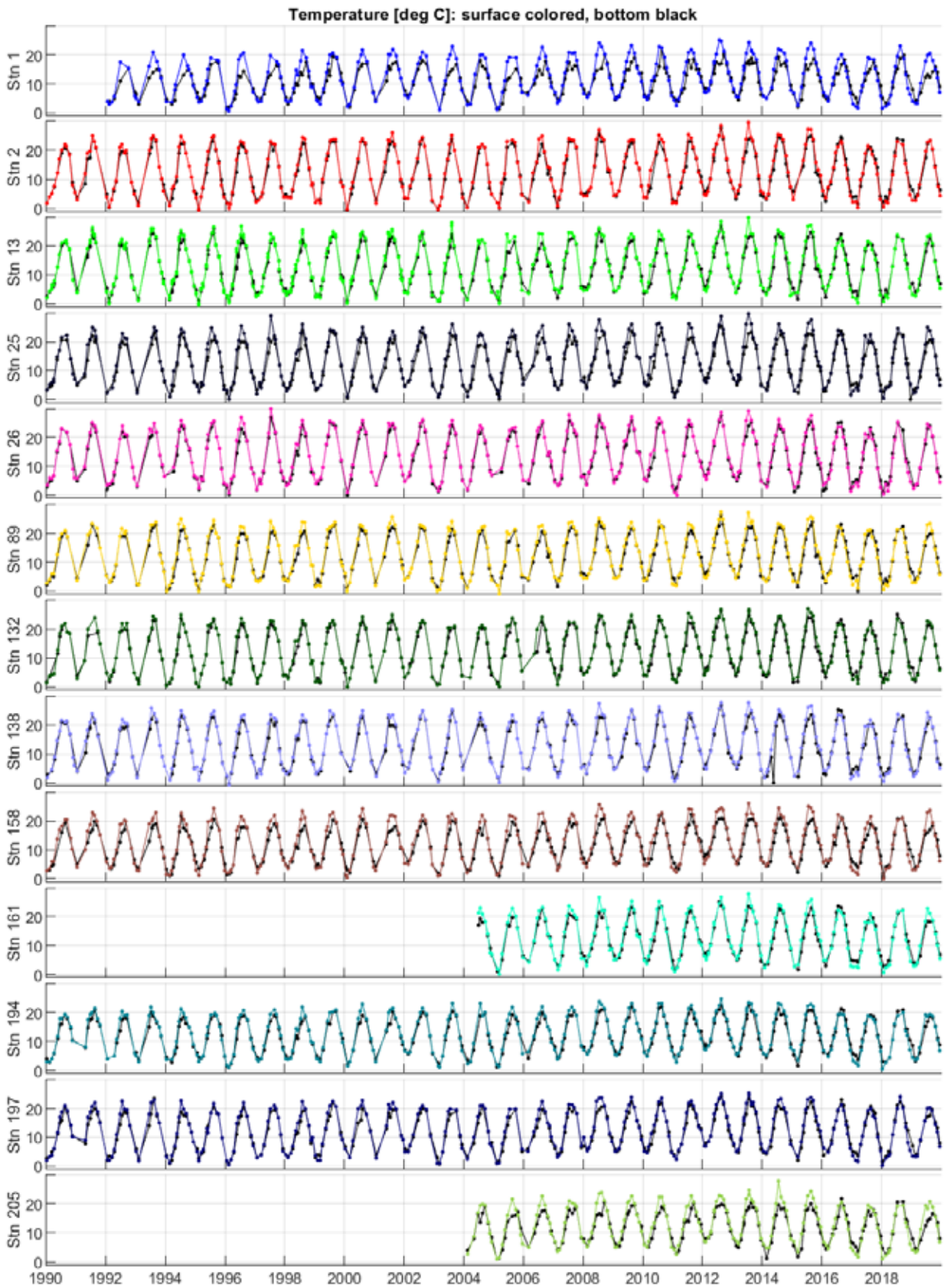


Figure 7-6. Post data-reduction NOAA Newport tidal station measurements.

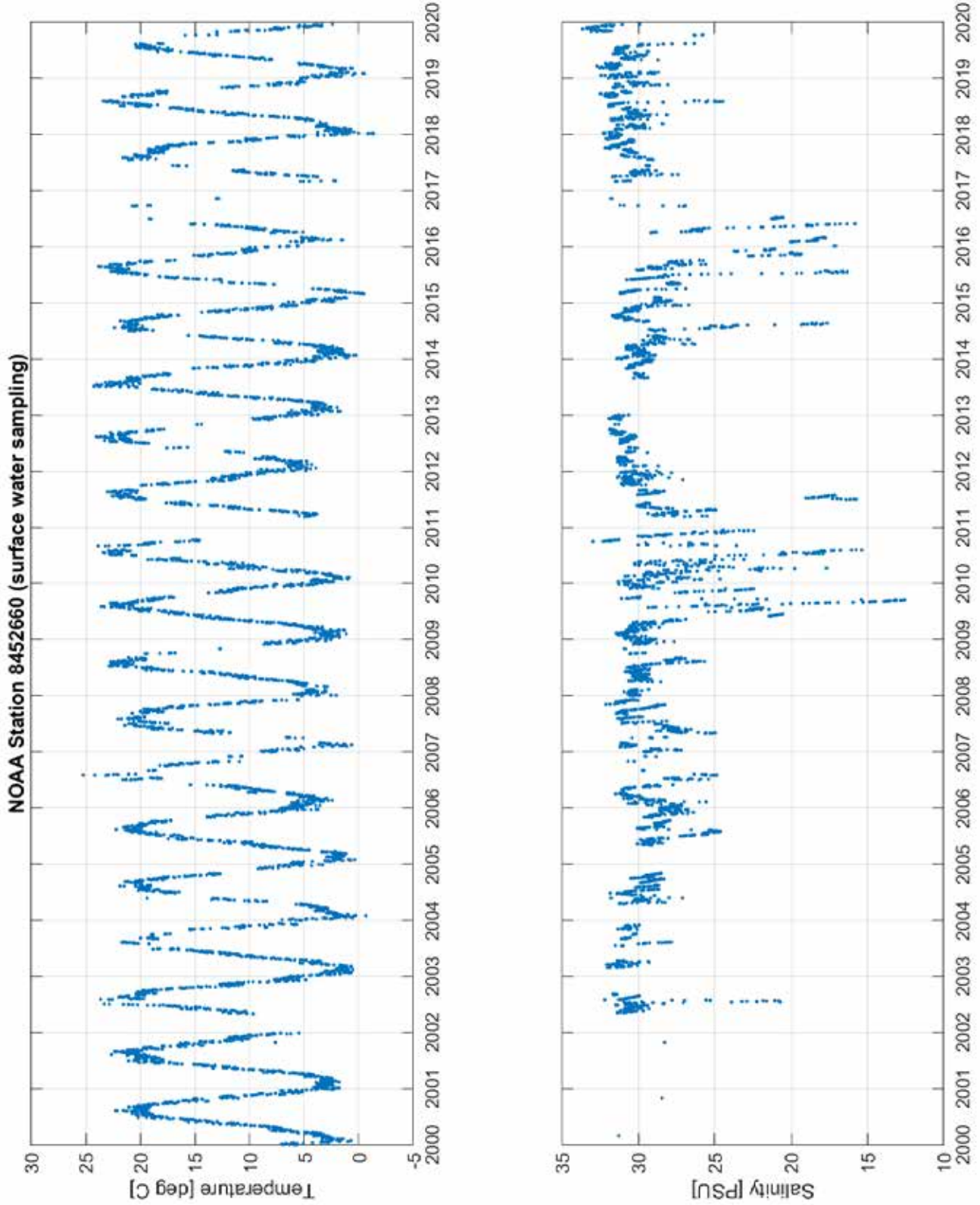


Figure 7-7. Example time series treatment and trend calculation results.

Bullocks Reach, surface temperature. Green is monthly-mean measurements, black is mean seasonal cycle computed from them, red is deseasoned result (green less black), and cyan is Thiel-Sen trend through red values.



Figure 7-8. Trend results for all fixed site (NBFSMN) stations, year range 2006-2019, 5-month mid-May to mid-Oct date range.

Uncertainty bars are the range of lower to upper confidence interval from the Theil-Sen method. Left side of panel with solid bars is shallower ("Sh") near-surface depth and right side with open bars is deeper ("Dp") near-bottom depth. Stations ordered by increasing bathymetric depth (shown in parentheses in frame title), followed by GSO Dock "GD" where only surface sampling occurs.

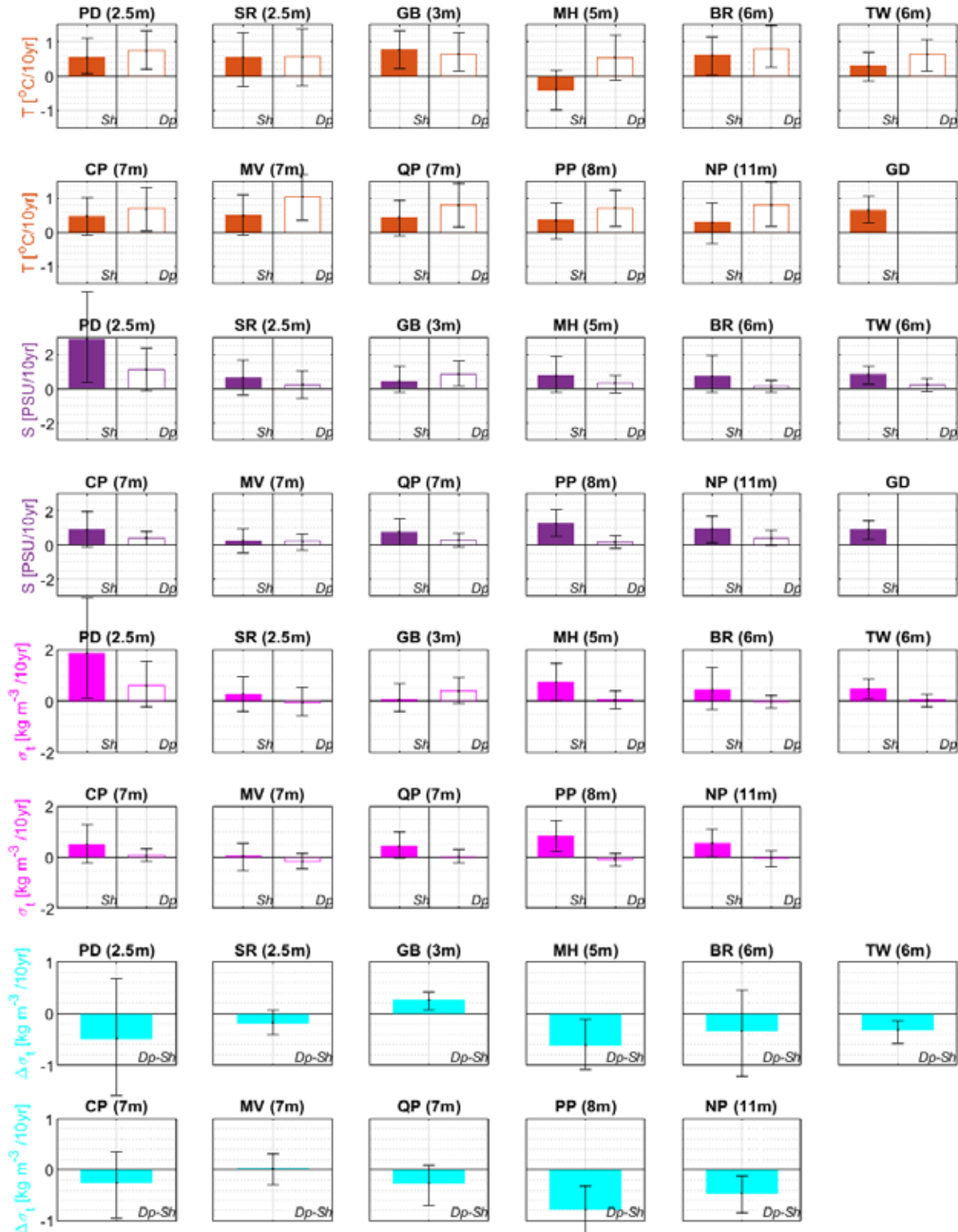


Figure 7-9. Trend results for the four fixed site stations where year-round sampling occurs, presented similarly to Figure 7-8 (same ranges on vertical axes, and colors, for the four variables).

The horizontal axis labels are S for summer-centered 6 months (start of May through end of Oct; most similar to Figure 7-8), A for annual period (12 months; start of Nov of prior year through end of Oct), and W for winter-centered 6 months (start of prior Nov through end of Apr).

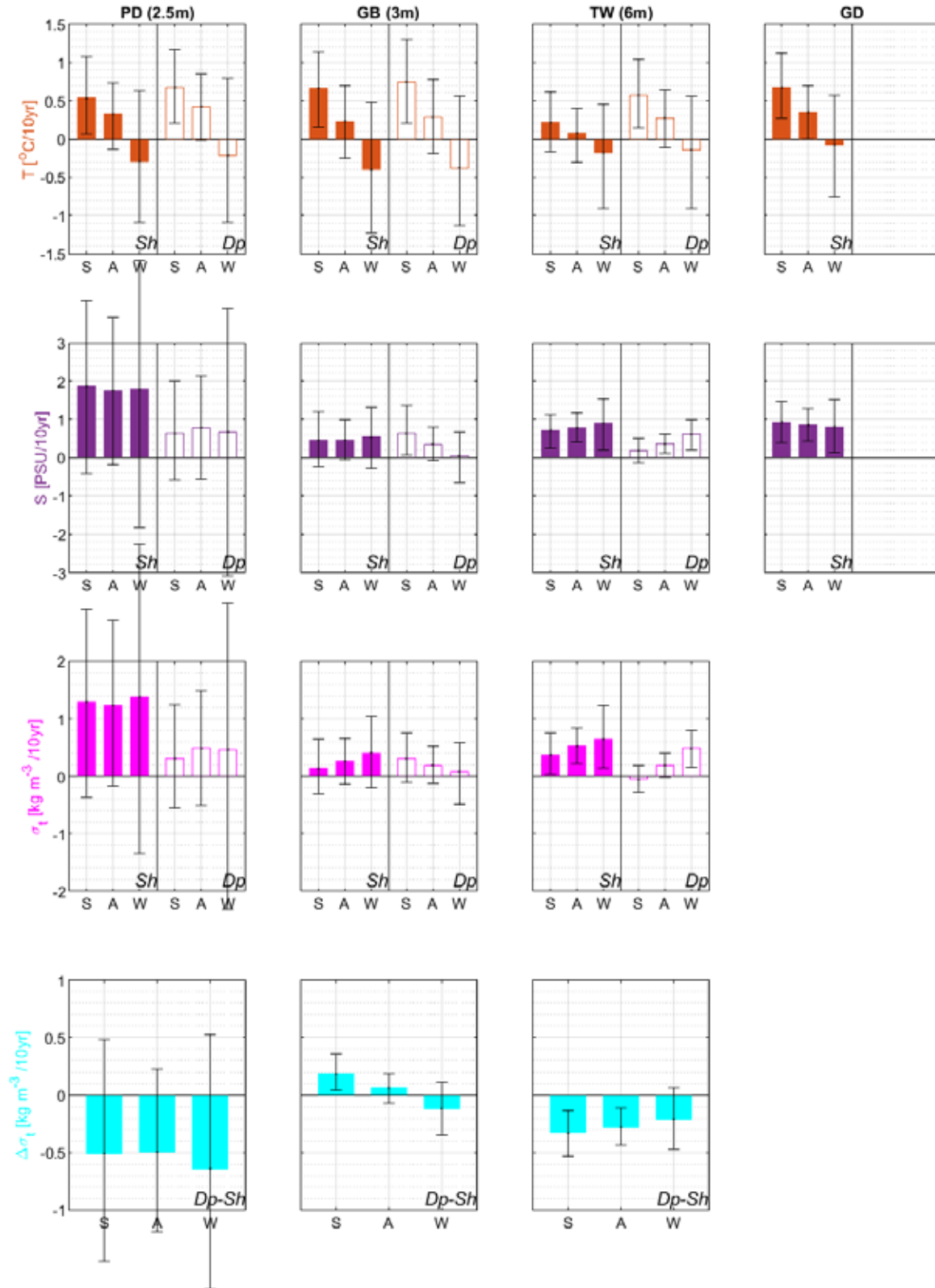


Figure 7-10. Bootstrap results. From monthly means from raw 15-min data, denoted "q" for quarter-hour, are same as in Figure 7-8. Weekly "w" and monthly "m" results are from bootstrap.

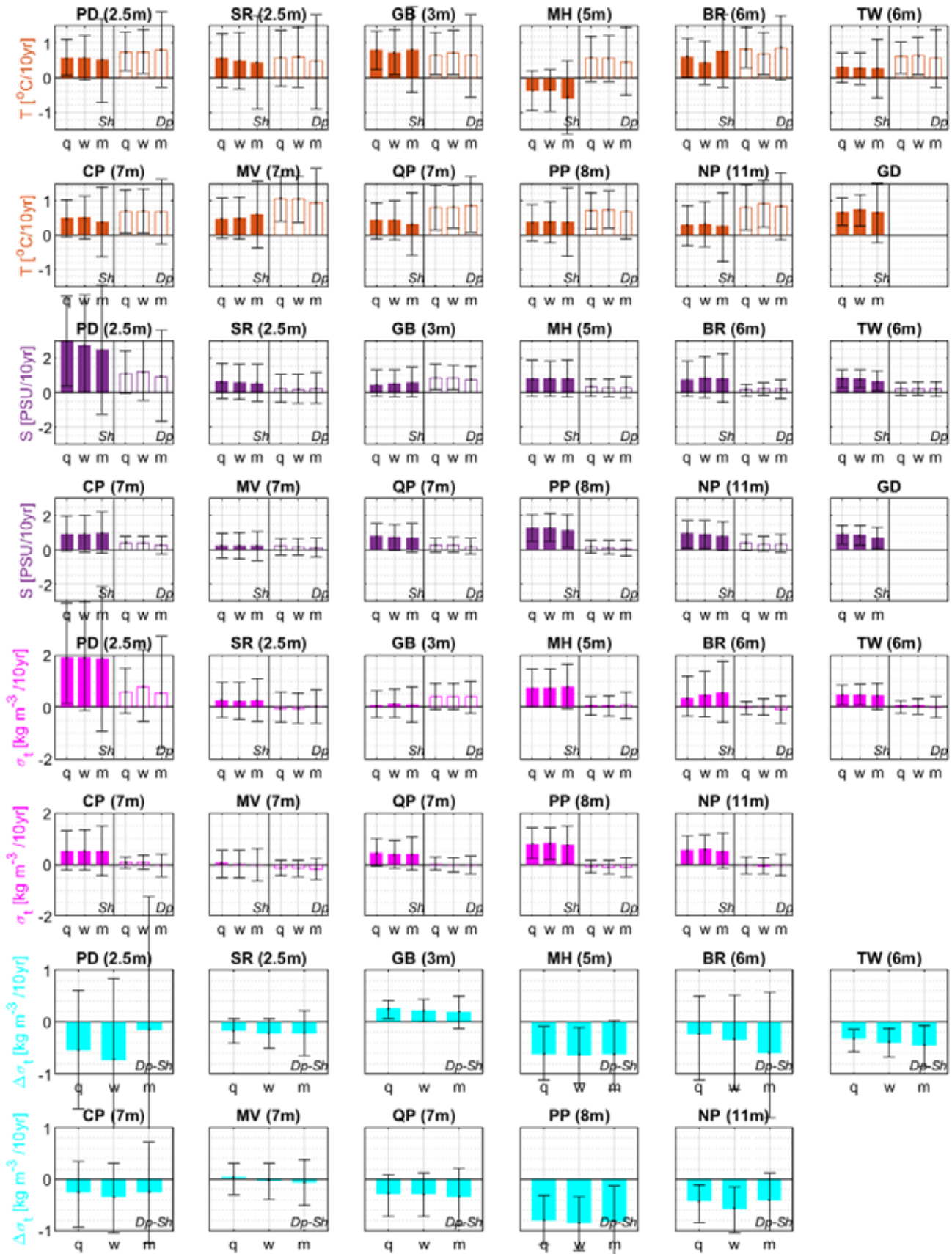


Figure 7-11. Trend results for GSO Long-term Plankton (station S2), GSO Fish Trawl (stations FI and WR), and Newport. Shown as in Figure 7-9 (same ranges on vertical axes, and colors, for the four variables), with S, A, and W indicating summer, annual, and winter periods.

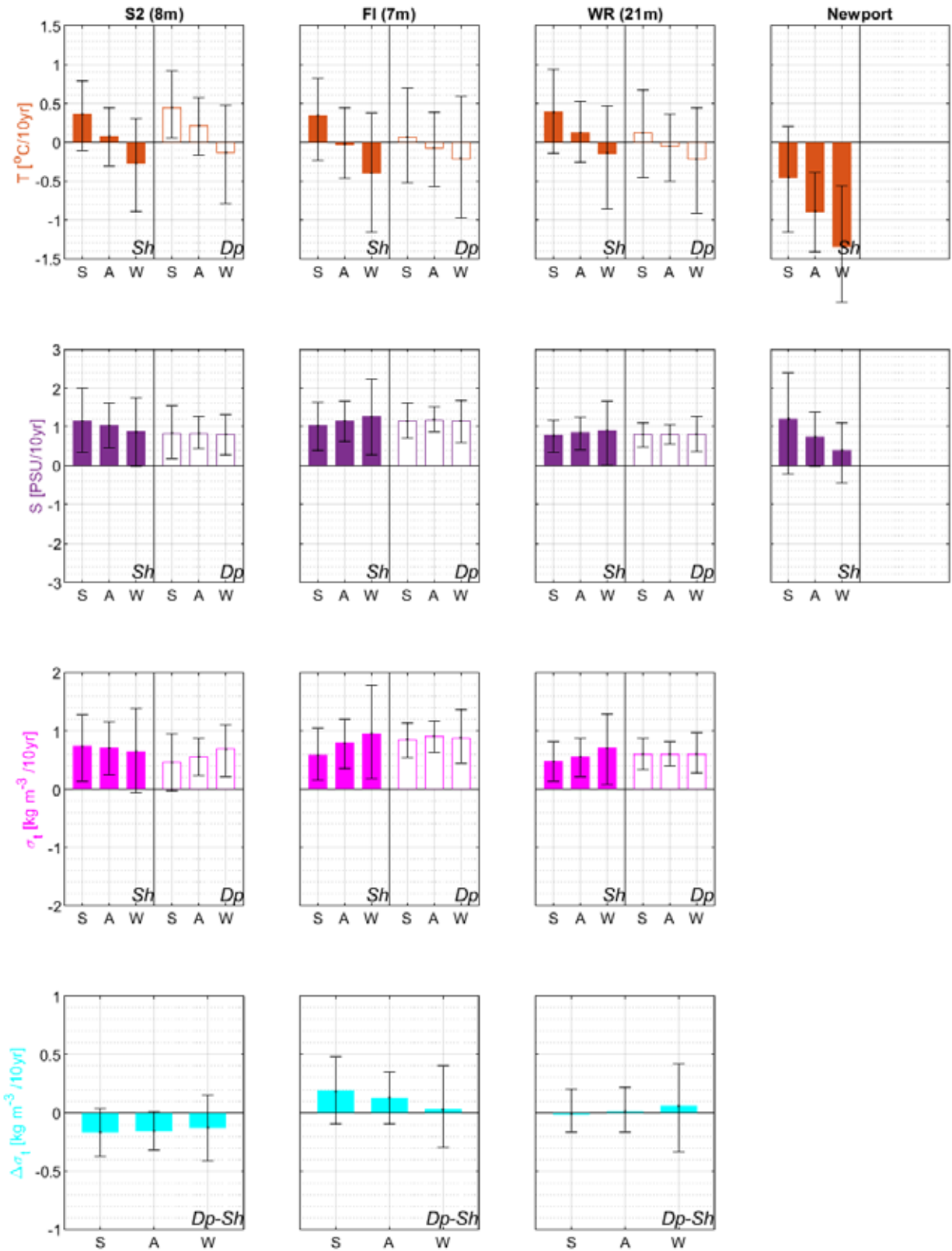
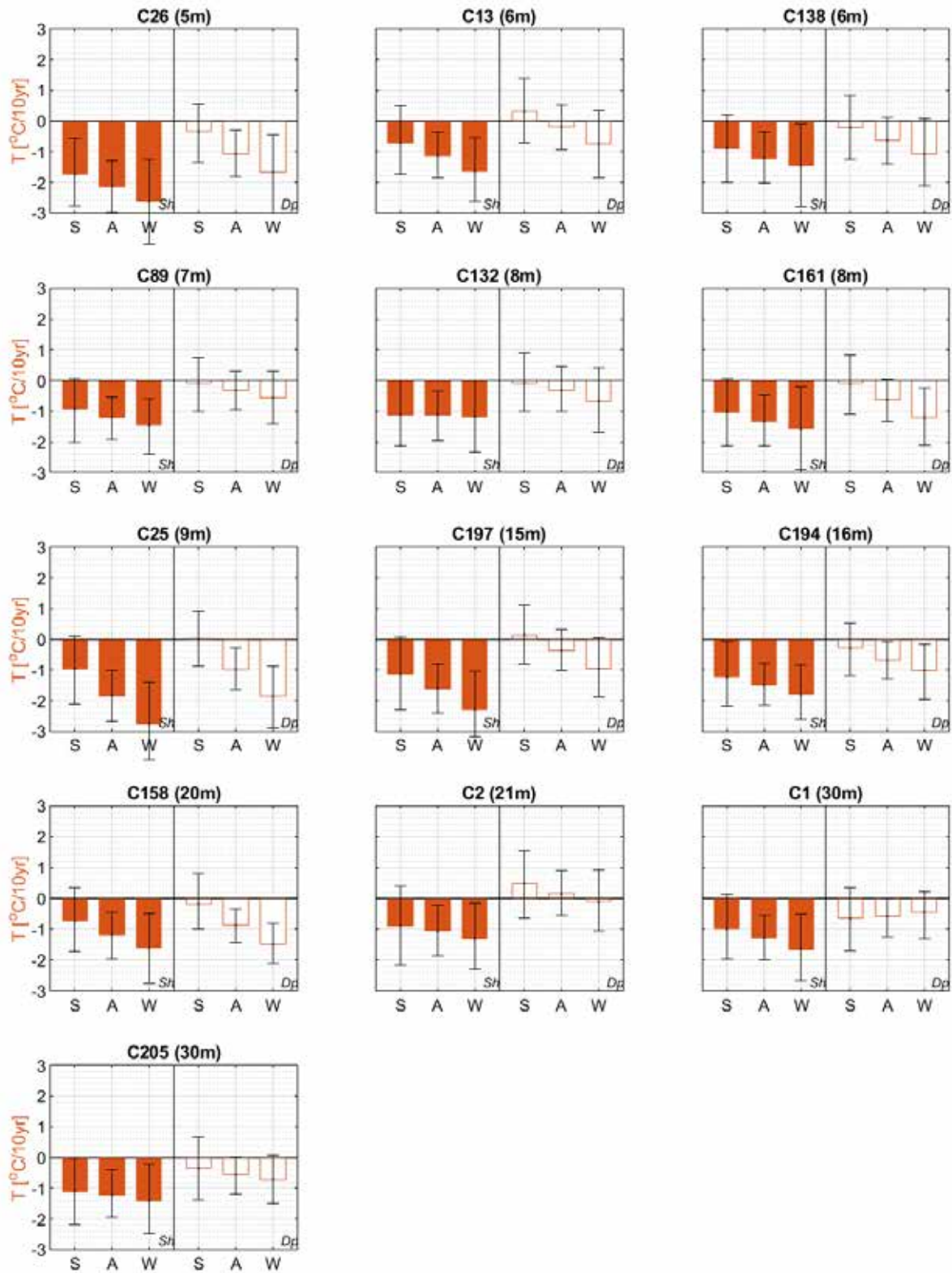


Figure 7-12. Trend results for DEM Coastal Trawl dataset. Presented as in prior two figures except that the range for the vertical axis is two times as large.



Some Recommended Future Research Needs

1. Complete an update to this analysis that includes years through at least 2021. This report was finalized in September 2021 after a summer with historically high rainfall conditions. If hypoxia is as weak during 2021 as in the several years prior, particularly if 2021 has summer river flow comparable to or higher than the wettest years prior to 2013, it will further reinforce the present conclusions that the bay has reached a new changed state in response to the nitrogen reductions. In contrast, if that is not the case, it will necessitate some reevaluation and reinterpretation.

2. Focus on understanding the different variability of shallow embayment stations (Phillipsdale, Greenwich Bay, Sally Rock). Most prior analysis has mainly focused on deeper stations (excluding these three) because the patterns of variability for the deeper stations are more coherent with each other. Compared to the deeper stations the three shallowest embayment stations have more pronounced inter-annual variability, are not as coherent with each other, and show counterintuitive results in some cases (for example, low chlorophyll and hypoxia in relatively wet years at Phillipsdale). The processes underlying these characteristics are not understood.

3. Apply the Weighted Regressions of Time, Discharge, and Season (WRTDS) method. The well-established WRTDS method of Hirsch and colleagues should be suited for application to the Narragansett Bay datasets. It is complementary to the previous work, specifically tailored to isolate variability over multi-year periods from inter-annual variability. It is a framework that has been adopted and applied in numerous systems worldwide over the past few decades, so applying it to Narragansett Bay should yield results understandable by many practitioners in the context of past work across other impacted estuaries. It could yield better isolation of multi-year changes, such as the decline in nitrogen load and response of chlorophyll and hypoxia, from the large inter-annual variability, as compared to the present analysis.

4. Non-GIS methods for spatial surveys dataset. Currently the *percent high-chlorophyll area* and *percent hypoxic area* from each spatial survey are computed by Brown University colleagues using a GIS-based method. An alternative method (e.g., objective analysis) could be developed to compute them without need for GIS. It is anticipated that the new method could give very similar results as the GIS-based method, but would be in the form of a script that should be faster and easier (requiring no manual treatment by a researcher using a graphical user interface within a GIS application). This would enable the metrics to be computed upon Brown making available the processed CTD cast files, potentially sooner than at present.

5. Further analysis of spatial surveys dataset. This would be pursued best on completing the above non-GIS methods. The dataset could be divided in to deeper and shallower stations, each analyzed independently, to investigate the extent to which results from the latter show tighter agreement with results from the fixed site stations (as expected given that the latter are from deeper on- and near-channel locations). An important question is the extent to which inter-annual variations in hypoxia of deeper areas are linked to inter-annual variations of chlorophyll in shallower areas. If they are strongly related it implies that lateral transport of chlorophyll from shallower to deeper areas is a crucial mechanism. This might be linked to the way hypoxia is strongest at mid-depth, instead of near the seafloor, in some years (for example, 2008), as noted by Prell and Deacutis in analysis of spatial surveys.

6. Database system for data management of fixed site and/or spatial surveys datasets. Currently there is no central database for the time series and spatial survey datasets that I am aware of. By constructing one, and making sure it adheres to tidy data principles, the datasets could be more easily and consistently distributed to end users. This effort could also include new tools that make it easier for GSO (Stoffel) and Brown (Prell/Murray) colleagues to enter their data in to the database. It would likely facilitate more efficient quality assurance procedures as well. This is a project for researchers with the appropriate database development and testing skills, in collaboration with researchers who bring familiarity with the datasets and how they are used scientifically.

7. Dashboard tools. In recent years powerful tools for near real-time interactive graphical display of datasets have been developed (for example Shiny in R, and Dash in python). The time series and spatial survey datasets are amenable to such presentations. Pursuing this goal would almost certainly be done most effectively in tandem with, or after completing, the above database goals.

8. Duration-only metrics analysis. Carry out a parallel analysis of the time series datasets that uses 'solely' event duration (for both high-chlorophyll and low-oxygen events) as the metric, instead of surplus-duration for chlorophyll and deficit-duration for hypoxia (i.e. instead of the 'area swept out' metrics on which the Chlorophyll Index and Hypoxia Index are based). This analysis can otherwise be identical to the calculations and plots already done here for surplus-duration and deficit-duration. The results would have units of days-- instead of $\mu\text{g L}^{-1} \text{ day}$ for chlorophyll and $\text{mg L}^{-1} \text{ day}$ for hypoxia—and would therefore be easier for some to understand—potentially of value, particularly for purposes of creating lay-friendly explanations. A goal for this effort would also be to include some idealized thought experiments and schematics to help isolate and make clear the differences and similarities of results using an Index (area under curve) vs a duration-only metric. These idealized cases could clarify the characteristics of time series events for which the two metrics are most similar, or most different, and why (for example, very rapid vs more gradual increases/declines at the starting/ending times of events). The overall conclusions using the duration metrics may well be similar to using the Indices; doing the calculations will test the extent to which that is actually the case.

9. Investigate possible improvements to quality of chlorophyll time series dataset by using only nighttime values to limit influence of non-photochemical quenching. Recent research indicates that commonly used fluorometers (including those in the fixed site network) are subject to non-photochemical quenching. This makes them inaccurate when there is strong sunlight. For some datasets it has been advocated that discarding daytime measurements entirely is the most defensible approach (e.g., Roesler, 2020). This could be applied to the fixed site timeseries dataset, and the results assessed (as done in Codiga 2020a) with respect to agreement with grab samples, to see if there is any improvement. If there is improvement and this treatment of the observations is adopted, it would mean that the Chlorophyll Index can no longer be used in the same way as a metric, because it requires equispaced data values without gaps and there will be no daytime measurements; some other metric for chlorophyll will need to be used, perhaps based on daily means computed using the nighttime values.

All Tasks: Data and Code Files Documentation

This is a task by task explanation of the data and code files used. All are in a single project repository accessible online at <https://figshare.com/s/a421d07c711a212ca7b2>. There are subfolders **Task1**, **Task2**, etc under the main folder of the repository, for data and code files associated with each task.

The code is in Matlab and generally structured in a series of “modules”. Each module has its own folder with identifying name indicating the task the module accomplishes (for example to manipulate data and save to disk newly calculated quantities; or to read in data and create a series of plots from it). In this folder is the main script, usually named the same as the main folder or similarly, and subfolders with some or all of the following names: **in**, **sub**, **out**, **plt**, and **diary**. The **in** subfolder holds configuration files containing information that is read in and used by the main script, for example input file locations. The **sub** subfolder holds functions or subscripts that the main script calls, if any. The **out** subfolder holds data files the module creates and saves to disk, if any. The **plt** subfolder holds plot files the module creates and saves to disk, if any. The **diary** folder holds logs of console messages during runs of the main script.

There is a set of utility functions (found in the repository under the folder **Utilities**), many of which facilitate, and depend on, the above subfolder and configuration input file structure for each module:

- **setpath.m**: This is the only utility that must be run manually. Run it prior to running the main script of a module, after changing directory in to the main folder for the module. It modifies the Matlab path to add the paths of the main module folder and all its subfolders (and remove from it the paths of the folders in the prior module that was run, if any). Subsequent runs of the main script do not require running setpath again, if the working directory has not been changed.
- **wipe.m**: This clears the workspace and deletes all figures. Every main script starts by calling it.
- **modprelims**: This is used in the main script to keep track of the run name and other diagnostics. It also provides convenient access to a few commonly used constants.
- **inputsdiary.m**: This is used to read information from configuration files stored in the **in** subfolder, and save a log of runtime console messages to a file in the **diary** subfolder.
- **getparams.m**: This is called by inputsdiary.m to read each individual configuration file.
- **figport.m**: Function to create 8.5”x11” size figure window, portrait orientation.
- **figland.m**: Function to create 8.5”x11” size figure window, landscape orientation.
- **tri_var_ss.m**: Function that applies triangle weight running mean as low-pass filter to time series data, and subsamples the results. Used during some data processing stages.

All of these utility functions are used by every module and therefore must be located in a folder that is on the Matlab path, in order for a module to successfully execute; the only exceptions are the last three (figport.m, figland.m, tri_var_ss.m), which are required only if the module uses them.

1. River Flow, Wind, Tidal Range, and Sea Level

Rivers. Supporting code is in folder “RiverFlow”. A series of Matlab modules is used, named ‘1GetData’, ‘2and5DiagnosticPlots’, ‘3FillGaps’, ‘4AddmaskerchuggHardig’, ‘6Baywide’, ‘WetIntDry’, ‘rivprms’, and ‘mat2xlsx’. The ‘1GetData’ module retrieves the raw data from the US Geological Survey website, and aligns all the records to a common time grid. The ‘2and5DiagnosticPlots’ module acts on the output of ‘1GetData’ or ‘4AddMaskerchuggHardig’ and creates a series of diagnostic plots. The ‘3FillGaps’ module fills gaps shorter than 3 days by linear interpolation and fills longer gaps using regression against a nearby river. The ‘4AddMaskerchuggHardig’ module computes the Maskerchugg and Hardig flows from the measured Hunt flow and appends them. The ‘6Baywide’ module computes

the river mouth flows, the bay-wide flow, and the ungauged flow. The 'WetIntDry' module applies the thresholds for designating individual years as wet, dry, or intermediate. The 'rivprms' module creates and appends 12-hr subsampled records. The 'mat2xlsx' module saves the data to an Excel spreadsheet file with the final results, Rivers.xlsx.

Output files

Data files: Rivers.mat, Rivers.xlsx.

In the Plots folder is a spreadsheet with data from Figure 1-2.

Supporting code: 1GetData, 2and5DiagnosticPlots, 3FillGaps, 4AddMaskerchuggHardig, 6Baywide, WetDryInterm, rivprms, mat2xlsx.

Winds. The Matlab module is called nc2wndprms. It retrieves the winds, computes a range of associated parameters from them-- eastward wind component, northward wind component, wind speed, wind direction, wind speed cubed (relevant to wind mixing), wind components directed towards the 16 cardinal directions i.e. toN, toNNE, toNE, ... For each such parameter it computes the daily mean and a low-pass filtered version (12-hour half-width triangle weight), in addition to the raw instantaneous NARR wind. All results are saved to the binary Matlab file WindsNARR.mat. A spreadsheet named WindsNARR.xlsx was generated, by a script mat2xlsx, to include the same contents as WindsNARR.mat. The first sheet of the spreadsheet provides all metadata for the other sheets.

Data files: WindsNARR.mat, WindsNARR.xlsx.

Supporting code: nc2wndprms, mat2xlsx.

Tidal Range. Module tidprms retrieves the data, does all manipulations, and saves all fields in the binary Matlab file TidalRange.mat. A spreadsheet named TidalRange.xlsx was generated, by a script mat2xlsx, to include the same contents as TidalRange.mat. The first sheet of the spreadsheet provides all metadata for the other sheets.

Data files: TidalRange.mat, TidalRange.xlsx.

Supporting code: tidprms, mat2xlsx.

Sea Level. Module slvprms retrieves the data, does all manipulations, and saves all fields to the binary Matlab file slvprms.mat. A spreadsheet named slvprms.xlsx was generated, by a script mat2xlsx, to include the same contents as slvprms.mat. The first sheet of the spreadsheet provides all metadata for the other sheets.

Data files: SeaLevel.mat, SeaLevel.xlsx.

Supporting code: slvprms, mat2xlsx.

2. Nitrogen Load

Results files

- **Daily2001to2019TNloadTNconcQflow18NBsources.xlsx**
 - The first sheet in this spreadsheet provides the metadata.
- **Daily2001to2019TNloadTNconcQflow18NBsources.mat**
 - This is a matlab binary storage file with the same contents as in the spreadsheet.

Raw input files (in spreadsheet format with flow and concentration observations)

- Treatment plants:
 - **Bristol, East Greenwich, East Providence, Jamestown, Newport, Quonset, and Warren:** File FromDEM20180619.xlsx, provided by Heidi Travers at Rhode Island Department of

- Environmental Management (RI DEM). The file also contains Fields Point and Bucklin Point data; these were used but only for the period prior to early 2004 (see below).
- **Somerset:** File **URI_MA_WWTFHistoricNutrient-cac.xlsx**, provided by Heidi Travers (RI DEM). File also contains Fall River data but they were not used (see Fall River below).
- **Field's Point and Bucklin Point:** Files **Field's Point Plant Data_Mar 2004-2017.xlsx** and **Bucklin Point Plant Data_Mar 2004-2017.xlsx**, from Narragansett Bay Commission (NBC), provided by Heidi Travers (RI DEM). The files include left-censored values, denoted with prefix string "LT" (less than). The censored values are a small portion of the dataset so it was determined acceptable for the analysis to treat them by substitution of the censoring level. Therefore, to make it easier to read values in to Matlab, a search and replace operation was applied manually to the files to remove all "LT" strings and the results saved as **Field's Point Plant Data_Mar 2004-2017_removedLTs.xlsx** and **Bucklin Point Plant Data_Mar 2004-2017_removedLTs.xlsx**, which are the files actually used by the analysis.
- **Fall River:** 204 files **YYYY-MM.XLS**, where YYYY is year 2001 through 2017 and MM is month 01 through 12, provided on request by Jeanne Wordell of the Fall River treatment plant.
- Rivers:
 - Files **YYYY NBC River and Nutrients Data.xlsx**, for years YYYY = 2005 through 2017, obtained from NBC via download from <http://snapshot.narrabay.com/WaterQualityInitiatives/NutrientMonitoring>.

Supporting code (a series of matlab modules)

- WWTFs (in **WWTFs** folder)
 - Seven WWTFs in Rhode Island (in **RI7** folder)
 - § Modules **Inventory**, to make diagnostic plots showing the temporal coverage/resolution of flow and concentration measurements, and **RI7LoadCalc**, for needed data manipulations to create the load timeseries.
 - Fields and Bucklin (in **FieldsBucklin** folder)
 - § Modules **FPBP1**, for needed data manipulations to create the load timeseries, and **FPBP2**, to save files and plots in a standard format used by all 18 sources.
 - Fall River (in **FallRiver** folder)
 - § Modules **Inventory**, to make diagnostic plots showing the temporal coverage/resolution of flow and concentration measurements, and **FRLoadCalc**, for needed data manipulations to create the load timeseries.
 - Somerset (in **Somerset** folder)
 - § Modules **Inventory**, to make diagnostic plots showing the temporal coverage/resolution of flow and concentration measurements, and **SomersetLoadCalc**, for needed data manipulations to create load timeseries.
- Rivers (in **Rivers** folder)
 - Modules **Inventory**, to make diagnostic plots showing the temporal coverage/resolution of flow and concentration measurements, and **RivLoadCalc**, which does the needed data manipulations to create the load timeseries.
- Ungauged/riparian area (matlab module **UngaugedLoad**), which uses river flow and area ratios and computes the load.
- All sources (in folder **AllSources**)
 - Module **Summary1**, which makes various plots of results for all 18 sources and saves the data from all sources to a single mat file and a single xlsx file ("Results files" above).

3. Fixed-Site Monitoring Network: Data Reduction

Data files: The modified corrected files are in a folder **ModifiedCorrected**, with a subfolder for each of the 11 stations using 4-letter codes (phdl, bulr, cnpt, npru, mtvw, qnpt, popt, twhf, mthp, grby, and srck). In each such subfolder there is an xlsx file with filename XYYYYY.xlsx where XX is the two-letter code for the station (PD, BR, CP, NP, MV, QP, PP, TW, MH, GB, and SR) and YYYY is the four-digit year of the data it contains. The metadata (parameters, units, source contact person, etc) is included in each spreadsheet; the files are all “corrected” versions of the data from Heather Stoffel (URI GSO), with minor modifications to the formatting in order to make them compatible with the Matlab-based processing scripts applied to them. In the **Plots** folder is HypoxiaIndex.xls, containing data from Figure 4-1, as generated by the script mat2xlsx.m included under supporting code.

Supporting Code:

Script “Location.m”. A stand-alone script in which the station location information is kept, and a simple map plot is made.

Module “xls2mat”. For each of the XYYYYY.xlsx modified corrected files, it creates a matlab data file XYYYYYqh.mat, containing the raw data in matlab structures (“qh” refers to the quarter-hourly temporal resolution), and some metadata including the latitude-longitude coordinates of the station, the bathymetric depth at the station, and the depths of the shallow and deep sensors.

Module “strt”. This module reads in the temperature and salinity data and computes the density and density difference (stratification), as well as other auxiliary parameters such as the temperature difference and salinity difference. saving the results as output files (one per station-year).

Module “rawplot”. For each station it uses the XYYYYYqh.mat file from the xls2mat module and makes a one-page plot for each station (with one frame for each year of data) for oxygen; for chlorophyll. These plots are for visual inspection. They annotate the percent of time between mid-May and mid-Oct that has good quality data for each year. Also makes a similar one-page plot for each station showing near-surface density anomaly (sigma-t), near-seafloor density anomaly, and density stratification (density difference between near-surface and near-seafloor density).

Module “MergeStrt”. This module pulls the density difference from the output files of the strt module, organizes them in to a format equivalent to that of the Hypoxia Index results (task 4) and Chlorophyll Index results (Task 5), to help enable use of them all for Task 6.

4. Fixed-Site Monitoring Network: Hypoxia Index

Module “1MWT”. Uses the XYYYYYqh.mat files from the xls2mat module. For each, if percent good data is 55% or higher, it applies the moving window trigger (MWT) algorithm to determine events relative to the three thresholds (1.4 mg L^{-1} , 2.9 mg L^{-1} , 4.8 mg L^{-1}) and save the statistics of events in output files named with format XYYYYY-Txpy-May15Oct15.mat where xpy is 1p4, 2p9, or 4p8 respectively. It also generates plots showing sections of timeseries, from each year of data at each station, during which there were events, with the identified events marked in color for easy visual inspection.

Module “2Merge”. Uses output files from the MWT module and merges all stations and all years. It creates one file for results relative to each of the three thresholds: T1p4-May15Oct15-min55.mat, T2p9-May15Oct15-min55.mat, and T4p8-May15Oct15-min55.mat.

Module “3Stats”. Uses the three output files from the Merge module and computes the statistics necessary to estimate uncertainties based on data gaps, saving them in three output files: T1p4-May15Oct15-min55-2wk1dy-90th10th.mat, T2p9-May15Oct15-min55-2wk1dy-90th10th.mat, and T4p8-May15Oct15-min55-2wk1dy-90th10th.mat.

Module “4Metrics”. Uses the output from the Merge and Stats modules and computes the seasonal Hypoxia Index values, with their uncertainties, saving them in output files T1p4-May15Oct15-min55.mat, T2p9-May15Oct15-min55.mat, and T4p8-May15Oct15-min55.mat.

Module “5IndStns”. Uses the output from the Metrics module, together with the ‘wet’/‘normal’/‘dry’ designations of years based on analysis of basin-wide river flows in Task 6 below, and creates Figures 4-1 through 4-3, and 4-5.

Module “6StnGrps”. With the same inputs as IndStns, creates Figure 4-4.

Script “mat2xlsx”. Saves results in spreadsheet file **HypoxiaIndex.xls**.

5. Fixed-Site Monitoring Network: Chlorophyll Index

A series of modules parallel to those of Task 4 were used: **1MWT_BW**, **2MergeBW**, **3StatsBW**, **4MetricsBW**, **5IndStnsBW**, **6StnGrpsBW**. The suffix BW indicates “bay-wide”; the thresholds used were calculated using observations from all stations bay-wide, and were applied to all stations. A script “**mat2xlsx**” saves results in spreadsheet file **ChlIndexBayWide.xls**.

6. Synthesis of Hypoxia, Chlorophyll, Nitrogen Load, Physical Drivers

Figures 6-1 and 6-2, showing TN load results with river flow superposed, are generated by module “**Upgrades**” which uses as inputs the files created in Tasks 1 and 2; the plotted values are saved in spreadsheet file **MayToOctRiverAndTNLoad18Sources.xlsx**. Using the same inputs, the module “**Seas**” generates Figure 6-4, showing seasonality of TN load and river flow; the plotted values are saved in spreadsheet file **RiverAndTNLoadSummedOverPortionsOfYear.xlsx**.

The spatial surveys raw data are in spreadsheets **CHL%AREA 05-19.xlsx** (for percent area high chlorophyll) and **MASTER HYPOXIA 05-19 WLP_corrected.xls** (for percent area hypoxic); the latter is a copy of the file provided by Prell, but with one correction, the year of the 9/4/2018 survey was changed to 2018 from its incorrect 2008 value. The module **SptISrvRdn** performs simple reduction of the spatial surveys data files, including making plots (not shown) of individual survey data, parallel to Figure 11-9 (chlorophyll) and Figure 7-10 (oxygen) in Codiga 2020a, used to verify data integrity.

The “**Calcs**” module reads all variables (TN load, river flow, chlorophyll metrics, hypoxia metrics, physical drivers) from the data files created in earlier tasks and modules, does the needed averaging manipulations (over periods of the year, and groups of stations or sources, etc), and saves them in a uniform format to a single file **rsIts_Config001.mat** (and corresponding spreadsheet **AllParamsVariousAnnualPeriodsAndStationGroupsSynthesis.xlsx**) that is used as input to the modules “**TimeSer1**” and “**Scatter1**”. The latter are the modules used to generate components (either time series, or scatter plot, respectively) in all other figures. Figure 6-3 is the lower frame from Scatter1 with input Config001. Figure 6-5 upper is from TimeSer1 with input Config002, and Figure 6-5 lower is the upper frame from Scatter1 with input Config001. Figure 6-6 is from TimeSer1 with input Config002. Figure 6-7 is from Scatter1 with input Config002. Figure 6-8 is from Scatter1 with input Config003. Figure 6-9 is from TimeSer1 with input Config003.

7. Long-Term Trends in Temperature, Salinity, and Stratification

The stations map (Figure 7-1) is generated by the **CommonMap** module. Data reduction and diagnostic plots (Figure 7-2 to Figure 7-6) are completed by modules **FixedSites**, **GSOTrawl**, **GSOPlank**, **DEMTrawl**,

and **Newport** in the **DataPrep** folder, which also includes the **Merge** module that groups together the reduced data from all datasets. The **Calcs** module applies monthly averaging and trend analysis to the outputs from **Merge**. From the outputs of **Calcs** the **TimeserPlots** and **TrendPlots** modules create time series plots (including Figure 7-7) and bar plots (Figure 7-8, Figure 7-9, Figure 7-11, and Figure 7-12) of the trend results, respectively. In the **Bootstrap** folder are the modules **BootstrapCalcs** and **BootstrapPlot**, which carry out the bootstrap calculations and generate Figure 7-10, respectively.

References Cited

- Bergondo, DL, DR Kester, HE Stoffel, WL Woods, 2005. Time-series observations during the low sub-surface oxygen events in Narragansett Bay during summer 2001. *Marine Chemistry*, 97(1), 90–103. <https://doi.org/10.1016/j.marchem.2005.01.006>
- Codiga, D.L., Stoffel, H., Deacutis, C., Kiernan, S., & Oviatt, C., 2009. Narragansett Bay Hypoxic Event Characteristics Based on Fixed-Site Monitoring Network Time Series: Intermittency, Geographic Distribution, Spatial Synchronicity, and Interannual Variability. *Estuaries and Coasts*, 32(4), 621-641.
- Codiga, D.L. 2012. Density stratification in an estuary with complex geometry: Driving processes and relationship to hypoxia on monthly to inter-annual timescales. *J. Geophys. Res.* 117. C12004. DOI 10.1029/2012JC008473.
- Codiga, D.L. 2020a. Further Analysis and Synthesis of Narragansett Bay (RI/MA USA) Oxygen, Chlorophyll, and Temperature. NBEP Technical Report. NBEP 20-231A. URL: <https://figshare.com/s/7d51f2540df6638a4552>. DOI: 10.6084/m9.figshare.12547676
- Codiga, D.L. 2020b. Daily-Resolution 2001-2017 Time Series of Total Nitrogen Load to Narragansett Bay (RI/MA USA) from Bay-Wide Treatment Facility and Watershed Sources. NBEP Technical Report. NBEP 20-231B. URL: <https://figshare.com/s/95abe0296139515ffb88>. DOI: 10.6084/m9.figshare.12573851.
- Efron, B., & Gong, G. 1983. A Leisurely Look at the Bootstrap, the Jackknife, and Cross-Validation. *The American Statistician*, 37(1), 36-48. doi:10.2307/2685844
- Fulweiler, RW, A.J. Oczkowski, K.M. Miller, C.A. Oviatt, M.E.Q. Pilson, 2015. Whole truths vs. half truths – And a search for clarity in long-term water temperature records, *Estuarine, Coastal and Shelf Science*, Volume 157, Pages A1-A6, ISSN 0272-7714, <https://doi.org/10.1016/j.ecss.2015.01.021>.
- Gilbert, R.O. 1987. *Statistical Methods for Environmental Pollution Monitoring*, Wiley, NY.
- Kellogg, D.Q., 2018. Freshwater flow to Narragansett Bay: An analysis of long-term trends. EPA Southern New England Program, Healthy Communities Grant Program.
- Kendall, M.G. 1975. *Rank Correlation Methods*, 4th edition, Charles Griffin, London.
- Leroy, S.S., J. G. Anderson, J. Dykema, and R. Goody, 2008. Testing climate models using thermal infrared spectra. *J. Climate*, 21, 1863–1875, doi:10.1175/2007JCLI2061.1.
- Mann, H.B. 1945. Non-parametric tests against trend, *Econometrica* 13:163-171.
- Mesinger, F., G. DiMego, E. Kalnay, K. Mitchell, P.C. Shafran, W. Ebisuzaki, D. Jovic, J. Woollen, E. Rogers, E.H. Berbery, M.B. Ek, Y. Fan, R. Grumbine, W. Higgins, H. Li, Y. Lin, G. Manikin, D. Parrish, and W. Shi, 2006. North American Regional Reanalysis. *Bulletin of the American Meteorological Society* 87 (3): 343–360. doi:10.1175/BAMS-87-3-343.
- NBEP, 2009. *Currents of Change: Environmental Status & Trends of the Narragansett Bay Region*. Final Technical Draft. Narragansett Bay Estuary Program.

NBEP, 2017. State of Narragansett Bay and Its Watershed. Technical Report. Narragansett Bay Estuary Program. Providence, RI.

Nixon, SW, SL Granger, BL Nowicki, 1995. An assessment of the annual mass balance of carbon, nitrogen, and phosphorus in Narragansett Bay. *Biogeochemistry*, 31(1), 15–61.
<https://doi.org/10.1007/BF00000805>

Nixon, SW, BA Buckley, SL Granger, LA Harris, AJ Oczkowski, RW Fulweiler, LW Cole, 2008. Nitrogen and phosphorus inputs to Narragansett Bay: past, present, and future. In *Science for ecosystem-based management* (pp. 101–175). Springer.

Nixon, S, Fulweiler, W, Buckley, B, Granger, S, Nowicki, B, Henry, K., 2009. The impact of changing climate on phenology, productivity, and benthic–pelagic coupling in Narragansett Bay. *Estuarine, Coastal and Shelf Science*. 82. 1-18. 10.1016/j.ecss.2008.12.016.

Oviatt, C.A. The changing ecology of temperate coastal waters during a warming trend. *Estuaries* 27, 895–904 (2004). <https://doi.org/10.1007/BF02803416>.

Parkins, CJ and SD Olszewski, 2019. Assessment of recreationally important finfish stocks in Rhode Island Waters. 2018 Annual Performance Reports F-61-R-21.
http://www.dem.ri.gov/programs/bnatres/marine/pdf/F61_2018Report.pdf

Phojanamongkolkij, N., Kato, S., Wielicki, BA, Taylor, PC, Mlynczak, MG, 2014. A comparison of Climate Signal Trend Detection Uncertainty Methods. *J. Climate*. 27, 3363-3376. DOI: 10.1175/JCLI-D-13-00400.1

Pilson M.E., 2008. Narragansett Bay Amidst a Globally Changing Climate. In: Desbonnet A., Costa-Pierce B.A. (eds) *Science for Ecosystem-based Management*. Springer Series on Environmental Management. Springer, New York, NY

Prell, W.L., Murray, D.W., Howell, P., 2015, Reanalysis of the Narragansett Bay Spatial Survey (Day Trippers) Water Column Data for Temperature, Salinity, Density, and Dissolved Oxygen (2005 to 2013), Narragansett Bay Estuary Program, NBEP-15-128. Providence, RI.

Prell, W.L, Murray, D.W., Carlson, L., and Thieleman, E., 2016, Update and integration of the 2014 and 2015 data into the Spatial Survey data set and generation of decade-long (2005-2015) trends of DO and Chlorophyll distribution in mid and upper Narragansett Bay for the Narragansett Bay Estuary Program's The State of Our Watershed Report. Narragansett Bay Estuary Program, NBEP-16-132. Providence, RI.

Ries, K. G. 1990. Estimating surface-water runoff to Narragansett Bay, Rhode Island and Massachusetts, U. S. Geol. Surv., Water-Resour. Invest. Rep., 89-4164, 1–49.

Rogers, JM, 2008. Circulation and transport in the heart of Narragansett Bay. Master's thesis, Graduate School of Oceanography, University of Rhode Island. 107pp.

Roesler CS. 2020. Continuous observations of chlorophyll fluorescence and related parameters in Massachusetts Bay, 2005 – 2019. Boston: Massachusetts Water Resources Authority. Report 2020-09. 27 p. <https://www.mwra.com/harbor/enquad/pdf/2020-09.pdf>

Rosa, K.K., 2020. "Coastal ocean modeling across length scales: From estuarine circulation to boundary currents". PhD Dissertation, University of Rhode Island, Graduate School of Oceanography. *Open Access Dissertations*. Paper 1196. https://digitalcommons.uri.edu/oa_diss/1196

Sen, P. K. (1968), "Estimates of the regression coefficient based on Kendall's tau", *Journal of the American Statistical Association*, 63 (324): 1379–1389, doi:10.2307/2285891

Smith, L. M., Whitehouse, S., & Oviatt, C. A. 2010. Impacts of Climate Change on Narragansett Bay. *Northeastern Naturalist*, 17(1), 77-90. doi: 10.1656/045.017.0106SNBIW

Theil, H. (1950), "A rank-invariant method of linear and polynomial regression analysis. I, II, III", *Nederl. Akad. Wetensch., Proc.*, 53: 386–392, 521–525, 1397–1412, MR 0036489

Tiao, G. C., and Coauthors, 1990: Effects of autocorrelation and temporal sampling schemes on estimates of trend and spatial correlation. *J. Geophys. Res.*, 95, 20 507–20 517, doi:10.1029/JD095iD12p20507.

Ullman, D.S., C. Kincaid, C. Balt, and D.L. Codiga, 2019. Hydrodynamic modeling of Narragansett Bay in Support of the EcoGEM ecological model. GSO Technical Report 2019-01. University of Rhode Island, Graduate School of Oceanography. Narragansett, RI.

USEPA, 2015. National Coastal Condition Assessment 2010 (EPA 841-R-15-006). Office of Water and Office of Research and Development. Washington, DC. <http://www.epa.gov/national-aquatic-resource-surveys/ncca>

Weatherhead, E. C., and Coauthors, 1998: Factors affecting the detection of trends: Statistical considerations and applications to environmental data. *J. Geophys. Res.*, 103, 17 149–17 161, doi:10.1029/98JD00995.

Acknowledgements

David Borkman (RIDEM)
Crystal Charbonneau (RIDEM)
Shelly Clark (NEIWPCC)
Jeremy Collie (URI)
Chris Deacutis (RIDEM)
Jesselyn Dugas (Veolia)
Richard Freisner (NEIWPCC)
Mike Gerel (NBEP)
Joe Habarek (RIDEM)
Kristin Huizenga (URI)
Eliza Moore (NBC)
Scott Olszewski (RIDEM)
Candace Oviatt (URI)
Chris Parkins (RIDEM)
Warren Prell (Brown)
Tatiana Rynearson (URI)
Nina Santos (URI)
Courtney Schmidt (NBEP)
Heather Stoffel (URI)
Jacob Strock (URI)
Tricia Thibodeau (URI)
Heidi Travers (RIDEM)
Molly Welsh (NBC)

Although the information in this document has been funded by the EPA, it has not undergone the EPA's publications review process and therefore, may not reflect the views of EPA and no official endorsement is inferred. The viewpoints expressed do not necessarily represent those of NEIWPCC or EPA. Mention of trade names, commercial products, or causes do not constitute endorsement or recommendation for use.